5-2006

Simulation Study of Digitized Enhanced Feher Quadrature Phase Shift Keying (EFQPSK)

Fall Bernard Taylor
University of Tennessee - Knoxville

To the Graduate Council:

I am submitting herewith a thesis written by Fall Bernard Taylor entitled "Simulation Study of Digitized Enhanced Feher Quadrature Phase Shift Keying (EFQPSK)." I have examined the final electronic copy of this thesis for form and content and recommend that it be accepted in partial fulfillment of the requirements for the degree of Master of Science, with a major in Electrical Engineering.

Mostofa K. Howlader, Major Professor

We have read this thesis and recommend its acceptance:

Stephen F. Smith, Donald W. Bouldin, Michael J. Roberts

Accepted for the Council:
Dixie L. Thompson

Vice Provost and Dean of the Graduate School

(Original signatures are on file with official student records.)

To the Graduate Council:

I am submitting herewith a thesis written by Fall Bernard Taylor entitled “Simulation Study of Digitized Enhanced Feher Quadrature Phase Shift Keying (EFQPSK)”. I have examined the final electronic copy of this thesis for form and content and recommend that it be accepted in partial fulfillment of the requirements for the degree of Master of Science, with a major in Electrical Engineering.

Mostofa K. Howlader

Major Professor

We have read this thesis
and recommend its acceptance:

Stephen F. Smith

Donald W. Bouldin

Michael J. Roberts

Accepted for the Council:

Anne Mayhew

Vice Chancellor and
Dean of Graduate Studies

(Original signatures are on file with official student records.)

Simulation Study of Digitized Enhanced Feher Quadrature Phase Shift Keying (EFQPSK)

A thesis presented for the Masters of Science Degree at
The University of Tennessee, Knoxville

Fall Bernard Taylor Jr.

May, 2006

DEDICATION

This thesis is dedicated my father, Fall B. Taylor Sr., for encouraging and enabling me to further my education. It was his wish to see me off to college before he passed away. I have no doubt that he would be proud of my accomplishments thus far. This thesis is also dedicated to my mother, Sharolyn M. Taylor, for encouraging me to further my education and giving me valuable advice over the years. Finally, this thesis is dedicated to the rest of my family for their support.

ACKNOWLEDEMENTS

I would like to thank my major professor, Dr. Mostofa Howlader, for giving me the opportunity to advance my learning by pursuing a master's degree. I would also like to thank him for always trying to help me and for being patient with me. I would like to thank my mentor Mike Moore for his many contributions in the advancement of my knowledge. I would like to thank Dr. Steve Smith, Dr. Miljko Bobrek, Dr. Mark Buckner, and Michael Vann for their help. I would like to thank the students of WCRG at the University of Tennessee, Knoxville for their help. I would like to thank my Uncle Ralph and Aunt Vicki for reviewing this work. Finally, I would like to thank all of the professors in a technical field that have educated me over the course of my college career.

This research work has been performed in the Wireless Communications Research Group (WCRG) at University of Tennessee, Knoxville, sponsored by the RF & Microwave System Group (RFMSG) of the Oak Ridge National Laboratory (ORNL) under the contract UT-B 4000025441 and UT research account number R011344113. I am also especially indebted to Paul Ewing, leader of the RFMSG, who has provided me with this great opportunity.

ABSTRACT

Digitized enhanced Feher quadrature phase-shift keying (EFQPSK) can be realized with a set of parameters that define its efficiency relative to analog EFQPSK and quadrature phase-shift keying (QPSK). Both sampling frequency and quantization play a significant role in developing an EFQPSK signal that resembles its analog counterpart in spectral efficiency, envelope fluctuation, and BER. Sampling frequency and quantization can be used to determine spectral efficiency as compared to analog EFQPSK and QPSK. Through simulation, this study compares and quantifies trade-offs between spectral efficiency, envelope fluctuation, and BER. By quantifying the trade-off between these parameters, system designers can quickly determine how to meet bandwidth efficiency and power efficiency requirements.

Keywords: Feher, QPSK, Spectral Efficient, Bandwidth Efficient, Constant Envelope, Power Efficient, Pulse Shaping, Trellis Code, Average Matched Filter, Sampling Frequency, Quantization, Discrete Fourier Transform, Distortion, Correlation, Energy-Per-Bit

TABLE OF CONTENTS

LIST OF TABLES

LIST OF FIGURES

LIST OF ABBREVIATIONS

BER	bit-error-rate
PSD	power spectral density
QPSK	quadrature phase shift keying
IJF-QPSK	interference and jitter-free quadrature phase shift keying
EFQPSK	enhanced Feher quadrature phase shift keying
OQPSK	offset quadrature phase shift keying
DFT	discrete Fourier transform
BPSK	binary phase shift keying
NRZ	non-return to zero
SQORC	staggered quadrature overlapped raised-cosine
MSK	minimum shift keying
XPSK	cross-correlated phase shift keying
FQPSK	Feher quadrature phase shift keying
“quasi”	refers to an envelope with very little amplitude modulation
TCM	Trellis coded modulation
CPFSK	continuous phase frequency shift keying
ROM	read only memory
ADC	analog-to-digital converter
N_q	Nyquist frequency
AM	amplitude modulation
PM	phase modulation
AWGN	additive white Gaussian noise
SQNR	signal-to-quantization noise ratio
DC	direct current

Chapter 1: INTRODUCTION

1.1 Overview of the Problem

For robust link designs, physical layer parameters such as spectral efficiency, power efficiency when transmitting over long distances, and bit-error rate (BER) are of major concern. Spectral efficiency defines the amount of power wasted given a certain bandwidth. Spectral efficiency can be classified by two terms: power spectral density (PSD) efficiency and out-of-band power efficiency. Power spectral density depicts the amount of power the side-bands of a given modulation scheme occupy. Out-of-band power measures the percentage of power outside of the bandwidth of interest. Power efficiency has to do with how much spectral re-growth can be expected when transmitting a signal over long distances using a non-linear amplifier. This aspect is dependent upon envelope fluctuation. Finally, BER measures the amount of errors expected with a given signal-to-noise ratio in a certain modulation scheme.

There are many modulation schemes that achieve at least one of these at one time but few that achieve three of these at one time. For example, quadrature phase shift keying (QPSK) is a modulation scheme that provides good BER and good power efficiency but poor spectral efficiency [1], [2]. Interference and Jitter-Free QPSK (IJF-QPSK) is a modulation scheme that provides good spectral efficiency characteristics but slightly degraded BER compared to QPSK and poor power efficiency since it is not constant envelope [2].

In this thesis, we study a type of modulation named enhanced Feher quadrature phase shift keying (EFQPSK) that offers excellent spectral efficiency characteristics, power efficiency characteristics comparable to that of constant envelope, and acceptable BER. More specifically, we study the effects that digitizing EFQPSK has on the performance of the aforementioned parameters.

1.2 Contributions

In this study, we will show the effects digitization has on a bandwidth efficient and power efficient modulation scheme. Specifically we will show the degradation digitization has on the bandwidth and power efficiency and both the improvement and degradation digitization has on BER. This study makes several distinct contributions to the literature:

1. We examine the impact digitization has on the spectrum, out-of-band power, and maximum envelope fluctuation of EFQPSK.
2. We illustrate the impact soft-limiting has on the digitized EFQPSK signal in terms of spectrum and out-of-band power.
3. We illustrate that digitizing EFQPSK can both improve and degrade BER over analog EFQPSK.

This thesis is organized as follows: Section 2.1 of Chapter 2 discusses the spectrum, out-of-band power, and BER of QPSK. Section 2.2 discusses the improvement OQPSK has over QPSK when hard limiting the transmitted signal. Section 2.3 discusses the improved spectral efficiency IJF-QPSK has over both QPSK and OQPSK and also discusses the method in which an IJF-QPSK signal is generated. Section 2.4 further illustrates the improved spectral efficiency cross-correlated phase shift keying (XPSK) offers over IJF-QPSK and the method in which a XPSK signal is generated. Section 2.5 introduces EFQPSK and how it is more spectrally efficient than the aforementioned modulation schemes and the method in which an EFQPSK signal is generated.

In Chapter 3 we lay the foundation of the system model used in this study starting with a discussion of the analog-to-digital converter model used in digitizing EFQPSK and finish this section with the effects taking the discrete Fourier transform (DFT) has on the spectrum of a signal. Section 3.3 discusses the amplifier model used in this study. Section 3.4 discusses the type receiver model used in this study. Finally, Section 3.5 summarizes the system model.

Chapter 4 presents the results obtained using the system model of Chapter 3. Namely, Section 4.1 compares the spectra of various digitized EFQPSK signals versus the

spectrum of analog EFQPSK. Section 4.2 compares the out-of-band power of various digital EFQPSK signals versus the out-of-band power of analog EFQPSK. Section 4.3 takes several digital EFQPSK signals and compares their respective maximum envelope fluctuations to that of analog EFQPSK. Section 4.4 analyzes BER of a variety of digital EFQPSK signals, comparing them to the BER of analog EFQPSK. Sections 4.5 and 4.6 compare spectral efficiency of assorted digital EFQPSK signals that are soft limited to soft limited analog EFQPSK. Finally, Chapter 5 concludes this study and discusses future research that may be conducted utilizing this system.

Chapter 2: BACKGROUND

2.1 QPSK

QPSK is a modulation scheme that offers constant envelope and good BER but poor spectral efficiency. QPSK has twice the bandwidth efficiency as binary phase shift keying (BPSK) for the same energy because two bits are transmitted in QPSK instead of one [1]. A QPSK signal is described by

$$S_{QPSK}(t) = \sqrt{\frac{2E_S}{T_S}} \cos\left[2\pi f_c t + (i-1)\frac{\pi}{2}\right] \qquad 0 \le t \le T_S \qquad i = 1,2,3,4\,, \qquad (2.1)$$

Where T_S is the symbol time and is equal to twice the bit period and E_S is the energy-per-symbol and is twice the energy per bit. The variable i in (2.1) describes the four different phases that QPSK can take. The phase of the I-channel and Q-channel is influenced by the incoming data bits and there can be a maximum of 180° discrete phase transition in the transmitted signal. If we assume QPSK uses binary data with rectangular pulse shaping, the PSD of QPSK is given by

$$P_{QPSK}(f) = \left[\frac{\sin(2\pi f T_b)}{2\pi f T_b}\right]^2 . \qquad (2.2)$$

Fig. 2.1 shows the PSD of conventional QPSK. Notice that the side-lobe power is rather high for higher frequencies, clearly not a desirable characteristic. Since the power in the side-lobes of QPSK is rather high for higher bandwidth, one would expect the out-of-band power to be high as well. Fig. 2.2 shows the out-of-band power of QPSK, where the normalized bandwidth B is $[BT_b]$ and T_b is the bit period. Note the bandwidth that contains 90% of the power is located at $\frac{1}{T_b}$ Hz and the bandwidth that contains 99% of the power is located at $\frac{8}{T_b}$ Hz [3].

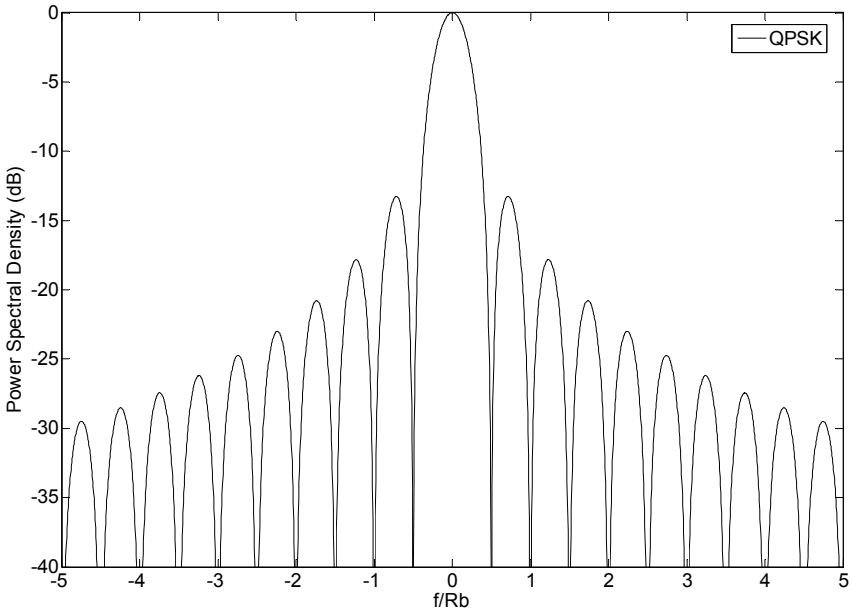

Fig. 2.1. Power spectral density of conventional QPSK.

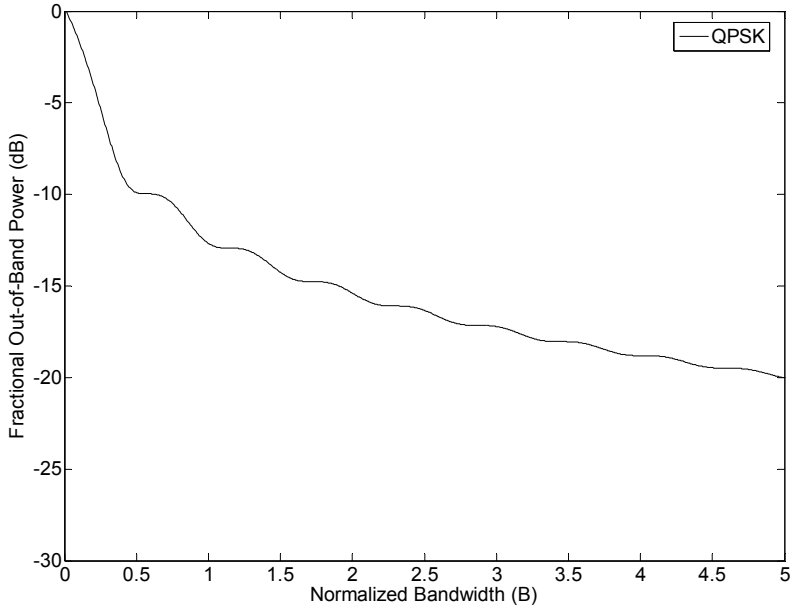

Fig. 2.2. Out-of-band power of QPSK.

Finally, the BER of conventional QPSK is equivalent to that of binary phase shift keying (BPSK). Therefore, given the same energy efficiency, QPSK has twice the spectral efficiency as BPSK. The BER for QPSK is

$$P_e = Q\left(\sqrt{\frac{2E_b}{N_0}}\right), \qquad (2.3)$$

Where N_0 is the additive white Gaussian noise (AWGN) power spectral density. Fig. 2.3 plots the BER of conventional QPSK. Note the good error performance for mid-to-high E_b/N_0 levels. As shown thus far, QPSK offers constant envelope and good BER. Both of these characteristics make it a good modulation scheme in a system that requires transmitting over long distances and in a system that must have lower BER. However, QPSK occupies a large amount of bandwidth for the given energy in the modulation scheme. The out-of-band power is considerably large for a given bandwidth. Overall, QPSK satisfies only two of the four parameters discussed previously in this document.

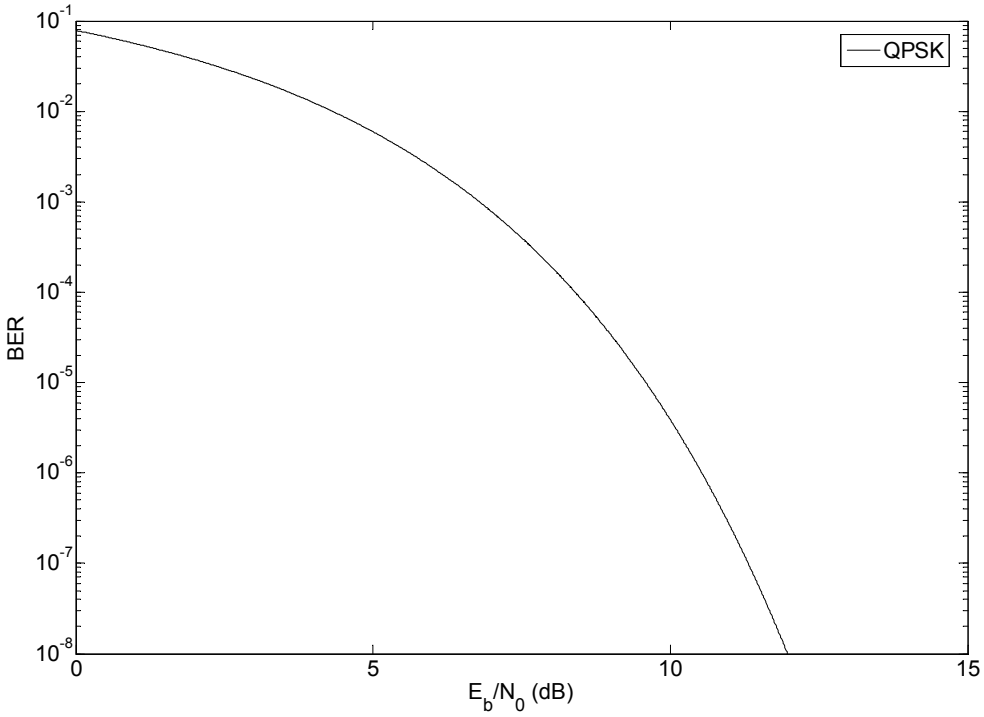

Fig. 2.3. BER of conventional QPSK.

2.2 OQPSK

It is a well-known fact that conventional QPSK is ideally constant envelope. However if the signal is band-limited in this modulation scheme, the envelope is no longer constant. When the phase change is $180°$ for one-quarter of the time, the envelope crosses zero one quarter of the time, which means that the envelope is not constant during that instant [1]. When this happens during nonlinear amplification, the original frequency side-lobes will be restored to their original state prior to band limiting, thus negating the band-limiting carried out in the transmission of the QPSK signal [4].

Offset QPSK (OQPSK) was introduced to limit the maximum amount of phase transition to $90°$. By limiting the maximum phase transition to only $90°$, band limiting the signal no longer causes the envelope to go to zero. Since the maximum phase transitions in OQPSK are much less than QPSK, nonlinear amplification of the envelope will not restore as many of the high frequency side-lobes [4]. However, since band limiting is performed, there will be some high frequency side-lobes generated at the maximum $90°$ phase transition.

OQPSK offers the same spectral efficiency, out-of-band power, and BER as QPSK because OQPSK and QPSK are of the same design, except with an offset of one of the channels in OQPSK. In other words, the delaying by a half symbol of one of the channels in OQPSK affects only the maximum phase transition, which in turn, only affects the envelope when band limiting and hard limiting is utilized.

Fig. 2.4 is a conceptual block diagram of an OQPSK transmitter. The incoming data bits are assumed to be random and uniformly distributed. The serial-to-parallel converter separates the data bits into an in-phase and quadrature-phase channel. The quadrature-phase channel is delayed by a half symbol. The in-phase branch is modulated onto a sinusoidal or co-sinusoidal carrier. The quadrature-phase branch is modulated on the $90°$ phase- shifted version of the in-phase carrier. Finally, the in-phase and quadrature-phase channels are added to form the OQPSK signal.

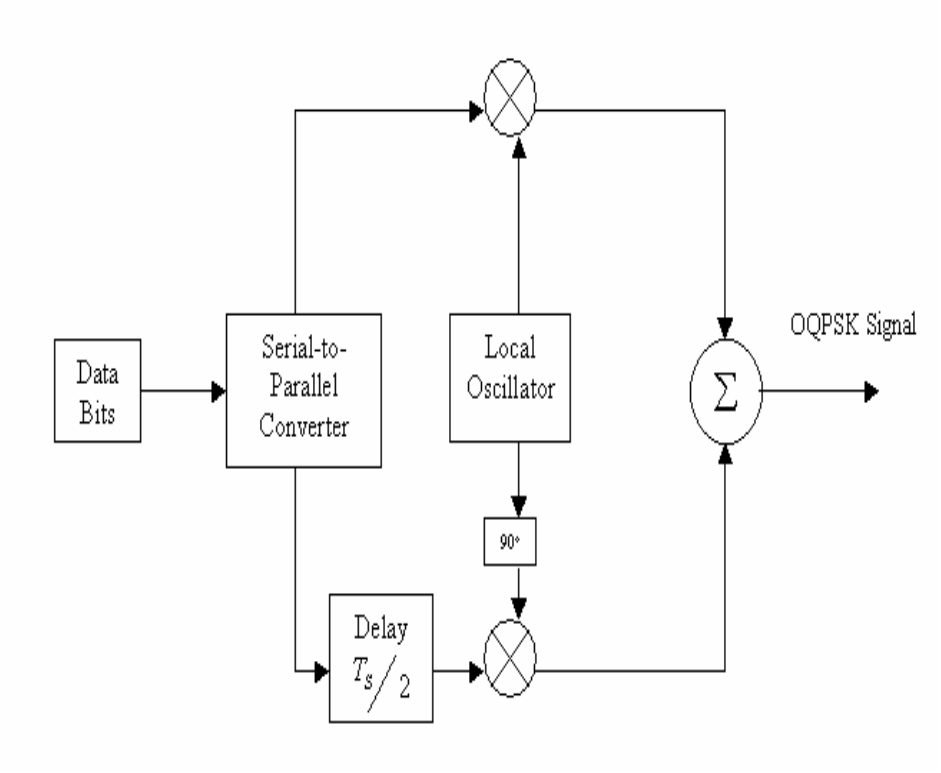

Fig. 2.4. Conceptual block diagram of an OQPSK transmitter.

2.3 IJF-QPSK

The transmission scheme IJF-QPSK was developed as a means to improve spectral efficiency over conventional QPSK. The inherent transmitter architecture for IJF-QPSK is OQPSK and IJF-QPSK works according to the following: two waveforms are defined as

$$\left.\begin{aligned} s_e(t) &= 1, && -\frac{T_S}{2} \le t \le \frac{T_S}{2} \\ s_o(t) &= \sin\left(\frac{\pi t}{T_S}\right), && -\frac{T_S}{2} \le t \le \frac{T_S}{2} \end{aligned}\right\}, \tag{2.4}$$

Where $s_e(t)$ is the even waveform, $s_o(t)$ is the odd waveform, and T_S is the symbol time [2]. During the interval $(n-[1/2])T_S \le t \le (n+[1/2])T_S$, the in-phase channel transmitted waveform, $x_I(t)$, is determined by

$$\left.\begin{array}{ll} x_I(t) = s_e(t - nT_S) = s_0(t - nT_S) & if\ d_{I,n-1} = 1,\ d_{I,n} = 1 \\ x_I(t) = -s_e(t - nT_S) = s_1(t - nT_S) & if\ d_{I,n-1} = -1,\ d_{I,n} = -1 \\ x_I(t) = s_o(t - nT_S) = s_2(t - nT_S) & if\ d_{I,n-1} = -1,\ d_{I,n} = 1 \\ x_I(t) = -s_o(t - nT_S) = s_4(t - nT_S) & if\ d_{I,n-1} = 1,\ d_{I,n} = -1 \end{array}\right\}, \qquad (2.5)$$

Where $d_{I,n-1}$ is the previous bit, $d_{I,n}$ is the present bit, and $s_i(t)\ for\ i = 1, 2, 3, 4$ are the four possible transmitted signals on the in-phase channel [2]. The equivalent quadrature-phase transmitted signal, $x_Q(t)$, is selected the same way except $d_{Q,n-1}$ and $d_{Q,n}$ replace $d_{I,n-1}$ and $d_{I,n}$ and the signaling interval is $nT_S \le t \le (n+1)T_S$, because the quadrature-phase channel is delayed by a half symbol [2]. Fig. 2.5 depicts a conceptual block diagram of an IJF-QPSK transmitter. Note that the incoming data bits must be pulse shaped with non-return to zero (NRZ) pulse shaping. The IJF-QPSK modulation scheme is equivalent to staggered quadrature overlapped raised-cosine (SQORC) modulation scheme if we define the raised-cosine pulse shape

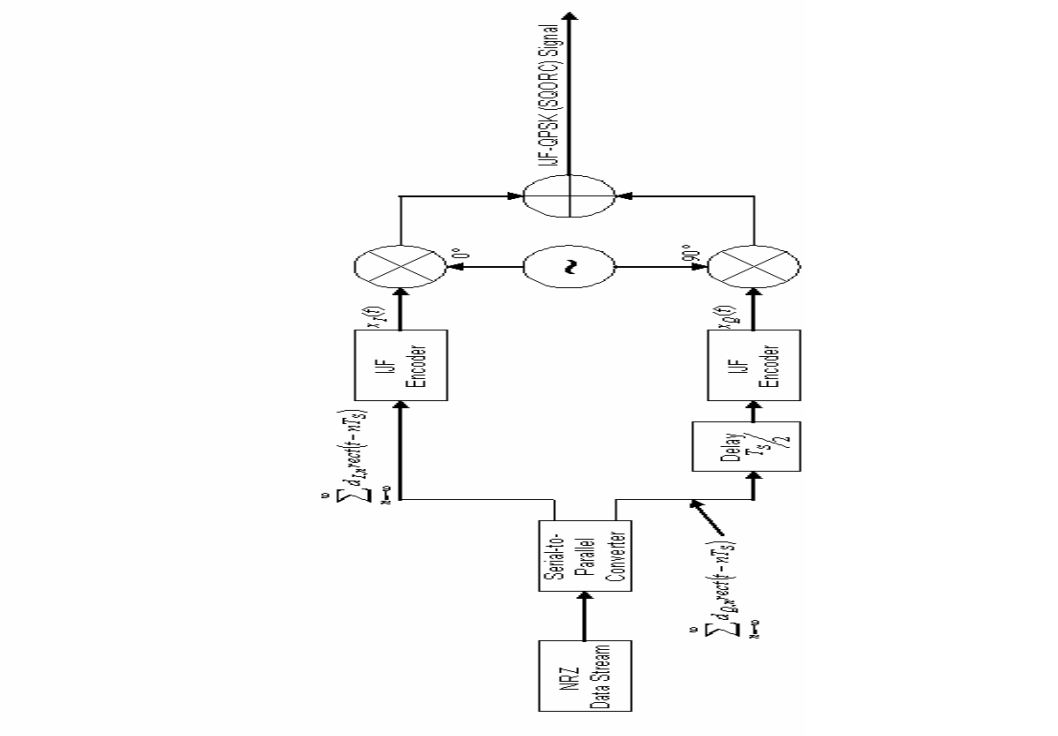

Fig. 2.5. Conceptual block diagram of an IJF-QPSK transmitter. Reproduced from [2].

$$p(t) = \sin^2\left(\frac{\pi\left(t+\frac{T_S}{2}\right)}{2T_S}\right), \qquad -\frac{T_S}{2} \le t \le \frac{3T_S}{2}. \tag{2.6}$$

The equivalent in-phase transmitted signal is given by

$$x_I(t) = \sum_{n=-\infty}^{\infty} d_{I,n}\, p\left(t - nT_S\right) \tag{2.7}$$

And the equivalent quadrature-phase transmitted signal is given by

$$x_Q(t) = \sum_{n=-\infty}^{\infty} d_{Q,n}\, p\left(t - \left(n+\frac{1}{2}\right)T_S\right), \tag{2.8}$$

where $x_I(t)$ and $x_Q(t)$ in (2.7) and (2.8) are equivalent to $x_I(t)$ and $x_Q(t)$ given in (2.5), assuming the waveforms in (2.4) are utilized [5]. The power spectral density of SQORC is given by

$$S_{SQORC}(f) = \left(\frac{\sin(\pi f T_S)}{\pi f T_S}\right)^2 \frac{\cos^2(2\pi f T_S)}{(1-16f^2T_S^2)^2}, \tag{2.9}$$

where (2.9) is the combination of PSD's for conventional QPSK and minimum shift keying (MSK) [2]. The cost for improving the spectral efficiency in this modulation scheme is a maximum of a $3\ dB$ fluctuation in the envelope. This amount of envelope fluctuation is not optimal in any sense because if this envelope were hard limited, a large amount of spectral re-growth would occur, causing interference between adjacent channels. Since the quadrature branch of the transmitted signal is delayed by a half-symbol, the maximum phase transition on the modulated signal of OQPSK is $90°$. Since the quadrature branch of IJF-QPSK is delayed by a half-symbol and both the in-phase and quadrature branches are band-limited, the maximum phase transition is slightly less than $90°$ because pulse-shaping smoothes the phase transitions in the modulated signal. However, since there is still a discrete phase transition in the envelope, there will be some spectral splatter. Fig. 2.6 shows the PSD of IJF-QPSK compared to the PSD of conventional QPSK. Note that the spectral efficiency of IJF-QPSK is much better than QPSK. Fig. 2.7 compares the out-of-band power of conventional QPSK to IJF-QPSK. Clearly IJF-QPSK is superior to QPSK in terms of spectral efficiency and out-of-band power, but the $3\ dB$ envelope fluctuation makes this

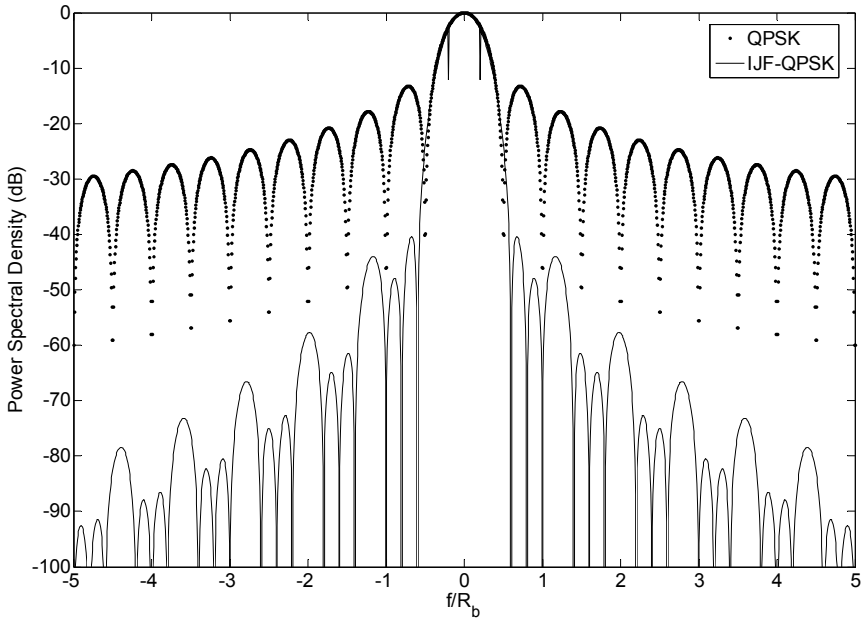

Fig. 2.6. Power spectral density of IJF-QPSK.

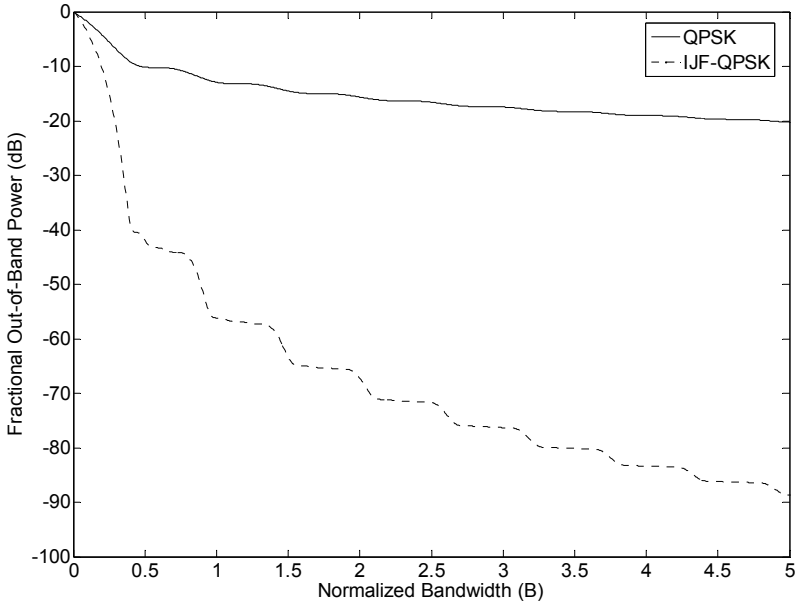

Fig. 2.7. Out-of-band power of IJF-QPSK.

modulation scheme a poor choice for a system that requires hard limiting.

2.4 Cross-Correlated Phase Shift Keying (XPSK)

Since QPSK does not yield good spectral efficiency characteristics, IJF-QPSK was introduced as a modulation scheme that does yield good spectral efficiency characteristics. Another topic of major concern is envelope fluctuation. Since IJF-QPSK exhibits a maximum of $3\ dB$ in envelope fluctuation, we have focused our attention on another modulation scheme.

XPSK is a modulation scheme derived from IJF-QPSK for purposes of minimizing envelope fluctuation from $3\ dB$ to almost $0\ dB$, while maintaining very good spectral efficiency characteristics [6]. The transmission scheme XPSK takes the IJF-QPSK modulation scheme and modifies it as follows: there are two channels in the modulation scheme, each of which contain up to four possibilities of transmitted waveforms. Therefore, there are $2^4 = 16$ possible signal components that can be input to the cross-correlator [2]. The cross-correlator was introduced as a means for reducing the maximum envelope fluctuation from $3\ dB$ to near $0\ dB$ [6]. Sixteen new signals are generated at the output of the cross-correlator and are given in Table 2.1.

Table 2.1. I and Q cross-correlated signal combinations. Reproduced from [2].

$s_I(t)$ $(or\ s_Q(t))$	$s_Q(t)$ $(or\ s_I(t))$	Number of Combinations
$\pm\cos\left(\frac{\pi t}{T_S}\right)$	$\pm\sin\left(\frac{\pi t}{T_S}\right)$	4
$\pm A\cos\left(\frac{\pi t}{T_S}\right)$	$f_1(t)$ or $f_3(t)$	4
$\pm A\sin\left(\frac{\pi t}{T_S}\right)$	$f_2(t)$ or $f_4(t)$	4
$\pm A$	$\pm A$	4

The transition functions $f_i(t)$ for $i = 1, 2, 3, 4$ from Table 2.1 are given by

$$\left.\begin{aligned} f_1(t) &= 1-(1-A)\cos^2\left(\frac{\pi t}{T_S}\right) \\ f_2(t) &= 1-(1-A)\sin^2\left(\frac{\pi t}{T_S}\right) \\ f_3(t) &= -1+(1-A)\cos^2\left(\frac{\pi t}{T_S}\right) \\ f_4(t) &= -1+(1-A)\sin^2\left(\frac{\pi t}{T_S}\right) \end{aligned}\right\}, \qquad (2.10)$$

each of which are defined over the signaling interval $0 \le t \le \frac{T_S}{2}$ [2]. The amplitude parameter, A, is used to control the amount of envelope fluctuation in XPSK. For $A = 1$, XPSK becomes IJF-QPSK and for $A = 1/\sqrt{2}$, the maximum envelope fluctuation is $0.18\ dB$ [6]. The cost of reducing the envelope fluctuation in XPSK is witnessed in the slight decrease in spectral efficiency. For the results of this study, the amplitude parameter is selected to be $A = 1/\sqrt{2}$. Fig. 2.8 is a conceptual block diagram of an XPSK transmitter.

Feher-patented quadrature phase-shift keying (FQPSK) is a term that is interchangeable with XPSK if FQPSK is in its unfiltered state [2]. Hence, FQPSK will be used for the rest of the study since the results shown in this paper of FQPSK are of the unfiltered form. Fig. 2.9 shows the PSD of FQPSK compared with the PSD's of QPSK and IJF-QPSK. Note that the spectrum of FQPSK is slightly worse than that of IJF-QPSK. From Fig. 2.9, there is an almost $50\ dB$ decrease in side-band power compared to QPSK at higher frequencies. This clearly is a better modulation scheme than QPSK for systems in which bandwidth is very limited and efficient amplification for long distance transmission is required. Fig. 2.10 shows the out-of-band power of FQPSK compared to that of QPSK and IJF-QPSK. Note that the out-of-band power of FQPSK is about 1.5 orders of

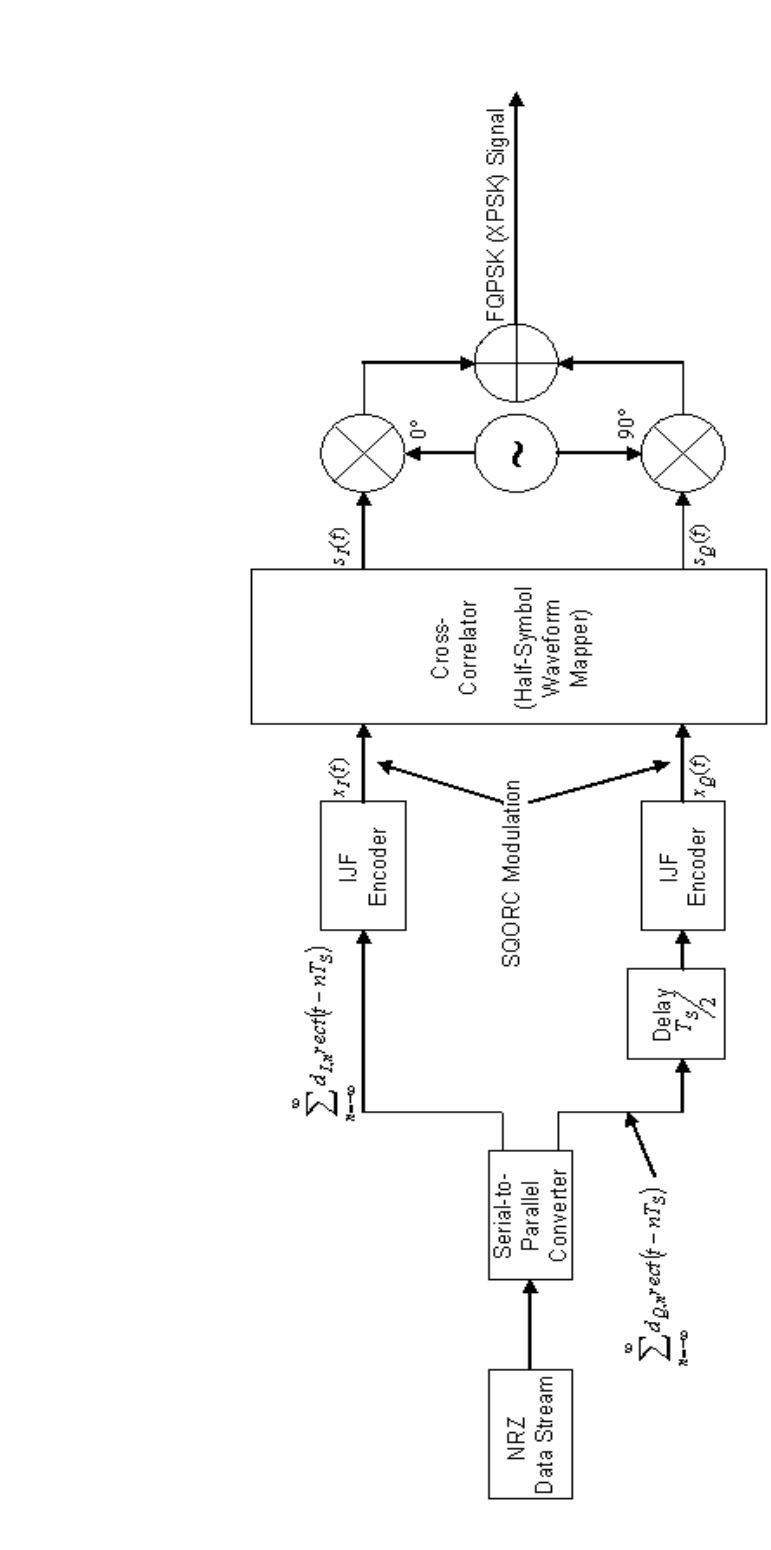

Fig. 2.8. Conceptual block diagram of an XPSK transmitter. Reproduced from [2].

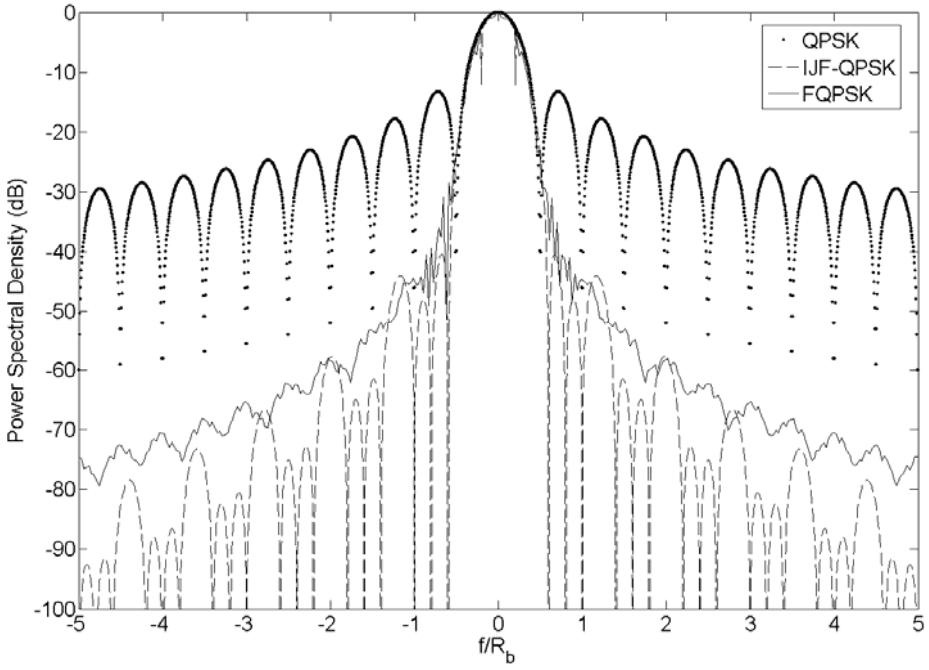

Fig. 2.9. The PSD of FQPSK as opposed to that of QPSK and IJF-QPSK.

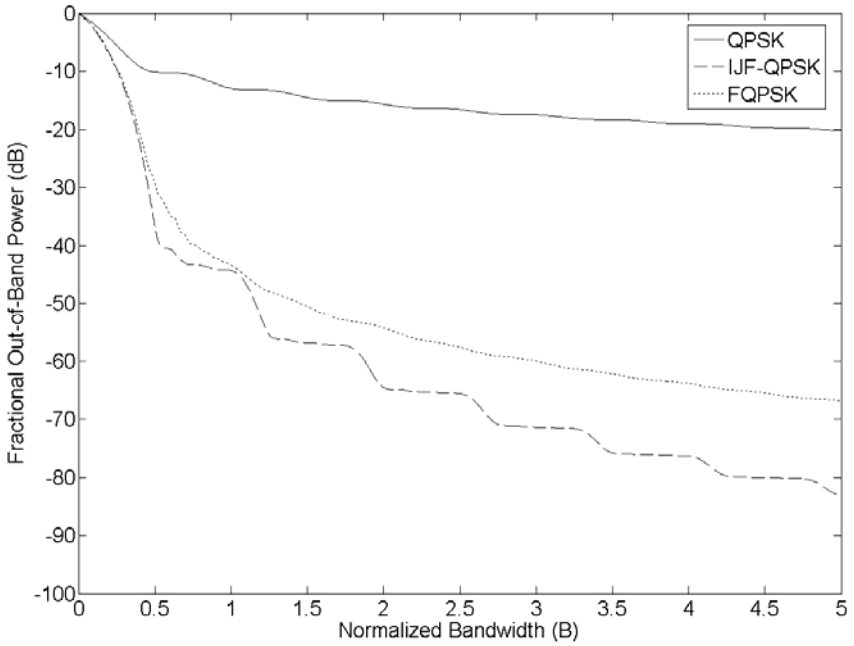

Fig. 2.10. The out-of-band power of FQPSK as opposed to that of QPSK and IJF-QPSK.

magnitude greater than that of IJF-QPSK at higher frequencies. This is a fair trade since the envelope of FQPSK is about 3 orders of magnitude smaller than that of IJF-QPSK.

Another major topic concerning the quality of a given modulation scheme is BER. Fig. 2.11 plots the BER of conventional QPSK with FQPSK. Note that at $P_e = 10^{-4}$, the BER of QPSK is almost 2 dB better than that of FQPSK. In a system in which BER must be very low, FQPSK is not a choice modulation scheme. However, in a system in which bandwidth is limited, efficient long distance transmission is required, and relaxed BER requirements exist, then FQPSK is a modulation scheme that could be considered.

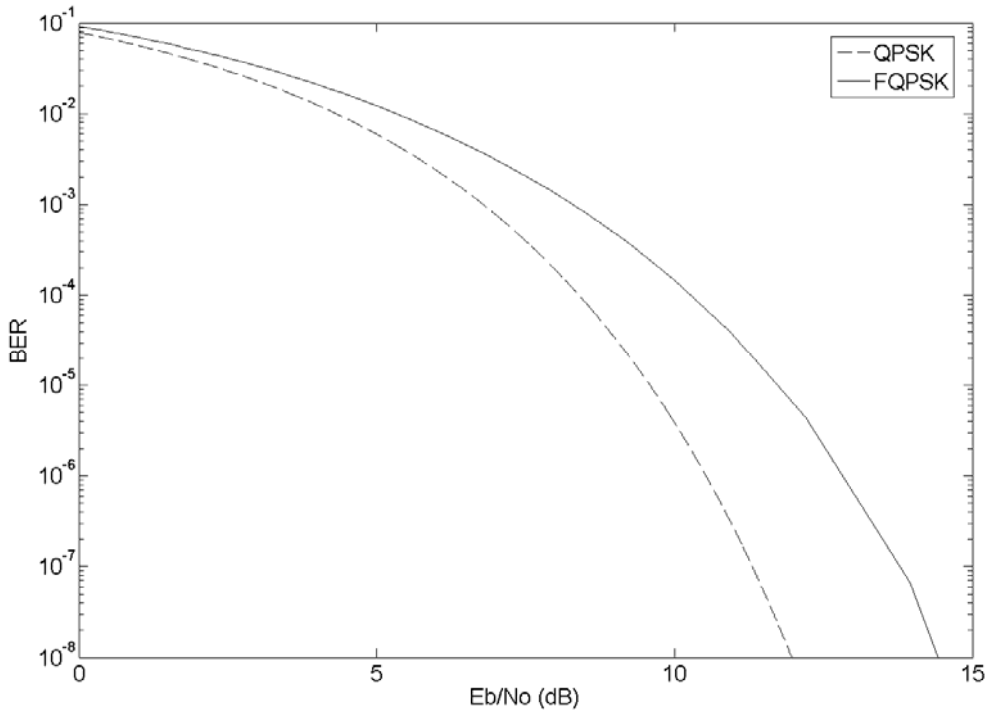

Fig. 2.11. BER of FQPSK compared to that of QPSK.

2.5 Enhanced FQPSK (EFQPSK)

2.5.1 Pulse Shaping

Many transmitter architectures modulate data bits that are rectangular in pulse shape. Other transmitter architectures use raised-cosine pulse shaping, Gaussian pulse shaping or some other type of pulse shaping. EFQPSK shapes polar NRZ data with 16 waveforms. These waveforms provide two distinct benefits for the transmitted signal. One benefit is good spectral efficiency characteristics and the other is a “quasi” constant envelope property. First we will describe the mapping of these 16 waveforms with the incoming data stream. From [7], the 16 waveforms are given in (2.10), where T_S is the symbol period and for the results of this thesis, $T_S = 2 \times 10^{-4}\, s$. The variable A in (2.10) is the amplitude parameter that was designed to range from $1/\sqrt{2} \le A \le 1$ [6]. The results of this thesis have $A = 1/\sqrt{2}$ in order to approach constant envelope as closely as possible.

All of the waveforms in (2.10) have continuous slopes at their respective midpoints and have zero slopes at their endpoints [7]. Having zero slopes at their endpoints allows for the concatenation of any waveform to any other waveform without any discontinuities [7]. Having a continuous slope at their midpoints means fewer high frequency components in the spectrum. Fig. 2.12 plots the 16 full-symbol waveforms of EFQPSK.

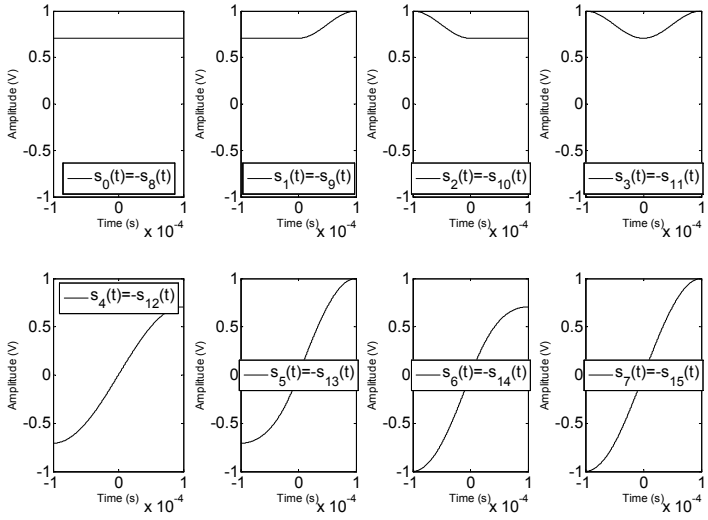

Fig. 2.12. 16 Full-symbol waveforms of EFQPSK.

$$
\left.
\begin{aligned}
s_0(t) &= A, && -\frac{T_S}{2} \le t \le \frac{T_S}{2}, \quad s_8(t) = -s_0(t) \\
s_1(t) &= \begin{cases} A, & -\frac{T_S}{2} \le t \le 0, \\ 1-(1-A)\cos^2\frac{\pi t}{T_S}, & 0 \le t \le \frac{T_S}{2}, \end{cases} && s_9(t) = -s_1(t) \\
s_2(t) &= \begin{cases} 1-(1-A)\cos^2\frac{\pi t}{T_S}, & -\frac{T_S}{2} \le t \le 0, \\ A, & 0 \le t \le \frac{T_S}{2}, \end{cases} && s_{10}(t) = -s_2(t) \\
s_3(t) &= 1-(1-A)\cos^2\frac{\pi t}{T_S}, && -\frac{T_S}{2} \le t \le \frac{T_S}{2}, \quad s_{11}(t) = -s_3(t) \\
s_4(t) &= A\sin\frac{\pi t}{T_S}, && -\frac{T_S}{2} \le t \le \frac{T_S}{2}, \quad s_{12}(t) = -s_4(t) \\
s_5(t) &= \begin{cases} \sin\frac{\pi t}{T_S} + (1-A)\sin^2\frac{\pi t}{T_S}, & -\frac{T_S}{2} \le t \le 0, \\ \sin\frac{\pi t}{T_S}, & 0 \le t \le \frac{T_S}{2}, \end{cases} && s_{13}(t) = -s_5(t) \\
s_6(t) &= \begin{cases} \sin\frac{\pi t}{T_S}, & -\frac{T_S}{2} \le t \le 0, \\ \sin\frac{\pi t}{T_S} - (1-A)\sin^2\frac{\pi t}{T_S}, & 0 \le t \le \frac{T_S}{2}, \end{cases} && s_{14}(t) = -s_6(t) \\
s_7(t) &= \sin\frac{\pi t}{T_S}, && -\frac{T_S}{2} \le t \le \frac{T_S}{2}, \quad s_{15}(t) = -s_7(t)
\end{aligned}
\right\} \qquad (2.10)
$$

For our study we categorize digital EFQPSK in terms of sampling frequency and quantization bits. Of the 8 waveforms, 4 of them in (2.10) have two parts: the first part contains a waveform defined only for the first half of the symbol period and the second part contains a waveform defined only for the second half of the symbol period. The model used for the results of this study take every $s_i(t)$ that has two parts and concatenates the two parts into one waveform defined over the symbol period. After all $s_i(t)$ have been combined to form one waveform for one symbol period, digitization is performed. The sampling process takes X samples over the period $-\frac{T_S}{2} \le t \le \frac{T_S}{2}$, where $X \in \{3, 5, 10, 20, 50, 100\}$ for the results of this study. In QPSK two bits make one symbol, where one I-channel bit is added with one Q-channel bit. However, for the digitized versions of EFQPSK in this study, X samples are taken over one symbol period, where the symbol containing the samples is not one I-channel bit added with one Q-channel bit, but rather is two concatenated I-channel bits or two concatenated Q-channel bits. For example if $X = 10$ then 10 samples are taken over the symbol period $-\frac{T_S}{2} \le t \le \frac{T_S}{2}$ for each I-channel symbol and each Q-channel symbol. In essence, for one EFQPSK symbol we have taken 20 samples because the $X = 10$ samples of the I-channel are added with the $X = 10$ samples of the Q-channel. To eliminate confusion while being precise, we will refer to the sampling frequency simply as "X sample" instead of "X sample-per-symbol". For example if we have a $X = 10$ sample-per-symbol EFQPSK signal, the "sample-per-symbol" term is misleading. However, if we say we have a $X = 10$ sample EFQPSK signal, we can more easily identify that this signal contains 10 samples (per pulse shape).

2.5.2 Trellis Code

In Section 2.5.1 we talked about the type of pulse shaping used in EFQPSK. In this section we talk about the methods used for shaping data with the 16 waveforms.

EFQPSK uses a type of Trellis-coded modulation (TCM) to map any of the 16 waveforms to each data bit. In terms of waveform selection, the operations performed on the I-channel are equivalent to the operations performed on the Q-channel. In selecting

a particular waveform to be mapped to a data bit given a certain signaling interval, the channel of interest depends on the most recent data transition on that channel and the two most recent and consecutive data transitions on the other channel [7]. For example, if the previous bit on the I-channel $d_{I,n-1}=1$, the present bit on the I-channel $d_{In}=1$, and, from the two previous transitions on the Q-channel, if the transitions $d_{Q,n-2}=0$, $d_{Q,n-1}=0$, and $d_{Q,n-1}=0$, $d_{Qn}=0$, then the waveform $s_0(t)$ is selected during the signaling interval $(n-[1/2])T_S \le t \le (n+[1/2])T_S$. From [7], Tables 2.2a and 2.2b list all the possible waveform mappings for the I-channel and the Q-channel. We can represent Tables 2.2a and 2.2b with a set of equations that simplify the model. D_{In} and D_{Qn} replace d_{In} and d_{Qn}, namely,

$$\left.\begin{aligned} D_{In} &\equiv \frac{1-d_{In}}{2} \\ D_{Qn} &\equiv \frac{1-d_{Qn}}{2} \end{aligned}\right\}, \tag{2.11}$$

Table 2.2a. Mapping of I-channel base-band signal during interval $(n-[1/2])T_S \le t \le (n+[1/2])T_S$. Reproduced from [7].

$\left\lvert\frac{d_{In}-d_{I,n-1}}{2}\right\rvert$	$\left\lvert\frac{d_{Q,n-1}-d_{Q,n-2}}{2}\right\rvert$	$\left\lvert\frac{d_{Qn}-d_{Q,n-1}}{2}\right\rvert$	$s_I(t)$
0	0	0	$d_{In}s_0(t-nT_S)$
0	0	1	$d_{In}s_1(t-nT_S)$
0	1	0	$d_{In}s_2(t-nT_S)$
0	1	1	$d_{In}s_3(t-nT_S)$
1	0	0	$d_{In}s_4(t-nT_S)$
1	0	1	$d_{In}s_5(t-nT_S)$
1	1	0	$d_{In}s_6(t-nT_S)$
1	1	1	$d_{In}s_7(t-nT_S)$

Table 2.2b. Mapping of Q-channel base-band signal during interval $nT_S \le t \le (n+1)T_S$. Reproduced from [7].

$\left\lvert \frac{d_{Qn} - d_{Q,n-1}}{2} \right\rvert$	$\left\lvert \frac{d_{In} - d_{I,n-1}}{2} \right\rvert$	$\left\lvert \frac{d_{I,n+1} - d_{In}}{2} \right\rvert$	$s_Q(t)$
0	0	0	$d_{Qn}s_0(t-nT_S)$
0	0	1	$d_{Qn}s_1(t-nT_S)$
0	1	0	$d_{Qn}s_2(t-nT_S)$
0	1	1	$d_{Qn}s_3(t-nT_S)$
1	0	0	$d_{Qn}s_4(t-nT_S)$
1	0	1	$d_{Qn}s_5(t-nT_S)$
1	1	0	$d_{Qn}s_6(t-nT_S)$
1	1	1	$d_{Qn}s_7(t-nT_S)$

where $D_{In}, D_{Qn} \in (0,1)$ and

$$\left.\begin{aligned} i &= I_3 \times 2^3 + I_2 \times 2^2 + I_1 \times 2^1 + I_0 2^0 \\ j &= Q_3 \times 2^3 + Q_2 \times 2^2 + Q_1 \times 2^1 + Q_0 2^0 \end{aligned}\right\}, \tag{2.12}$$

where i and j are binary-coded decimal (BCD) representations of the I-channel and Q-channel mapping signals where

$$\left.\begin{aligned} I_0 &= D_{Qn} \oplus D_{Q,n-1}, & Q_0 &= D_{I,n+1} \oplus D_{In} \\ I_1 &= D_{Q,n-1} \oplus D_{Q,n-2}, & Q_1 &= D_{In} \oplus D_{I,n-1} = I_2 \\ I_2 &= D_{In} \oplus D_{I,n-1}, & Q_2 &= D_{Qn} \oplus D_{Q,n-1} = I_0 \\ I_3 &= D_{In}, & Q_3 &= D_{Qn} \end{aligned}\right\}. \tag{2.13}$$

From (2.13), the I-channel and Q-channel base-band signals are each chosen from the set of 16 waveforms as dictated by the indices i and j [7]. Therefore, the new I-channel signal is $s_i(t)$ and the new Q-channel signal is $s_j(t)$. Fig. 2.13 plots various outputs within the transmitter starting with the bits from each channel, D_{In} and D_{Qn}, the

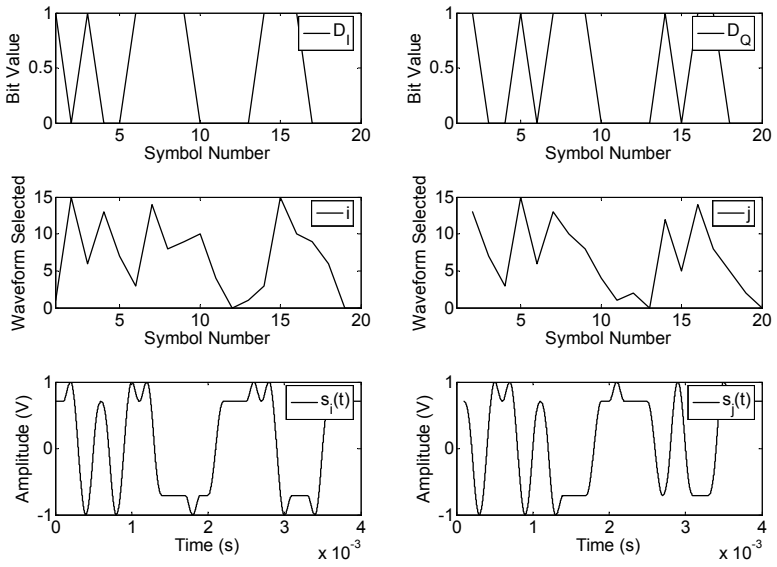

Fig. 2.13. I and Q-channel data bits, waveform selection indices, and pulse shaped I-channel and Q-channel over 20 symbols.

waveform mapping indices, i and j, and the new I-channel and Q-channel streams of pulse shaped data bits. The plots of Fig. 2.13 are 20 symbols long in duration. For example, look at Fig. 2.13: when $D_{In} = 1$ the index $i = 1$ and therefore $s_i(t) = s_1(t)$ for one symbol duration. Fig. 2.14 plots the EFQPSK transmitted signal, where the envelope appears constant but is deviating by a maximum of $0.28\ dB$. Note that the phase transition is slow enough that it is not noticeable. In other words, the phase transitions are continuous and not discrete. EFQPSK is actually a form of continuous-phase frequency shift keying (CPFSK) with minimum frequency deviation, because the transmitter architecture is OQPSK with sinusoidal pulse shaping [8].

Fig. 2.15 is a block diagram of an EFQPSK transmitter. From Fig. 2.15, i and j feed the read-only memory (ROM) blocks inside the waveform mapping block in Fig. 2.15. The details of the TCM and waveform mapping blocks of Fig. 2.15 are given in Fig. 2.16 and 2.17. The signals D_I and D_Q from Fig. 2.16 are equivalent to I and Q in Fig. 2.15. The ROM blocks of Fig. 2.17 store the 16 waveforms of EFQPSK.

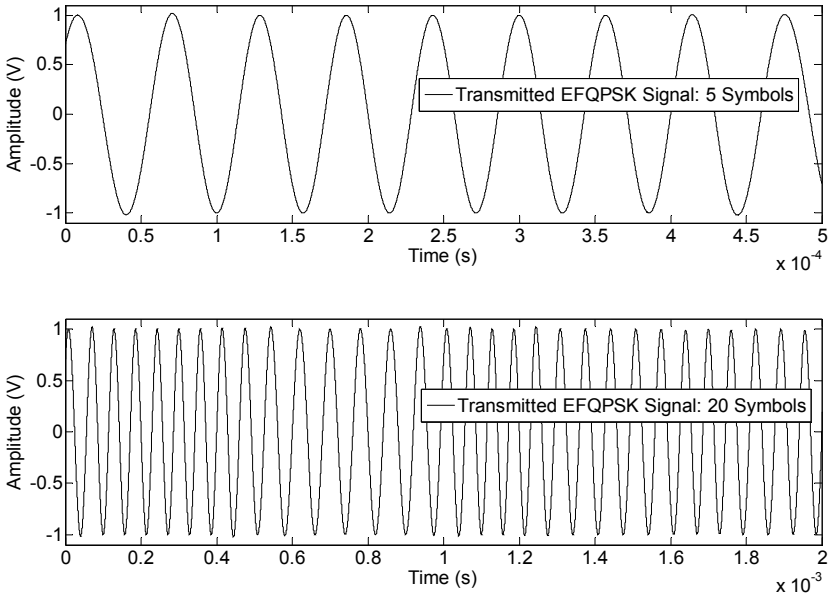

Fig. 2.14. Transmitted EFQPSK signal with 5 symbols and 20 symbols.

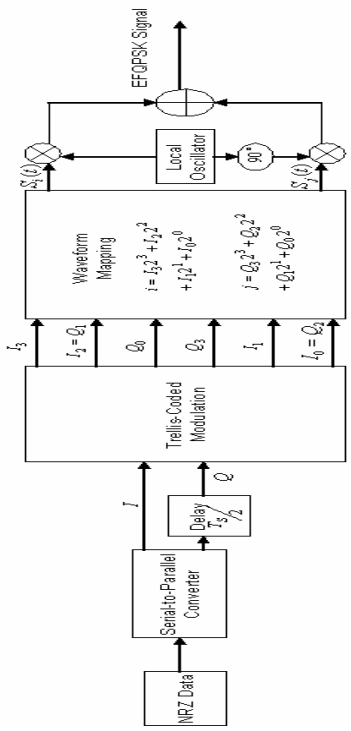

Fig. 2.15. Block Diagram of an EFQPSK Transmitter.

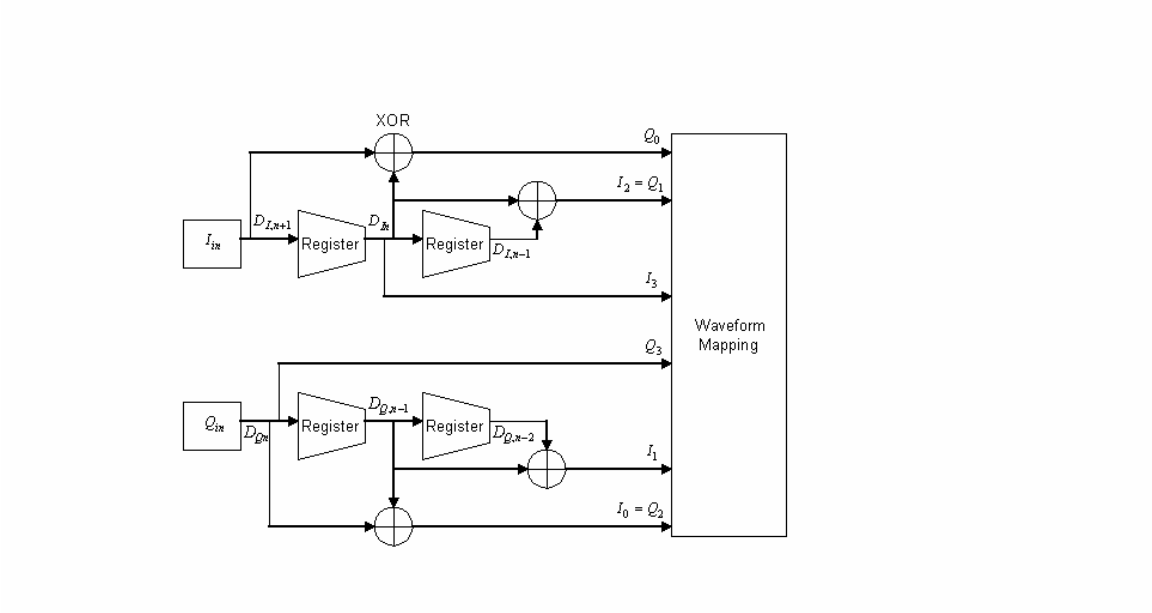

Fig. 2.16. TCM block from Fig. 2.15.

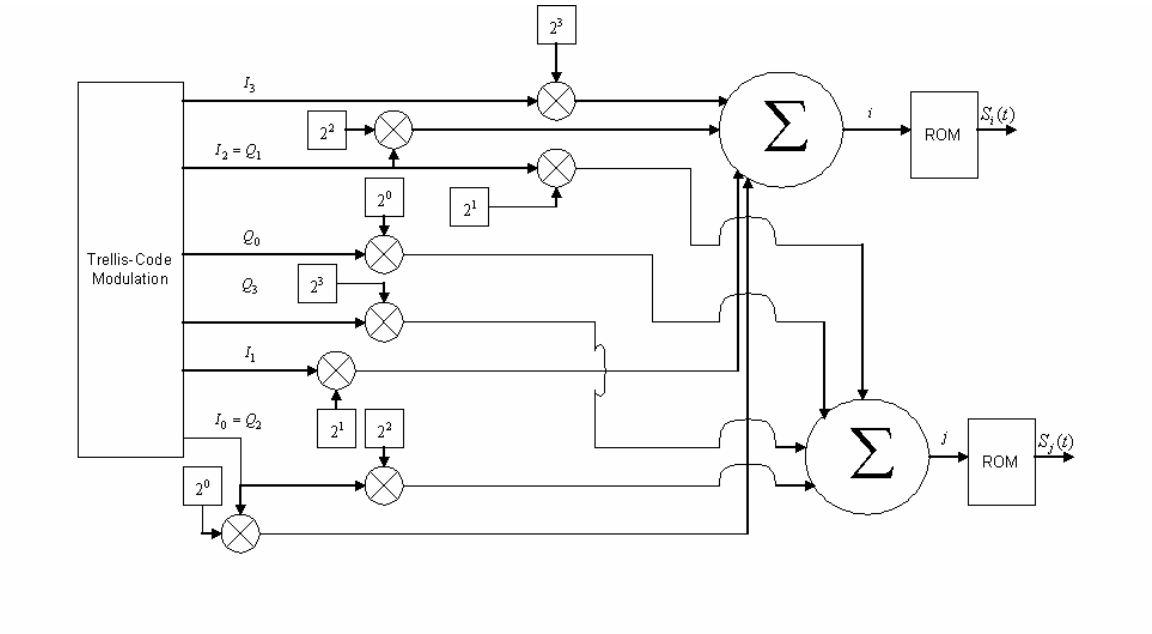

Fig. 2.17. Waveform mapping block of Fig. 2.15.

FQPSK is a modulation scheme that exhibits good spectral efficiency characteristics, is nearly constant envelope, and has tolerable BER. EFQPSK is the same as FQPSK except that 2 of the 8 waveforms in FQPSK are replaced for EFQPSK. From [7], the purpose of replacing 2 of the 8 waveforms is to eliminate the slope discontinuity inherent in 2 of the waveforms of FQPSK. Replacing 2 of these waveforms results in less spectral splatter in EFQPSK than FQPSK, because the derivative of anything discontinuous results in higher frequencies. The by-product of reducing the spectral splatter is a slight increase in maximum envelope fluctuation to about $0.28\ dB$. Fig. 2.18 compares the PSD of EFQPSK to that of FQPSK. Note that the side-band power in EFQPSK is almost $20\ dB$ less than that of FQPSK at higher frequencies. Substituting the EFQPSK modulation scheme for the FQPSK modulation scheme yields a 2 order of magnitude reduction in side-band energy with only a tenth of a magnitude increase in maximum envelope fluctuation. Fig. 2.19 shows the out-of-band power of EFQPSK compared to that of FQPSK. Note the out-of-band power of EFQPSK is about $20\ dB$ lower than that of FQPSK at higher bandwidths.

Thus far we have seen that EFQPSK exhibits better spectral efficiency than FQPSK in terms of PSD and out-of-band power. We have noted that the cost for increasing the spectral efficiency in EFQPSK is an $0.1\ dB$ increase in envelope fluctuation as opposed to FQPSK. The last major issue of concern in EFQPSK is BER. According to [7], substituting 2 of the waveforms in FQPSK with 2 improved waveforms, the spectral efficiency increases and the BER remains the same. In other words, the BER of EFQPSK is equivalent to the BER of FQPSK. To conclude, EFQPSK offers increased spectral efficiency over FQPSK, equivalent BER, and only a slight increase in envelope fluctuation.

2.6 Summary

Thus far in this study we have presented various modulation schemes that exhibit a multitude of both useful and degrading characteristics. The BER of QPSK is very good and has constant envelope while the spectral efficiency of it is poor.

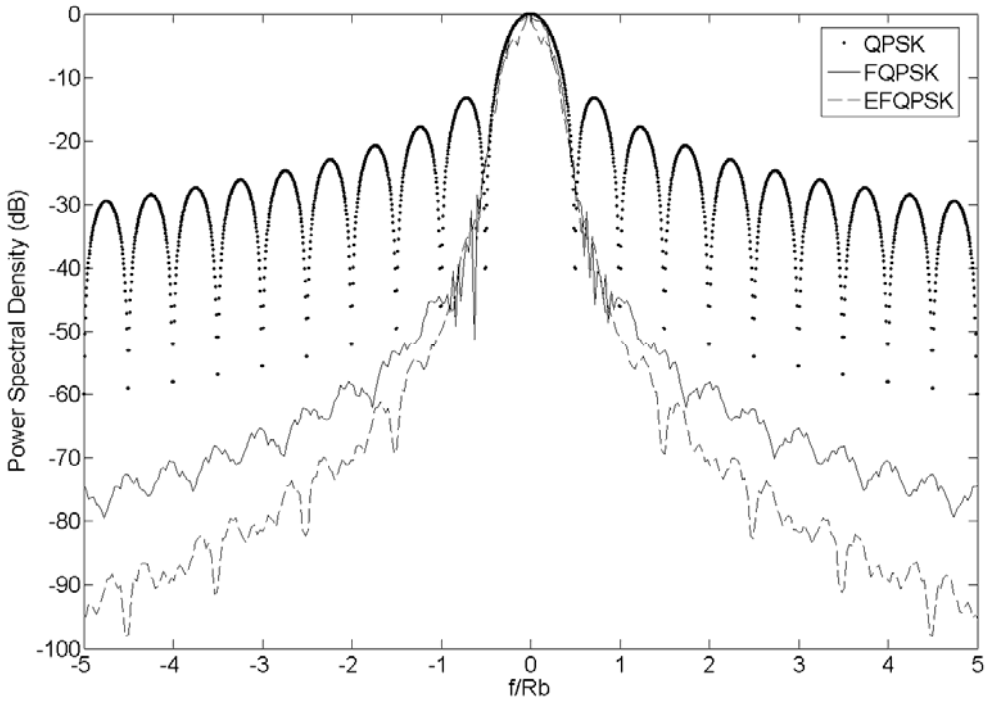

Fig 2.18. The PSD of EFQPSK compared to that of FQPSK.

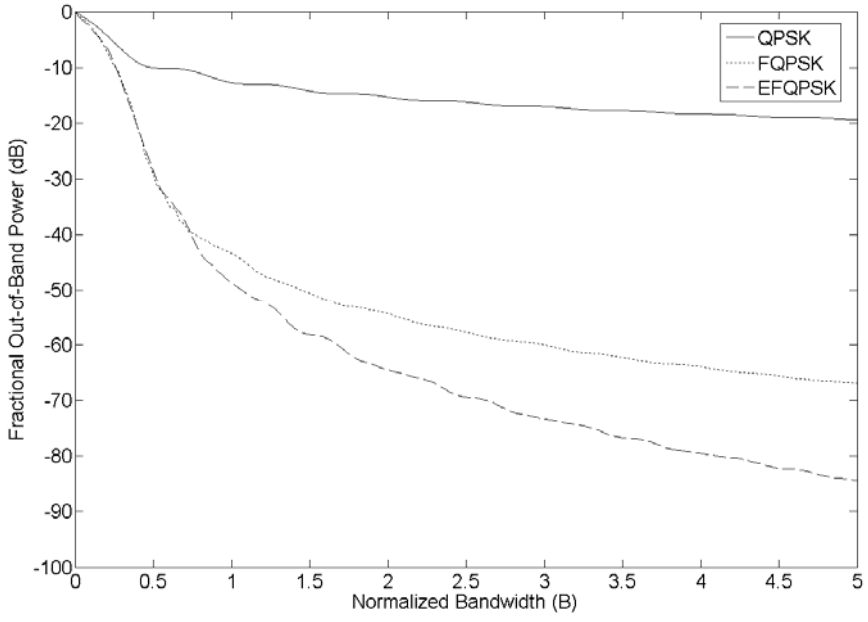

Fig 2.19. Out-of-band power of EFQPSK versus FQPSK.

One advantage OQPSK has over QPSK when hard-limiting the transmitted signal, no high frequency components are generated from the envelope crossing zero in the x-axis. The modulation scheme IJF-QPSK exhibits excellent spectral efficiency characteristics but does not have constant envelop. The modulation scheme FQPSK has good spectral efficiency characteristics and constant envelope with only a modest degradation in BER. Overall, EFQPSK is modulation scheme displays good spectral efficiency, “quasi” constant envelope, and tolerable BER.

Chapter 3: SYSTEM MODEL FOR DIGITAL EFQPSK

3.1 Introduction

In this chapter, we will outline in detail the system model used for this study. We will begin with a discussion about the fundamentals of analog-to-digital conversion (ADC). We will discuss in detail the fundamentals of the sampling operation, the quantization operation, and interpolation. Following the description of the ADC there will be an introduction to the type amplifier model used in this study. Section 3.4 will describe the type of receiver used in generating BER for EFQPSK.

3.2 Analog-to-Digital Conversion

This study was conducted to show the degradation of digital EFQPSK when compared to analog EFQPSK. Therefore a simple model of an analog-to-digital converter (ADC) will be presented.

The first operation performed in the ADC is the sampling operation. The sampled signal is expressed as

$$x(n) = X_a(nT) \qquad -\infty \le n \le \infty, \tag{3.1}$$

where X_a is the analog signal and T is the sampling period [9]. The type of sampling used in this study is uniform sampling, which takes an integer number of samples at uniformly spaced intervals within the analog signal. If X_a has period T_P, then $x(n)$ must have period $T < T_P$, which implies that at least two samples must be taken from X_a. For simplicity, we express the sampling period T as the number of samples taken, X. For the results of this study, the various cases taken were $X = \{3, 5, 10, 20, 50, 100\}$ samples each for the in-phase and quadrature phase channels. Fig. 3.1 shows the effect only the sampling operation has on a 10 symbol long sequence of EFQPSK pulse shaped bits of the in-phase channel. The x-axis of Fig. 3.1 shows the time duration of the 10 symbols. Note the sharp discontinuities in the 3-sample signal. The 10-sample signal appears to have no discontinuities. However, the results in Chapter 4 prove that the 10-sample signal has some discontinuities.

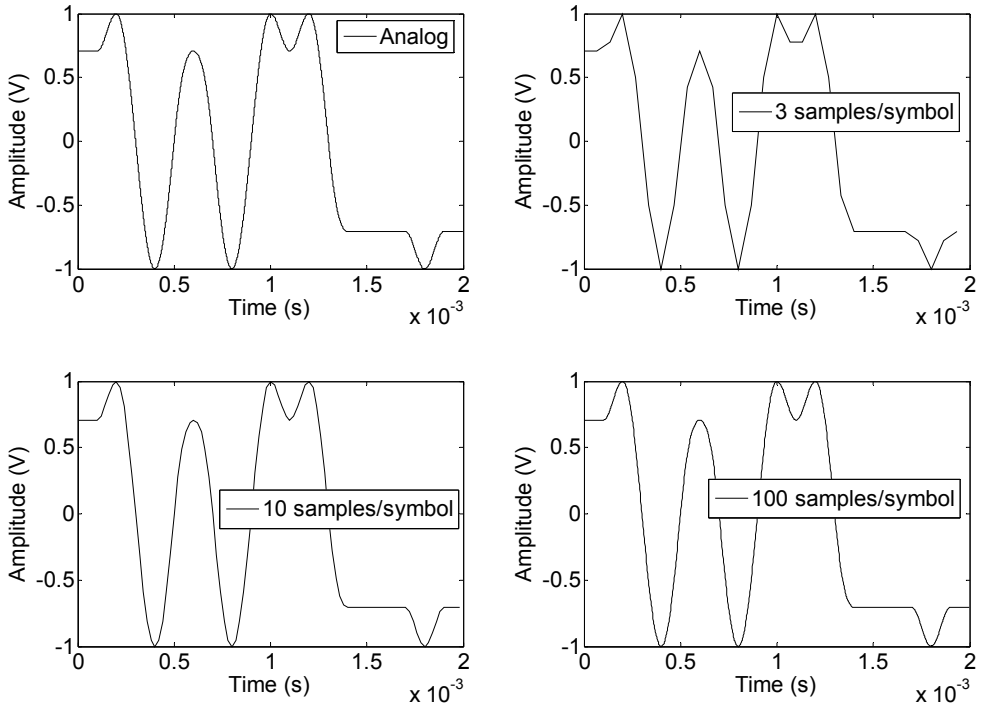

Fig. 3.1. The effect sampling has on the in-phase channel of an EFQPSK signal.

The 100-sample signal has no noticeable discontinuities and is a reasonable approximation to the analog signal. It should be noted that the resulting spectra of any signals with discontinuities has higher frequency components, thus increasing the bandwidth of these signals.

The next operation is the quantization operation. The effects of quantization on the signal may be studied by

$$\frac{S}{N_{avg}} = \frac{E[X_a{}^2]}{D} = \frac{\int_{-\infty}^{\infty} X_a{}^2 f_x(X_a)dx}{\sum_{k=1}^{n} \int_{X_{k-1}}^{X_k} (X_a - X_k)^2 f_x(X_a)dx}, \qquad (3.2)$$

where X_a is the analog signal, X_k is the discrete signal at time instant k, D is the distortion, and $f_x(X_a)$ is the probability density function (PDF) of X_a. For the results of this study uniform quantization is assumed and

$$f_x(X_a) = \begin{Bmatrix} \frac{1}{2^b}, & for & -\frac{V_{FS}}{2} \le X_a \le \frac{V_{FS}}{2} \\ 0, & for & else \end{Bmatrix}, \tag{3.3}$$

where b is the number of quantization bits and V_{FS} is the full scale signal voltage at the output of the ADC. In uniform quantization, a power of 2 integer number of quantization levels is utilized to map the analog voltages to a new voltage equal to the quantization levels. In this study, $x(n)$ from (3.1) replaces X_a in (3.2) and (3.3) and the new average signal-to-noise ratio is described by

$$\frac{S}{N}_{avg} = \frac{E[x(n)^2]}{D} = \frac{\int_{-\infty}^{\infty} x(n)^2 f_x(x(n))dx}{\sum_{k=1}^{n} \int_{X_{k-1}}^{X_k} (x(n) - X_k)^2 f_x(x(n))dx}, \tag{3.4}$$

where the PDF of $x(n)$ is still assumed to be uniform and is given by

$$f_x(x(n)) = \begin{Bmatrix} \frac{1}{2^b}, & for & -\frac{V_{FS}}{2} \le x(n) \le \frac{V_{FS}}{2} \\ 0, & for & else \end{Bmatrix}. \tag{3.5}$$

Fig. 3.2 shows the effect quantization has after the signal has been sampled. All signals in Fig. 3.2 have 4 quantization bits. The various sampling periods are the same as those in Fig. 3.1. Note that for the 3-sample plot the effects of quantization are not immediately evident because the quantization operation has few samples to distort. However, comparing Figs. 3.1 and 3.2, we can see that certain voltages in the 3-sample plot of Fig. 3.2 are different than corresponding voltages of Fig. 3.1. The quantization operation has distorted the original signals. Looking at Fig. 3.2 alone we see that for the 10 and 100 sample signals, the distortion from quantization has created sharp and jagged discontinuities in the waveforms. This is immediately evident because the quantization operation has many samples to distort. For example, if 20 samples are taken then the quantization operation has distorted a block of 20 samples, which is quite noticeable.

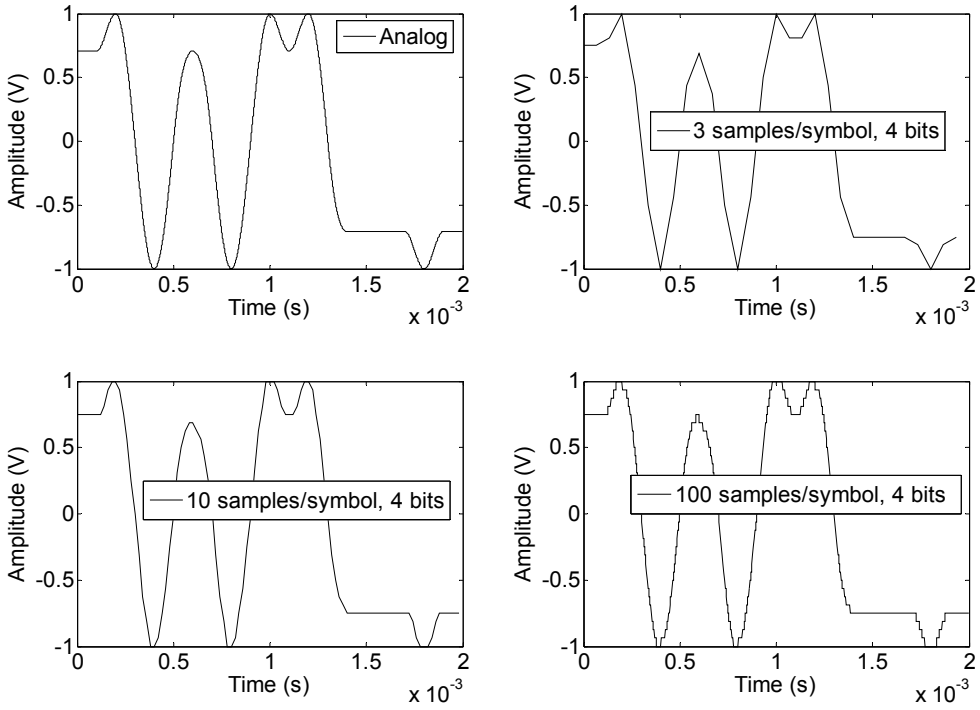

Fig. 3.2. The effect quantization after sampling has on the in-phase channel of an EFQPSK signal.

However, if 3 samples are taken then only a block of 3 samples is distorted from quantization, which may be less noticeable.

The final operation performed in this study's ADC is the interpolation operation. When a lower sampling frequency is used fewer samples are taken; therefore, the length of the discrete signal becomes shorter than the length for the analog signal. For example, when comparing the spectra of the sampled signals with the spectra of the analog signals, it is convenient to make the sampled signals long enough to allow a comparison between the two sets of signals, given a certain bandwidth of interest. If the sampled signals are not of sufficient length, then the corresponding spectrum will not be defined over the entire certain bandwidth of interest. If the sampled signal is not of sufficient length, then the corresponding spectrum of the sampled signal will not be defined over the entire bandwidth of interest. A zero-insertion interpolation was performed to achieve the aforementioned goal. This type of interpolation inserts zeros in between samples of a

signal and then low-pass filters the up-sampled signal [10]. Fig. 3.3 illustrates the effect interpolation has on the in-phase channel of a 10 symbol long EFQPSK signal. The software used for this operation requires a signal with a length of at least 9 samples for the signal to be interpolated. Because of this limitation, the only signals that are interpolated are signals whose length consists of 10, 20, and 50 samples. For the 100 sample signals, the lengths are sufficient to allow a comparison between the spectra of the 100 sample signals with the spectrum of the analog signal, given the bandwidth of interest. Note the discontinuities in the 10 and 20 sample signals of Fig. 3.3. These discontinuities exist at certain intervals in the interpolated waveforms. However, these discontinuities have a more degrading effect on the in-phase or quadrature-phase channel at the points of concatenation of one waveform to another waveform. This is because the interpolated value of the last sample in the previous waveform does not always equal the interpolated value of the first sample in the present waveform. The 50

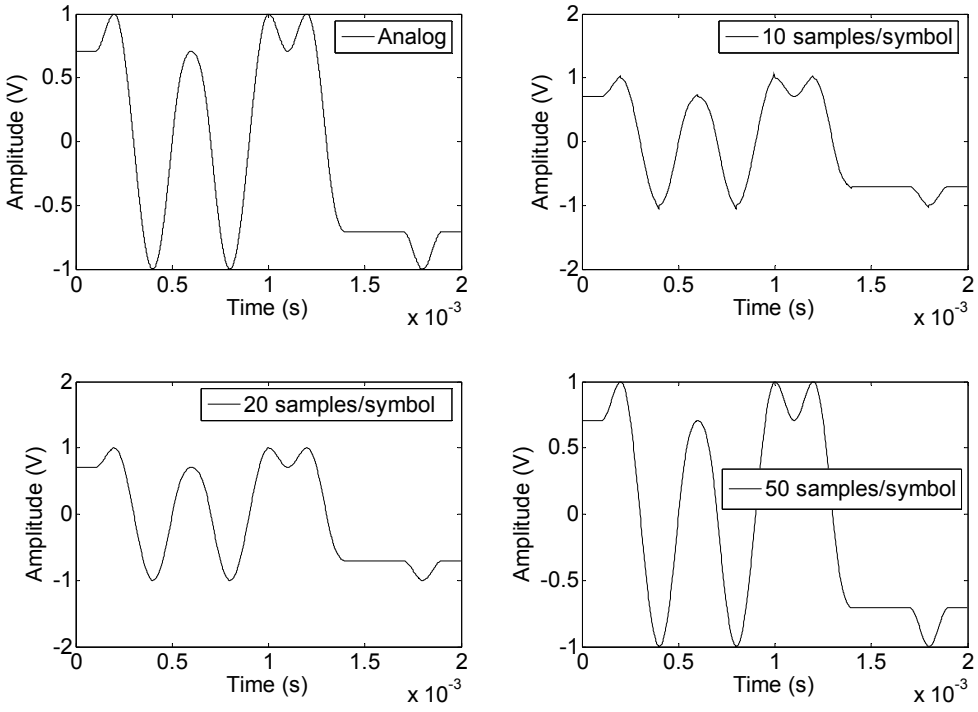

Fig. 3.3. The effect interpolation has on the in-phase channel of an EFQPSK signal.

sample signal has some discontinuities but with a lower magnitude than those of the 10 and 20 sample signals; which is why it is not evident that there are discontinuities in the 50-sample signal from Fig. 3.3. When taking samples of the analog signal X_a using (3.1), it is important to analyze the spectrum using

$$X(f) = F_S \sum_{k=-\infty}^{\infty} X_a[(f-k)F_S], \tag{3.4}$$

illustrating the periodicity of the digital signal's spectrum [9]. The variable F_S is the sampling frequency. The DFT of the sampled signal $x(n)$ in (3.1) is given by

$$X(f) = \sum_{n=-\infty}^{\infty} x(n)e^{-j2\pi fn}, \tag{3.5}$$

which suggests that the signal $x(n)$ is discrete and aperiodic [9]. Since the sampled signal is discrete and aperiodic its spectrum is continuous and periodic. From (3.4), if the sampling frequency is $F_S < 2N_q$, where N_q is the Nyquist frequency, the side-bands of one replicated adjacent spectrum of X_a will be added to the side-bands of the next adjacent replicated spectrum of X_a. However, if $F_S >> 2N_q$ then this problem is minor enough without much effect on the outcome of the spectrum. Figs. 3.4 and 3.5 illustrate the effect F_S has on the spectrum of $x(n)$. Figs. 3.4 and 3.5 are representations of a generic spectrum. If signals with spectra other than those shown in Figs. 3.4 and 3.5, F_S may have to be adjusted to achieve the same effects as those in Figs. 3.4 and 3.5. Note that if the signal is sampled with $F_S < 2N_q$, the side-bands interfere with each another as in Fig. 3.5. However, if the signal is sampled with $F_S >> 2N_q$ then the interference between the side-bands does not occur.

Chapter 4 deals with the spectrum of analog and digital EFQPSK. However, before presenting the results of Chapter 4 it is important to note that if the in-phase and quadrature-phase signals of EFQPSK are shaped from random data not independently and identically distributed, then spectrum of the EFQPSK signal will have a direct current (DC) term. This DC term will distort the spectrum, causing the corresponding side-band power to be larger in magnitude than the true spectrum of any version of EFQPSK. In other words, to witness the true spectrum of any version of EFQPSK we

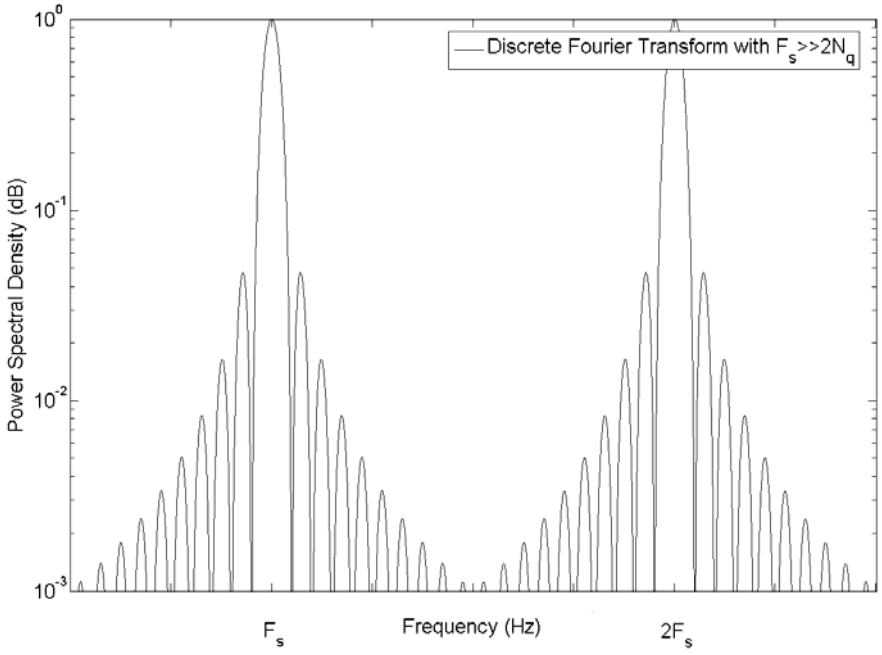

Fig. 3.4. DFT with $F_S >> 2N_q$.

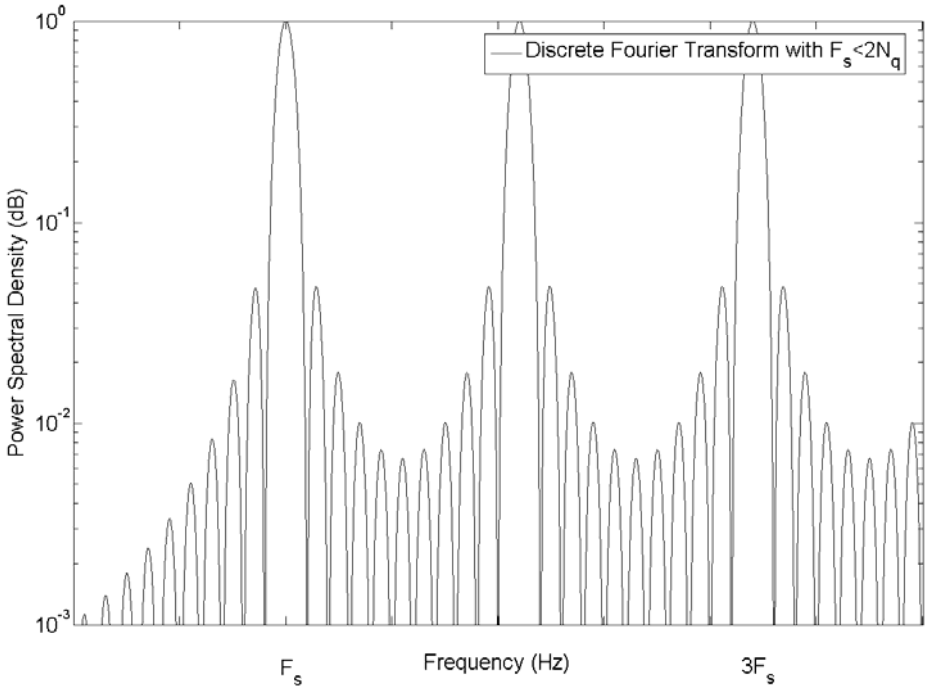

Fig. 3.5. DFT with $F_S < 2N_q$.

must ensure the correlation between the in-phase and quadrature-phase bits before pulse shaping is zero.

3.3 Limiter Model

To amplify the transmitted EFQPSK signal with an amplifier operating in saturation, which is the most efficient state in which the amplifier can operate, the waveforms of EFQPSK are tailored to produce an envelope that is almost constant. An amplifier operates in saturation in the following manner. If the magnitude of the input signal is larger than the magnitude of the of the amplifier's maximum output voltage,, then the amplifier rounds that input voltage to the maximum allowable voltage in the amplifier. In contrast, an ideal amplifier is an amplifier that clips or cuts off the maximum input voltage when that voltage exceeds the maximum allowable output voltage of the amplifier. A typical model of this type of amplifier is the hard limiter model, or clipper.

The model used for the amplifier in this thesis is the soft limiter model, which can be described by the function

$$y(t) = \frac{M \operatorname{sgn}(x(t))}{\left[1 + \left(m / |x(t)|\right)^{s}\right]^{1/s}}, \tag{3.6}$$

where m is the input limiting value, M is the output limiting value, $x(t)$ is the transmitted EFQPSK signal, and s is the shaping factor [11]. Fig. 3.6 plots (3.6) for various values of s. Comparing the plots for $s = 0.5$ and $s = 10$, we see that the plot for $s = 0.5$ corresponds to a harder limiter while the plot for $s = 10$ corresponds to a softer limiter. As s approaches ∞ the characteristic of the limiter becomes soft [11]. Therefore, the s selected for the model in this study is $s = 100$ because it is reasonably large compared to the soft limiting shaping parameter of $s = 10$. The input and output limiting voltages were both selected to be one since those are peak amplitudes of the envelope of conventional QPSK. In the remainder of this study, the term "amplification" will be used as a reference to non-linear amplification or soft limiting.

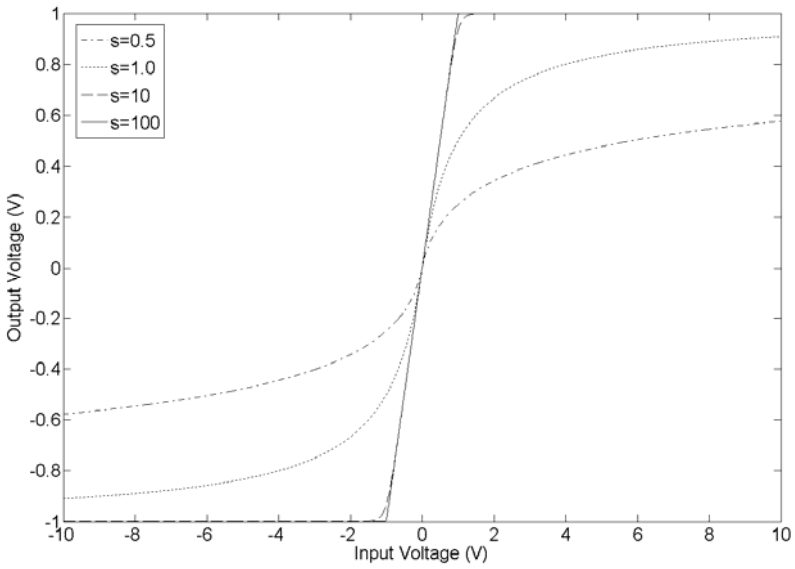

Fig. 3.6. Plot of the limiter model with various shaping parameters. Reproduced from [11].

Since our amplifier, or more equivalently soft limiter, is operating in saturation the amplitude modulation (AM) of the input may produce a change in AM in the output (AM/AM conversion). There is also a possibility that a change in the input signal's AM can create a change in phase modulation (PM) or phase drift in the output (AM/PM conversion) [12]. Suppose our complex envelope signal is described by

$$x(t) = A_x(t)e^{j\phi_x(t)}, \tag{3.7}$$

where $A_x(t)$ is the AM of the signal and $\phi_x(t)$ is the PM of the signal [12]. If the signal $x(t)$ is hard limited, then the output envelope will be

$$y(t) = g_A(A_x)e^{ig_\phi(A_x)}e^{j\phi(t)}, \tag{3.8}$$

where $g_A(\bullet)$ is the new AM and $g_\phi(\bullet)$ is the new PM [12]. Neither one of these two phenomena will exist if the envelope of the signal has no AM and continuous phase transitions, assuming we are operating in the linear portion of Fig. 3.6. Since the magnitude of AM in EFQPSK is only $0.28\ dB$ and with a continuous phase modulation scheme, we should expect that very little if any AM/AM conversion and AM/PM conversion will exist. However, when the magnitude of the input voltage is close to 1,

there will always be some AM/AM and AM/PM conversion because that part of the limiter is not linear. Fig. 3.7 illustrates the typical effect the soft limiter has on 10-sample EFQPSK signals with 2-bit and 14-bit quantization. Note that for the 14-bit quantization signal the top left AM/AM plot is almost linear and the top right AM/PM plot shows the same phase shape as that of a true 10-sample EFQPSK signal. The top right plot expresses some phase drift. The bottom 2 plots show a 10-sample EFQPSK signal with 2-bit quantization. Note that the bottom left AM/AM plot is not close to linear at higher voltages. The bottom right AM/PM plot expresses some phase drift. Note that for the 2-bit quantization case, the envelope is far from constant.

Fig. 3.8 shows typical AM/AM and AM/PM characteristics of 20-sample EFQPSK signals with 2-bit and 14-bit quantization. For both the 2-bit and 14-bit quantization signals, the non-constant envelopes coupled with the non-linear portions of the limiter have significantly changed both the output voltage and output phase of the EFQPSK signals.

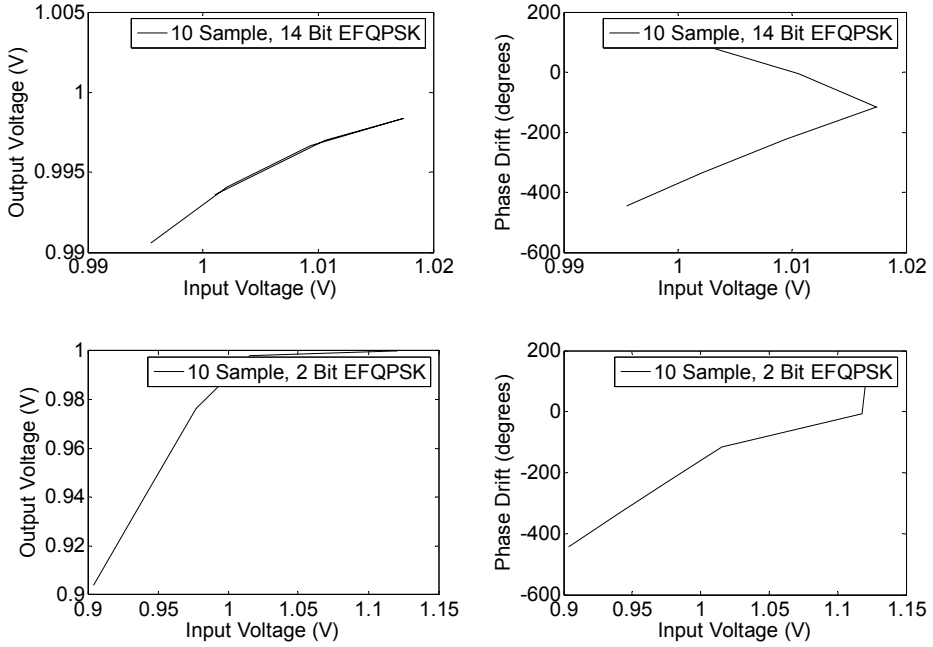

Fig. 3.7. Typical AM/AM and AM/PM conversion characteristics of 10-sample EFQPSK signals with 2-bit and 14-bit quantization.

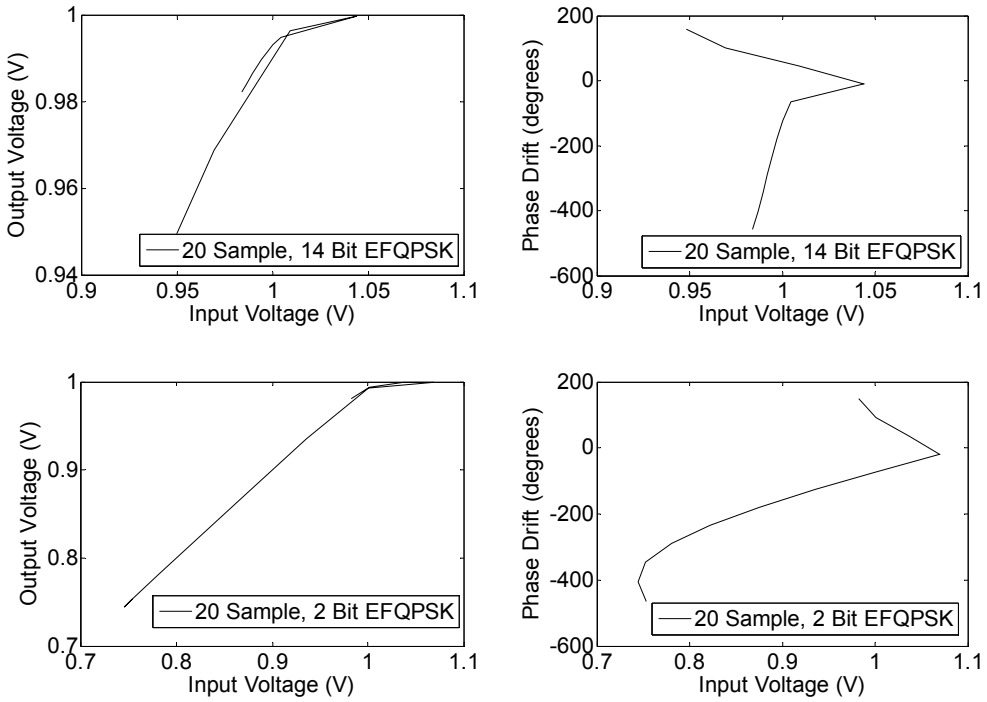

Fig. 3.8. Typical AM/AM and AM/PM conversion characteristics of 20-sample EFQPSK signals with 2-bit and 14-bit quantization.

Fig. 3.9 shows typical AM/AM and AM/PM characteristics of 50-sample EFQPSK signals with 2-bit and 14-bit quantization. The envelope of the 14-bit quantization signal does not fluctuate as much as those for the 10-sample and 20-sample signals, which is why the output voltage is almost linearly proportional to the input voltage. For this same reason, the output phase does not jitter as much as the sample signals' phases.. The amount of phase jitter describes how suddenly the phase jumps from one value to another. For the 50-sample, 2-bit quantization signal the output voltage is no longer linearly proportional to the input voltage and the phase jitter is unpredictable. Both of these characteristics are due to the ample envelope fluctuation of this particular signal.

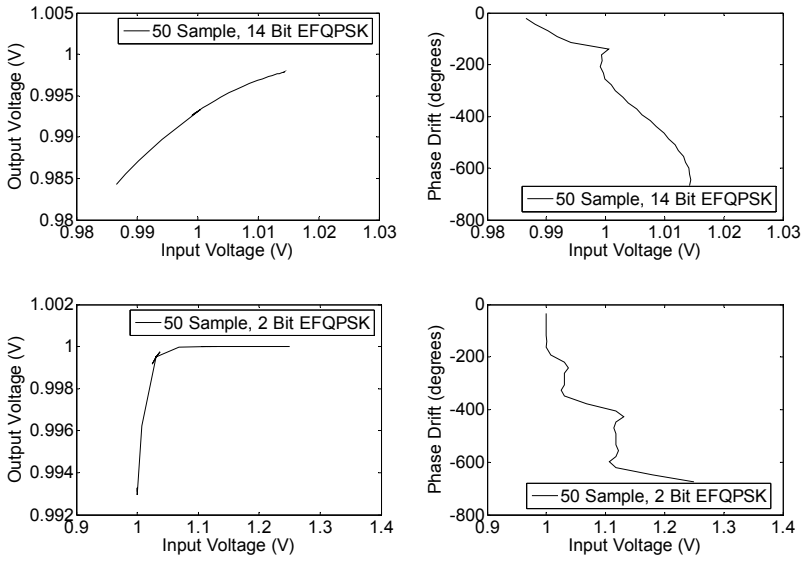

Fig. 3.9. Typical AM/AM and AM/PM conversion characteristics of 50-sample EFQPSK signals with 2-bit and 14-bit quantization.

Fig. 3.10 shows typical AM/AM and AM/PM characteristics of 100-sample EFQPSK signals with 2-bit and 14-bit quantization. Looking at the 14-bit quantization signal, we see that the relationship between the input voltage and the output voltage is idenitical to the shaping parameter $s = 100$ from Fig. 3.6. Looking at the top right AM/PM plot, we see no phase jitter. Both phenomena are due to very little envelope fluctuation in this signal. The 2-bit quantization signal of Fig. 3.10 expresses a linear relationship between the input voltage and the output voltage inside the maximum voltage range. However, outside of this range, i.e. $1.2\ V$, we notice a large amount of AM/AM conversion. Looking at the bottom right AM/PM, we see a considerable amount of phase jitter. These two characteristics are due to the large amount of envelope fluctuation in this signal.

Fig. 3.11 shows typical AM/AM and AM/PM characteristics of an analog EFQPSK signal. Note that the left AM/AM plot takes the shape of the shaping parameter $s = 100$ from Fig. 3.6. In the right plot we see no phase jitter. Both of these results are due to the fact that there is only $0.28\ dB$ of envelope fluctuation in the signal. It should be noted that the 100-sample, 14-bit quantization signal has almost the same envelope fluctuation as the analog signal, which is why the plots of Figs. 3.10 and 3.11 appear similar.

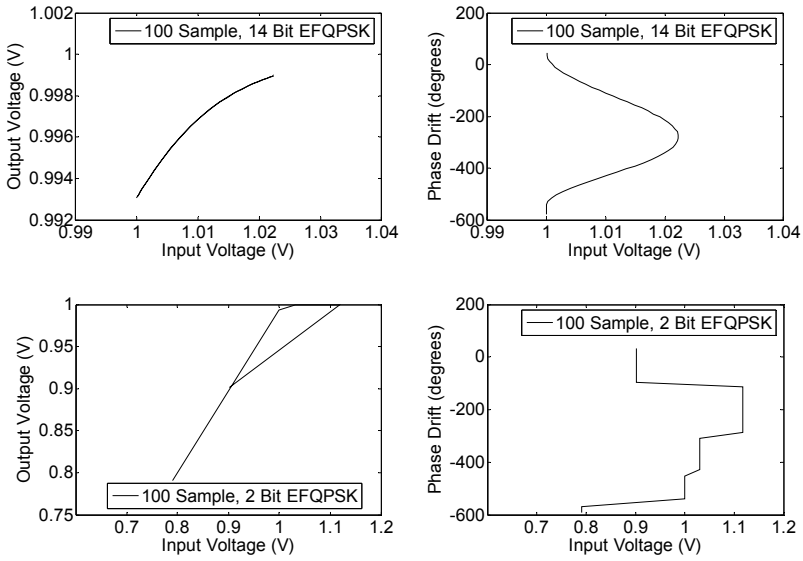

Fig. 3.10. Typical AM/AM and AM/PM conversion characteristics of 100-sample EFQPSK signals with 2-bit and 14-bit quantization.

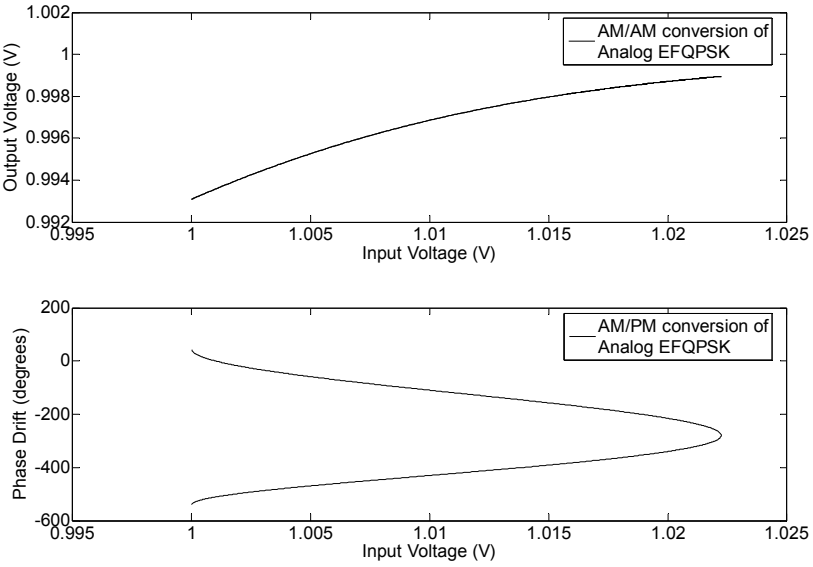

Fig. 3.11. Typical AM/AM and AM/PM conversion characteristics of an analog EFQPSK signal.

3.4 Reception

Although a conventional OQPSK receiver can be used to retrieve data from a transmitted EFQPSK signal, this is not an optimal choice for reception due to lower quality BER than in an average matched filter receiver of EFQPSK [2]. Since EFQPSK can be implemented with TCM, it can also be received using a Viterbi receiver [7]. However, while the Viterbi receiver of EFQPSK is the optimal receiver in terms of BER it is not the best choice for the model in this study because its computational complexity is large. Therefore, this study uses the average matched filter receiver of EFQPSK for better BER and smaller computational complexity. Before discussing a specific matched filter receiver of EFQPSK, we present the fundamental architecture of a matched filter receiver.

A matched filter is one in which the impulse response is given by

$$h(t) = s(T - t), \tag{3.9}$$

where $s(t)$ is the input signal after demodulation and low-pass filtering defined over the interval $0 \le t \le T$ [13]. When the signal $s(t)$ passes through the filter in (3.9), the response is given by

$$y(t) = \int_0^t s(\tau)s(T - t + \tau)d\tau, \tag{3.10}$$

which is basically the autocorrelation function of $s(t)$ [13]. There is an important property that makes this matched filter tremendously useful and is stated as follows: if the signal $s(t)$ is corrupted by additive white Gaussian noise (AWGN) and if the impulse response of the filter in (3.9) matches the signal $s(t)$, then the filter maximizes the signal-to-noise ratio [13]. Another important property of this filter is that it depends only on the energy of the signal $s(t)$, not on other any characteristics of $s(t)$ [13]. Fig. 3.12 is a block diagram of an average matched filter receiver of EFQPSK. The term “average matched filter” describes a matched filter that matches the incoming signal, $s(t)$, with the average shape of that signal. More will be said about this shortly. The variable $r_c(t)$ in

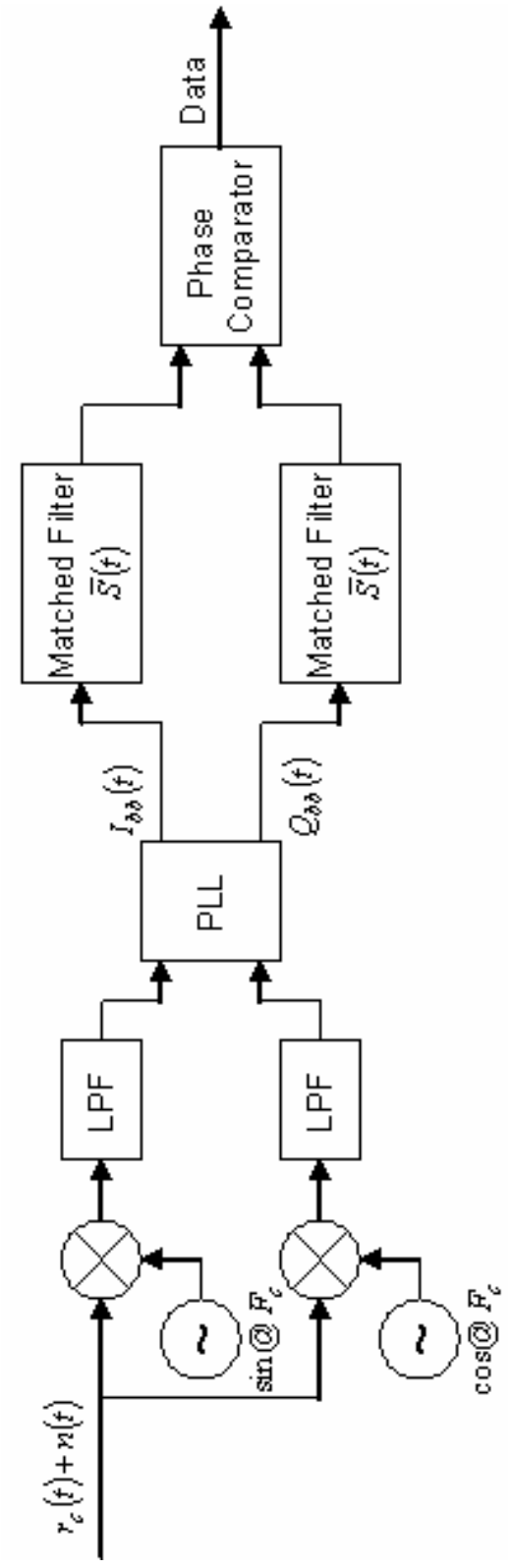

Fig. 3.12. Block diagram of an average matched filter receiver of EFQPSK.

Fig. 3.12 is the transmitted EFQPSK signal with carrier frequency F_c, and $n(t)$ is AWGN. The variables $I_{bb}(t)$ and $Q_{bb}(t)$ in Fig. 3.12 are the base-band in-phase and quadrature-phase bits, respectively. In this study for analog EFQPSK the results are analytical, taken from [14], while the results for digital EFQPSK are semi-analytical because the equations in [14] are digitized and simulated in software. From [14],

$$P_{si}(E) = \frac{1}{2} erfc\left(\sqrt{\frac{\overline{E}_b C_{S\overline{S}}}{\overline{E} N_0 \; E_{\overline{S}} / T_S}}\right), \tag{3.11}$$

and

$$P_S(E) = \frac{1}{8}\sum_{i=0}^{7} P_{si}(E) \tag{3.12}$$

where $\overline{E} = \frac{1}{8}\sum_{i=0}^{7} E_i$, where $E_i = \int_0^{T_S} S_i^2(t)dt$, $C_{S\overline{S}} = \left(\frac{1}{T_S}\int_0^{T_S} S_i(t)\overline{S}(t)dt\right)^2$, and $E_{\overline{S}} = \int_0^{T_S} \overline{S}^2(t)dt$, the BER of analog EFQPSK is obtained as in [14]. The variable $C_{S\overline{S}}$ in (3.11) is the product after the correlation between the received signal and average matched filter signal. For QPSK, the average matched filter signal is one (rectangular pulse shaping), and the correlations of each of the waveforms in $S_i(t)$ are simply the integral of $S_i(t)$ over one symbol period divided by the symbol period T_S. For an average matched filter receiver of EFQPSK, $\overline{S}(t)$ is the average pulse shape of EFQPSK. The correlations for each of the waveforms in an average matched filter receiver of EFQPSK are larger in magnitude than the correlations of a QPSK receiver of EFQPSK because in

$$\overline{S}(t) = \frac{1}{2}[(1+A) + (1+A)\sin(\pi t / T_S) - (1-A)\cos^2(\pi t / T_S)], \tag{3.13}$$

where $A = 1/\sqrt{2}$, the magnitude of (3.13) is larger than the magnitude of a one for rectangular pulse shaping in QPSK. This produces a superior BER since the magnitude inside $erfc$ in (3.11) is larger for an average matched filter receiver of EFQPSK than it is for a QPSK receiver of EFQPSK.

3.5 Summary

Thus far we have explained the main blocks used in the system model of this study. We started with the corrupting effects analog-to-digital conversion has on the resulting signals. Next we laid the foundation of the soft limiter model used in this study and discussed the effects soft-limiting can have on the transmitted signal. Finally, we described the type of receiver used in generating BER for EFQPSK with a presentation of typical receiver structures of an average matched filter receiver of EFQPSK and the corresponding P_e derivations for this receiver.

Chapter 4: SIMULATION RESULTS FOR DIGITAL EFQPSK

4.1 Power Spectral Density (PSD) for Digital EFQPSK

This chapter focuses on comparing the PSD, out-of-band power, envelope fluctuation, and BER of digital EFQPSK to those of analog EFQPSK and QPSK. More specifically, we consider 3, 5, 10, 20, 50, and 100 sample EFQPSK signals with varying quantization bits. Note that in several cases, we did not present the 3-sample and 5-sample signals because these signals are not of sufficient length for comparison to analog EFQPSK or QPSK.

In this study, the 10, 20, 50, and 100-sample signals satisfy Nyquist's theorem. However, for practical purposes, we limit the duration of the discrete sequence $x(n)$ to L samples, where $x(n)$ contains samples in the interval $0 \le n \le L-1$ [12]. This operation is equivalent to multiplying the discrete sequence $x(n)$ by a rectangular window $w(n)$ of length L where

$$w(n) = \begin{cases} 1, & 0 \le n \le L-1 \\ 0, & else \end{cases}, \tag{4.1}$$

creating a new sequence

$$\hat{x}(n) = x(n)w(n)\,. \tag{4.2}$$

Assuming $x(n)$ is a sequence of EFQPSK pulse shaped bits, the Fourier transform of $w(n)$ is given by

$$W(\omega) = \frac{\sin\left(\omega L/2\right)}{\sin\left(\omega/2\right)} e^{-j\omega(L-1)/2} \tag{4.3}$$

and the Fourier transform of $x(n)$ is given by

$$\hat{X}(\omega) = \frac{1}{2\pi}\int_{-\pi}^{\pi} X(\theta)W(\omega-\theta)d\theta\,. \tag{4.4}$$

Finally, the DFT of the windowed sequence $\hat{x}(n)$ is a sampled version of $X(\omega)$ and is given by

$$\hat{X}(k) = \hat{X}(\omega)\Big|_{\omega=2\pi k/N} = \frac{1}{2\pi}\int_{-\pi}^{\pi} X(\theta)W\left(\frac{2\pi k}{N}-\theta\right)d\theta \qquad k = 0,\ 1,...,\ N-1\,, \tag{4.5}$$

where N is the number of points in the DFT [12]. Fig. 4.1 illustrates how windowing the sequence $x(n)$ creates spectral leakage. The signals presented are for conventional QPSK, analog EFQPSK, and 10, 20, 50, and 100-sample versions of EFQPSK. The 10-sample EFQPSK signal is windowed with a window of length $L=10$. The spectrum of the 10-sample signal has reduced resolution and the spectrum of this signal has retained many of the characteristics of the spectrum of $w(n)$. This leakage characterizes how much power in the original sampled sequence $x(n)$ has been spread out by windowing. The 20-sample signal retains many of the spectral characteristics of the window, but the leakage is not as prominent as that of the 10-sample signal. The 50-sample signal retains some of the characteristics of the spectrum of the window, but leakage is not as prominent. For the 50-sample signal, the spectral resolution is increased. The 100-sample signal is windowed by a window of length 100 and therefore there appears to be no spectral leakage and the 100-sample signals converges to the analog signal. Therefore, as the length of $w(n)$ and $x(n)$ increases, the amount of spectral leakage decreases and the spectral resolution increases. The x-axis of all spectral plots in this study characterizes the total bit rate for a QPSK signal. For instance, at $f/R_b = 1$, the frequency is $f = 2/T_b$.

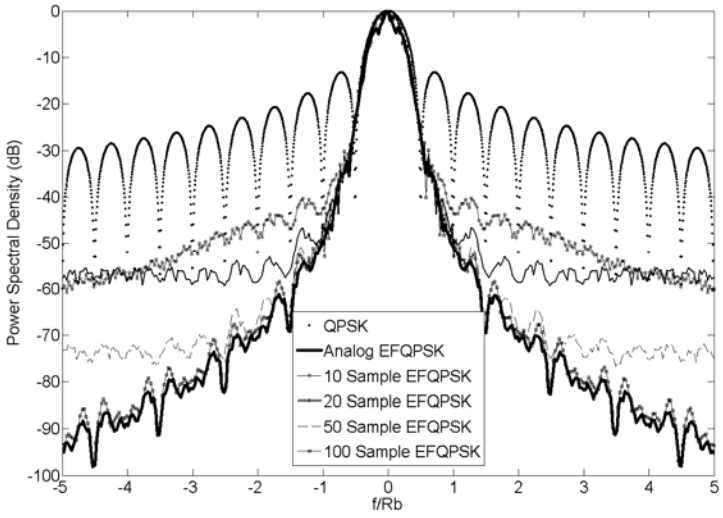

Fig. 4.1. Illustration of spectral leakage in discrete EFQPSK.

Section 4.1 focuses on comparing sample signals with varying quantization bits to analog EFQPSK and QPSK. Fig. 4.2 shows the effect that a 10-sample EFQPSK signal with varying quantization bits has on the power spectrum compared to the spectrum of analog EFQPSK. For the results in this study, the base-band bandwidth for pulse-shaping was selected to be $2.5\ kHz$, the bit period is $4\times10^{-4}\ s$, and the Nyquist frequency is $5\ kHz$. According to [13], a signal must be sampled at a minimum of twice the Nyquist frequency (N_q) to reconstruct a band-limited waveform without error. Since the 10 sample EFQPSK spectra in Fig. 4.1 have a sampling interval of $T=4\times10^{-5}\ s$ the signals are sampled at $F_S=5N_q$, where F_S is the sampling rate. Therefore, the highest frequency that can be reconstructed without error is $F_S/2=12.5\ kHz$. Since the range of frequencies shown in Fig. 4.2 is $-12.5kHz\le {}^{f}\!/_{R_b}\le 12.5kHz$, the aliasing of the 2.5 kHz is present at ${}^{f}\!/_{R_b}\ge 5$ in Fig. 4.2. Therefore, only two factors contribute to the degradation of the digital spectra compared to the analog spectrum: the quantization operation, which will be discussed shortly; and the other is in taking the discrete Fourier transform (DFT). Since $x(n)$ from (3.1) is discrete and aperiodic, the DFT can be expressed as

$$X(\omega)=\sum_{n=-\infty}^{\infty}x(n)e^{-j\omega n}\ , \qquad (4.6)$$

and $X(\omega)$ is the DFT of $x(n)$ [12]. The DFT takes a finite discrete sequence, $x(n)$, and transforms this sequence into a sequence of frequency samples, $X(k)$ [12]. In other words, the DFT takes the sampled spectrum and replicates it at intervals equal to the inverse of the sampling interval used with the original analog waveforms. Looking at ${}^{f}\!/_{R_b}\approx 0.7$, we see that all the 10-sample spectra start to deviate from the analog EFQPSK spectrum. As stated previously, the sampling period of the 10-sample signal is $T=4\times10^{-5}\ s$, which is of relatively long duration. Due to a long duration in the time domain this interval is short in the frequency domain. This means that the corresponding spectra of the 10-sample signal will be closely spaced in the frequency domain. In other words, some of the side-lobes of the 10-sample spectra will be bunched together with side-lobes of other replicated 10-sample spectra. This is an expected artifact from taking the DFT of a signal with such a large sampling interval. There is limit as to how good the

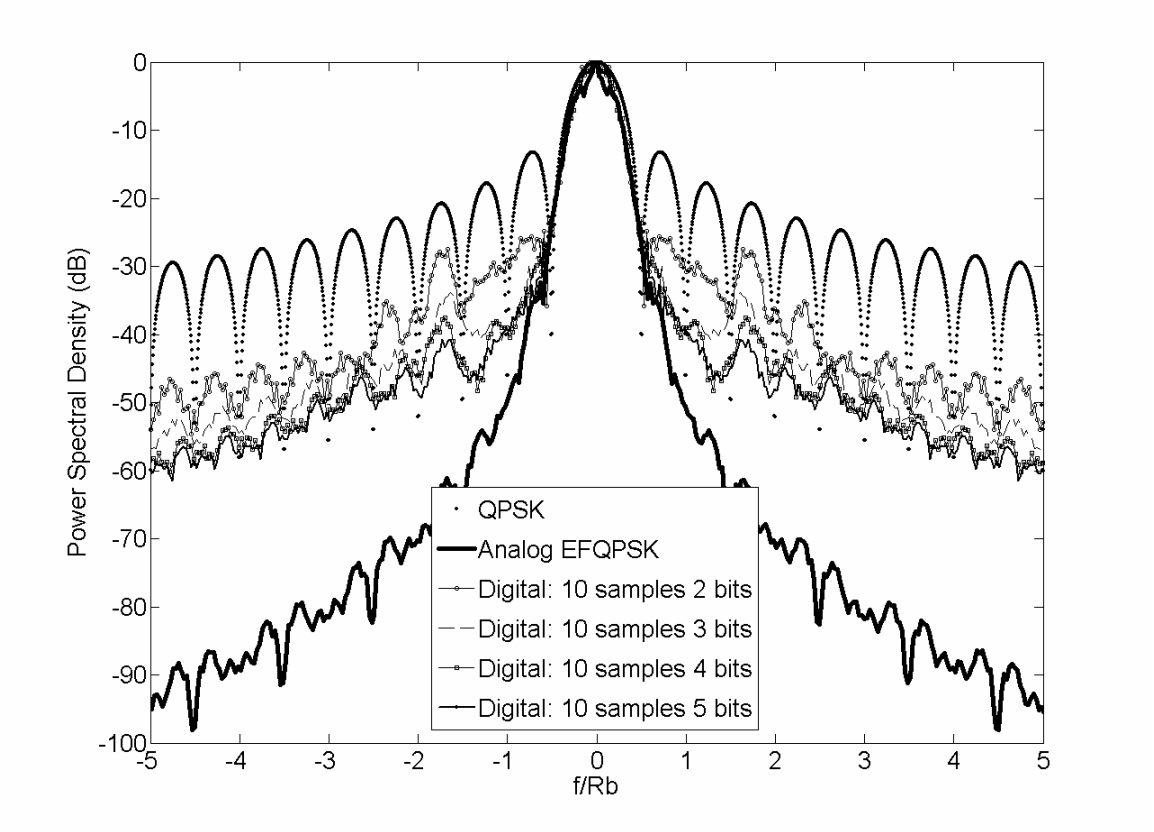

Fig. 4.2. The effect a 10-sample EFQPSK signal with various quantization bits has on the spectrum of EFQPSK.

spectral efficiency of the 10-sample signal can become. This limit is dictated by the artifact of taking the DFT of the 10-sample signal. Since there are so many side-lobes with high power, packed closely together over the frequency range $-12.5kHz \le {}^{f}\!/_{R_b} \le 12.5kHz$, the spectra of the 10-sample signals will never be as good as that of analog EFQPSK. Hence, this study will refer to this as spectral leakage. The spectral leakage of the 10-sample signal is high for two reasons: a) in taking the DFT, the side-lobes of one replica of the spectrum are added, or more appropriately, interfere with the side-lobes of another replica of the spectrum; and, b) the side-lobes that interfere with one another are high in power, leaving the power in the side-lobes especially high compared to the side-lobes of analog EFQPSK.

From Fig. 4.2, there are four cases of the 10-sample EFQPSK power spectrum: 2-bit, 3-bit, 4-bit, and, 5-bit quantization signals. From [12], the signal-to-quantization noise ratio is

$$SQNR(dB) = 1.25 + 6.02b\,, \tag{4.7}$$

where b is the number of quantization bits. According to (4.7), for a 2-bit quantization case, the SQNR (dB) is $13.8\ dB$. Since $13.8\ dB$ from quantization is much higher than the power in the spectral leakage, the distortion from 2-bit quantization in the 10-sample case is quite noticeable. The 2-bit quantization only distorts the spectrum at instances where side- lobes interfere with one another, as seen in Fig. 4.2. This is because the distortion brought on by quantization changes the shapes of the interfering side-lobes. Since the SQNR is 13.8 dB, which is low for quantization, the distortion swells the spectral content of the extra side-lobes that are packed tightly together.

Looking at Fig. 4.2, the other cases show that the interfering side-lobes do not swell as much as the 2-bit case. The SQNR's of the 3-bit, 4-bit, and 5-bit cases are $19.8\ dB$, $25.8\ dB$, and $31.8\ dB$, respectively. As the number of quantization bits increases the side-band power decreases with each respective case. This is because as the distortion becomes smaller and smaller, it will have a much lower effect on the shape of the spectra. In other words, as the distortion approaches zero so does the the spectra as it changes shape.

Fig. 4.3 illustrates the effect a high number of quantization bits has on the spectrum of a 10-sample EFQPSK signal. Looking at Fig. 4.3, we notice that the 6-bit quantization and 14-bit quantization cases are similar. The SQNR for the 6-bit case is $\sim 37.9\ dB$, and for the 14-bit case it is

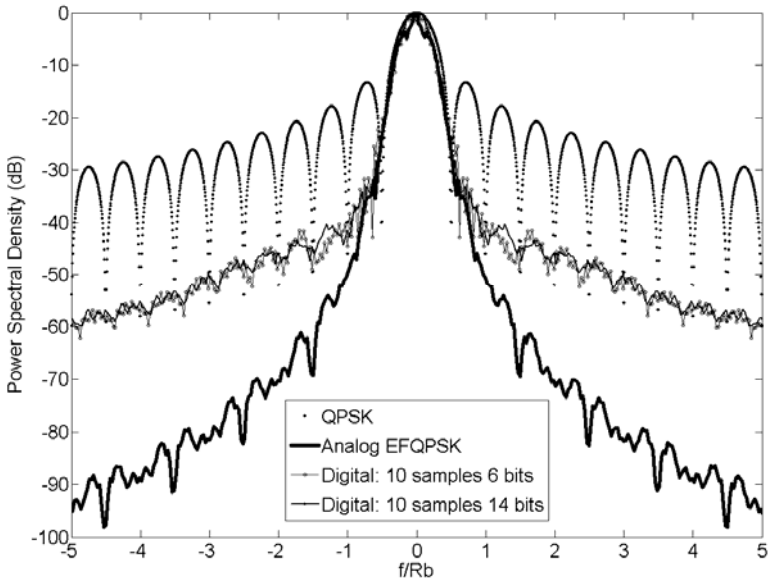

Fig. 4.3. The effect quantization with a higher number of bits has on a 10-sample EFQPSK signal.

$\sim 86\ dB$. The fact that there is a large difference between these two values is irrelevant because when 6 or more bits are used for quantization, the corresponding SQNRs fall at or below the power in spectral leakage. Once the SQNRs fall below the power in the spectral leakage, there is no longer any effect on changing the spectra since the power in the spectral leakage dominates all else in the system. Comparing Figs. 4.2 and 4.3, we notice that the 10- sample EFQPSK signal no longer exhibits a reduction in side-band power, as a moderate-to-high number of quantization bits are utilized. Once a 6-bit quantization is used, the spectrum of the 10-sample signal has converged to its best spectral state. Although it is obvious that quantization with 14 bits produces a much better effect on a signal in general, for the 10-sample case quantization with more than six bits is not advantageous when trying to reduce the side-band power because the power in the spectral leakage has a more dominant effect on the spectrum than does quantization.

Fig. 4.4 illustrates the effect a low-to-moderate number of quantization bits have on the spectrum of a 20-sample EFQPSK signal. The sampling interval for this signal is one-half of the 10-sample signal, and is $T = 2 \times 10^{-5}\ s$.

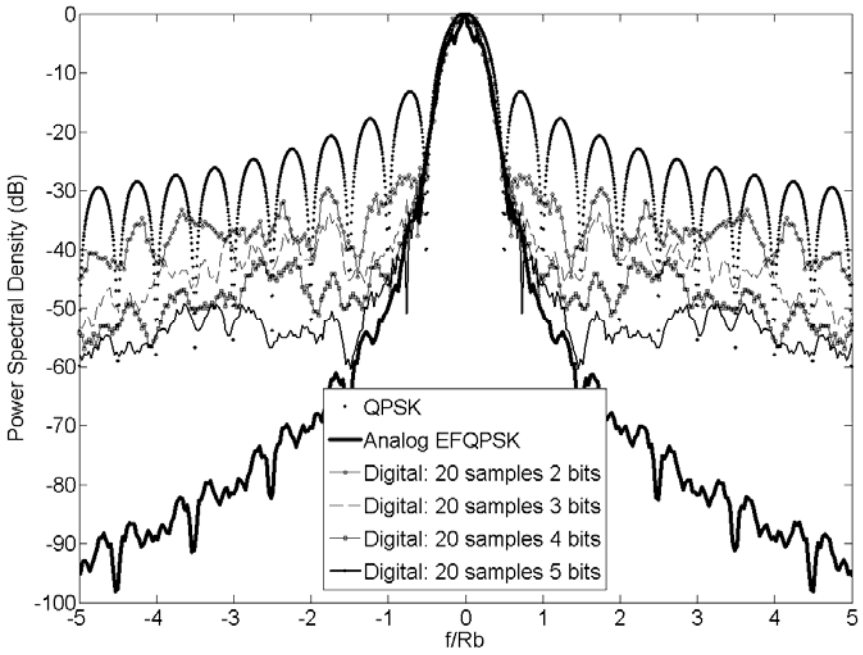

Fig. 4.4. The effect quantization with a low number of bits has on a 20-sample EFQPSK signal.

This is a shorter sampling interval than that of the 10-sample signal and we should expect the period of the spectrum to be twice that of the 10-sample spectrum. The sampling frequency of this signal is $F_S = 10N_q$ and the highest represented frequency without error is $25\ kHz$. Therefore, there is no aliasing present in Fig. 4.3. Only two reasons exist for the degradation of the digital EFQPSK spectra: the quantization operation and the artifact from taking the DFT. In Fig. 4.4, there are four cases of digital EFQPSK spectra: 2-bit, 3-bit, 4-bit, and 5-bit quantization cases. The SQNRs are the same for the 20-sample cases as in the 10-sample cases. Comparing Figs. 4.2 and 4.4, we notice that as the number of quantization bits increases, the degradation of spectra decreases. While evident for the 10-sample cases, in the 20-sample cases as each bit is added to quantization the roll-off rate becomes higher than that of the 10-sample cases. This is because in taking the DFT of the 20-sample cases, the side-lobes that are bunched together from replicas of the spectrum exist at twice the frequency of those in the 10-sample signal. In looking at the spectrum of analog EFQPSK, we notice that a decrease of $\sim 20\ dB/decade$ is witnessed in side-band power. The same characteristic

holds for the 20-sample signal. As each bit is added to quantization, the power in the side-bands at a given frequency in the aforementioned frequency range is one-half that of the 10-sample side-bands for the same number of quantization bits. Therefore, the spectral leakage of the 20-sample signal is one-half of that of the 10-sample signal. Even though the 20-sample signal has a much lower spectral leakage it is relatively large, as will be shown herein.

Fig. 4.5 plots the spectra of 20-sample signals with a moderate-to-high number of quantization bits. Note that the 6-bit quantized signal is almost as efficient as the 14-bit quantized signal. This is because once 6 bits of quantization are used the power in the distortion of the 6-bit quantization process is approximately equivalent to the power in spectral leakage. When more than 6 bits of quantization are used, the power in the distortion from quantization is lower than the power in the spectral leakage. Once the power in the spectral leakage has become larger than the power in the distortion from quantization, the signal has converged to its best spectral case. Therefore, when trying to reduce side-band power in a 20-sample EFQPSK signal it is not beneficial to use more than 6 quantization bits.

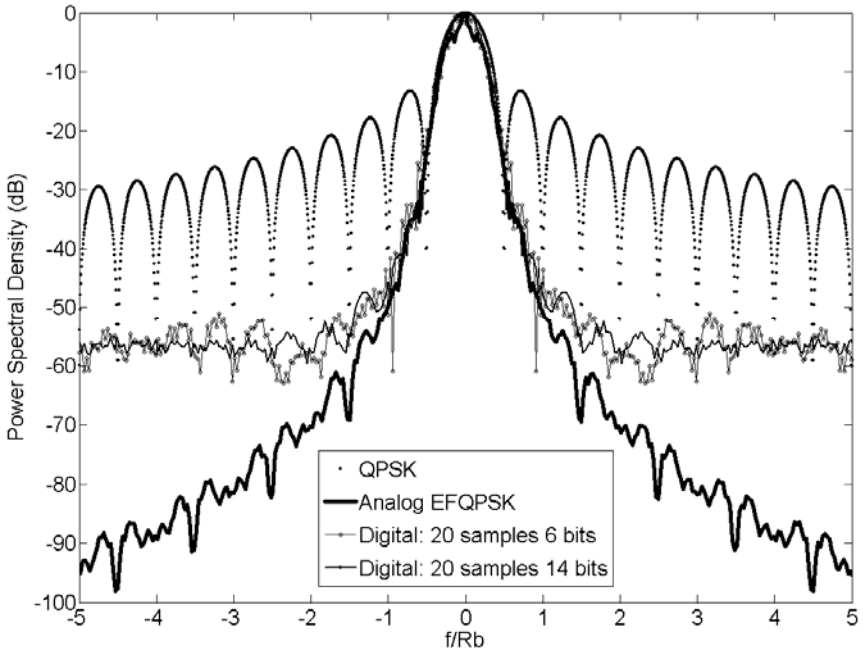

Fig. 4.5. The effect quantization with a moderate-to-high number of bits has on a 20-sample EFQPSK signal.

Fig. 4.6 illustrates the effect a low-to-moderate amount of quantization bits has on the spectrum of a 50-sample EFQPSK signal. The sampling interval for this signal is $T = 8 \times 10^{-6}\ s$ and the sampling frequency is $F_S = 25N_q$. The highest frequency represented without error is $62.5\ kHz$, which is outside the range of the plot. Therefore, as with the 20-sample case, the only two reasons the spectra of 50-sample cases are worse than the spectrum of the analog case is quantization and the leftover artifact in taking the DFT. The period of the spectra in Fig. 4.6 is $2.5\times$, the same as in the 20-sample case. Since the spectra of 50-sample cases are replicated at frequencies $2.5\times$, the side-bands that interfere with each other are even lower in power than the 20-sample case. Therefore, the power in spectral leakage of the 50-sample case is much lower than that of the 20-sample case. Fig. 4.6 plots a 2-bit quantization case, 3-bit quantization case, 4-bit quantization case, and a 6-bit quantization case. The SQNRs of each of these cases is the same as those for the 10-sample and 20-sample cases. Note that the side-band power of the 6-bit quantized case for the 50-sample spectrum is lower than in the 10-sample and 20-sample cases. This is due to the power in distortion from 6-bit quantization for the 50-sample case is higher than the spectral leakage, whereas in the 10-sample and 20-sample cases the power in the distortion from

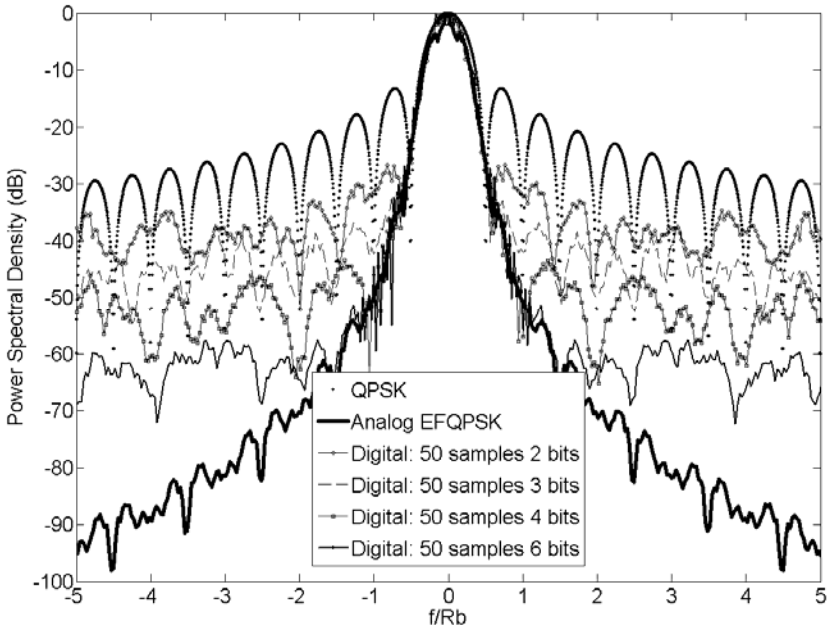

Fig. 4.6. The effect quantization with a low-to-moderate number of bits has on a 50-sample EFQPSK signal.

quantization is approximately equivalent to or higher than the spectral leakage. As with the 20-sample spectra, the 50-sample spectra experience the same effects when the number of quantization bits increases in the spectrum at about the same rate as the 20-sample cases.

Fig. 4.7 shows the effect a high number of quantization bits has on a 50-sample EFQPSK signal. Note that spectra from Fig. 4.6 are almost as acceptable as FQPSK from Fig. 2.9. Looking at Fig. 4.7, the 8-bit quantization case is approximately the same as the 14-bit quantization case. This results when more than 7 bits of quantization are used in the 50 sample EFQPSK signal, causing power in the distortion of the quantization process to become approximately equivalent to or less than the power in the spectral leakage. Therefore, it is not practical to use more than 8 quantization bits for a 50-sample EFQPSK signal when trying to reduce side-band power.

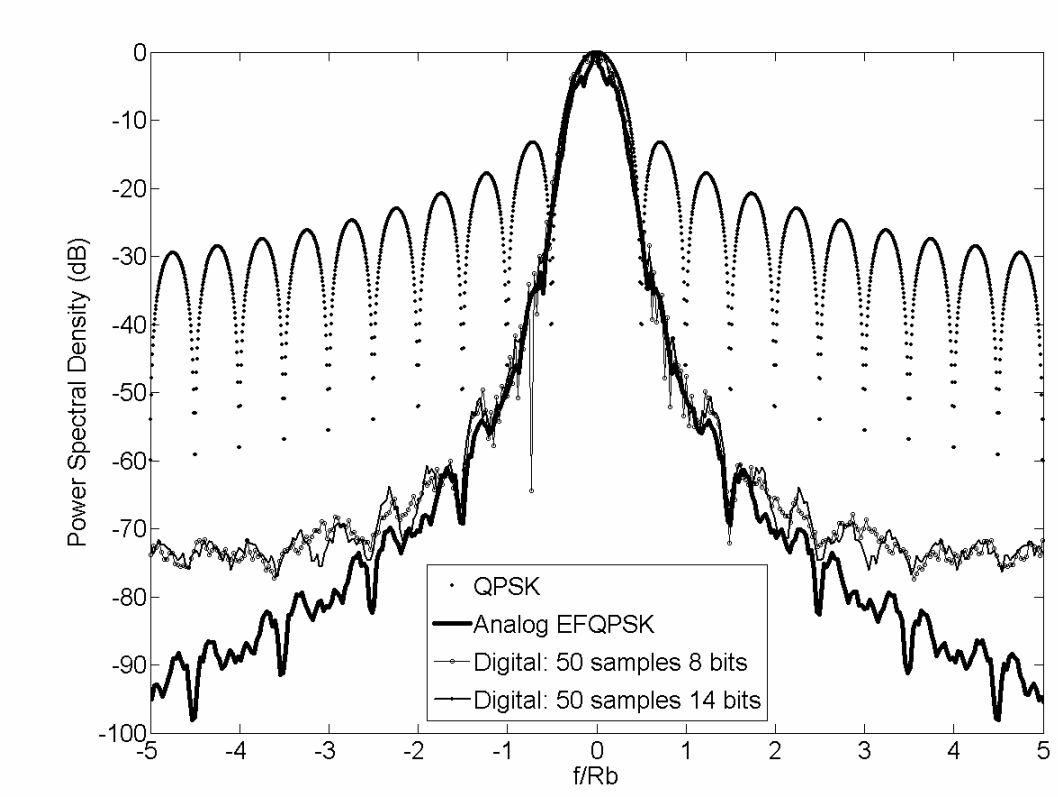

Fig. 4.7. The effect quantization with a high number of bits has on a 50-sample EFQPSK signal.

Fig. 4.8 illustrates the effect on a 100-sample EFQPSK signal from quantization with a moderate amount of bits. The cases presented are a 2-bit quantization case, 3-bit quantization case, 4-bit quantization case, 5-bit quantization case, and a 6-bit quantization case. The sampling interval for this signal is $T = 4 \times 10^{-6}\ s$ and the sampling frequency is $F_S = 50N_q$. Therefore, the highest represented frequency without error is $125\ kHz$. Looking at Fig. 4.8, it does not appear evident that side-lobes of one replica of the spectrum avoid interfering with the side-lobes of another replica of the spectrum. The reasons for this will be given shortly. Since no aliasing is present in Fig. 4.8, the only two factors that degrade the spectra are quantization and the leftover artifact in taking the DFT. Since the sampling interval is small, the period of the spectrum is large and therefore the side-bands that interfere with other side-bands in successive periods of the spectrum are very low in power. As a result, in the 100-sample signal the spectral leakage is very small, and all the undesirable spectral plots of EFQPSK in Fig. 4.8 are a result of quantization. Note that as the number of quantization bits increases, the roll-off rate decreases in a fashion comparable to the 50-sample cases from Fig. 4.6. In Fig. 4.8, power in the distortions of each quantization case is much larger than the power in the spectral leakage. The

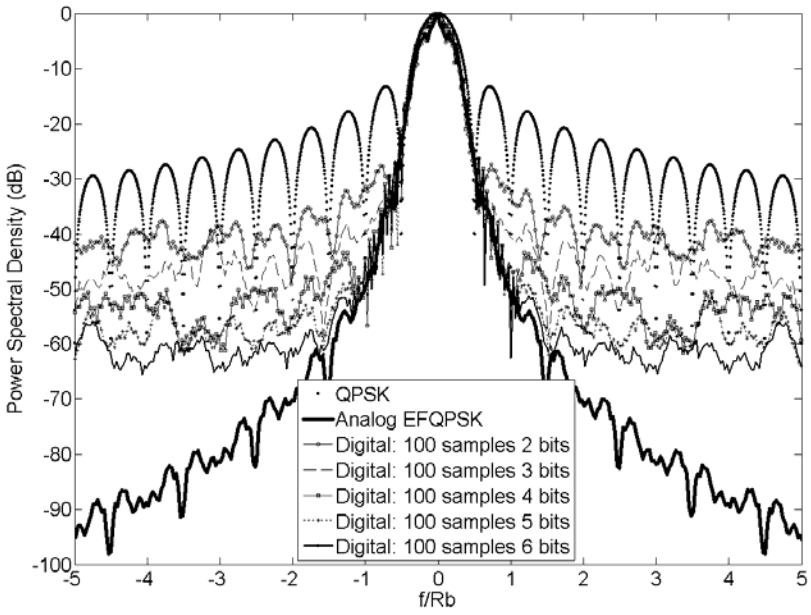

Fig. 4.8. The effect quantization with a low-to-moderate amount of bits has on a 100-sample EFQPSK signal.

100-sample, 6-bit quantization case is not much better than a 6 quantization bit, 20-sample or 50-sample signal. This is because the ratio of the distortion power to the power in the spectral leakage is much higher in the 100-sample signal than for the 20-sample and 50-sample signals. In other words, the distortion power has a more dominant effect on the 100-sample signal.

Fig. 4.9 illustrates the effect quantization with a high number of bits has on the spectrum of a 100-sample EFQPSK signal. Comparing Figs. 4.8 and 4.9 we see that the 8 quantization bit signal is about 20 dB lower in power than the 6-bit case. This is due to the SQNR of the 8-bit quantization process, which is almost 50 dB compared to the 37 dB of the 6-bit quantization process. The 8-bit quantization, 100-sample spectrum of EFQPSK yields lower power than the analog FQPSK spectrum of Fig. 2.9. The 10-bit and 12-bit cases have SQNRs of 62 dB and 74 dB. In Fig. 4.8 we compared a 6 quantization bit version of a 10-sample signal to a 14 quantization bit, 10-sample signal to show that quantization with greater than six bits is not advantageous when trying to reduce side-band power. In Fig. 4.9, the same concept is considered. A 12-bit quantized case of a 100-sample EFQPSK signal nearly matches that of its analog counterpart in the frequency range discussed previously. This is because the power in the distortion from quantization is

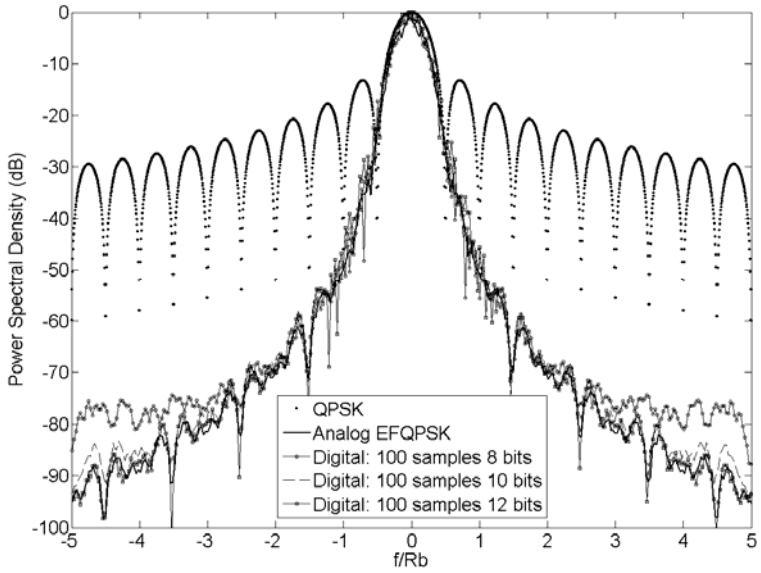

Fig. 4.9. The effect quantization with a high number of bits has on a 100-sample EFQPSK signal.

approximately equal to the power in the spectral leakage. In other words, since the distortion power is so close to zero, the shape of the signal hardly changes and the spectral leakage is approximately zero. Therefore, if a system designer is limited by very stringent bandwidth requirements then it is not advantageous to use more or less than 12 bits of quantization. However, if a system designer has slightly more relaxed bandwidth requirements, then the designer can afford to utilize 8 to 10 quantization bits in a 100 sample signal, both of which are clearly better in spectral efficiency that analog FQPSK.

Fig. 4.10 emphasizes that with certain sampling intervals, it is not advantageous to use the maximum number of quantization bits. The plots of Fig. 4.10 show a 10-sample, 6 quantization bit spectrum, a 20-sample, 6-bit spectrum, a 50-sample, 8 quantization bit spectrum, and a 100-sample, 12 quantization bit spectrum. Each signal converges to its best spectral state in the frequency range shown. If computational complexity is of concern and bandwidth is limited, then a designer may choose any of the signals in Fig. 4.10 knowing that the spectral efficiency will increase negligibly if at all.

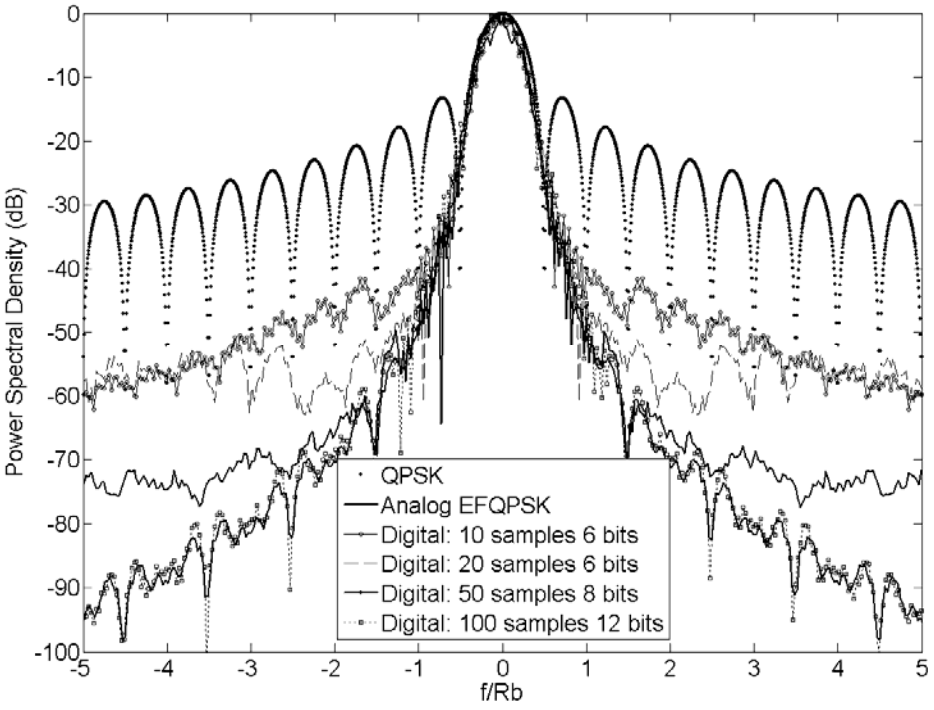

Fig. 4.10. Optimized plot of digital EFQPSK with various sampling frequencies and quantization bits.

4.2 Out-of-Band Power for Digital EFQPSK

The signals simulated in this section are QPSK, analog EFQPSK and digital EFQPSK with varying sized samples and quantization bits. Fig. 4.11 illustrates the effect 2-bit, 3-bit, and a 4-bit quantization has on the out-of-band power of a 10-sample EFQPSK signal. As stated previously, the 10-sample signal is sampled at $5N_q$, where the highest represented frequency without error is $12.5\ kHz$. Looking at $B \approx .3$, the equivalent frequency is $2.5\ kHz$, and the 10-sample signal starts to deviate from analog EFQPSK. The reason the digital signal deviates from the analog signal at this point is because the artifact from taking the DFT is present at this point in frequency. The results of Fig. 4.11 show an out-of-band power that is high for the 10-sample case compared to the analog case because of quantization, the leftover artifact of taking the DFT, and the aliasing of the $2.5\ kHz$. Similar to what was stated in Section 4.1 of this study, the 2-bit quantization signal experiences a swelling effect in the side-band power due to the distortion of the leftover artifact of taking the DFT. Since the side-bands expand in power, the out-of-band power is increased. Looking at the 3-bit and 4-bit quantization cases, the out-of-band power plot for 3-bit quantization is much better than the 2-bit quantization plot because the side-bands in the PSD of the 3-bit quantization signal are lower in power than the 2-bit case. This is due in large part to the 6 dB difference in SQNRs between the 2-bit and 3-bit cases. The 4-bit case is slightly better than the 3-bit case in both PSD and out-of-band power, as one would expect; but, since the SQNR of the 4-bit case does not dominate as much as a case with fewer quantization bits, the out-of-band power does not decay as much as going from 2-bits to 3-bits. This is because the SQNR of the 4-bit case is large enough that it starts to approach the spectral leakage, as discussed previously.

Fig. 4.12 shows the effect a moderate-to-high amount of quantization bits has on the out-of-band power of a 10-sample EFQPSK signal. Looking at the 5-bit quantization case, the out-of-band power is comparable to that of the 4-bit quantization case from

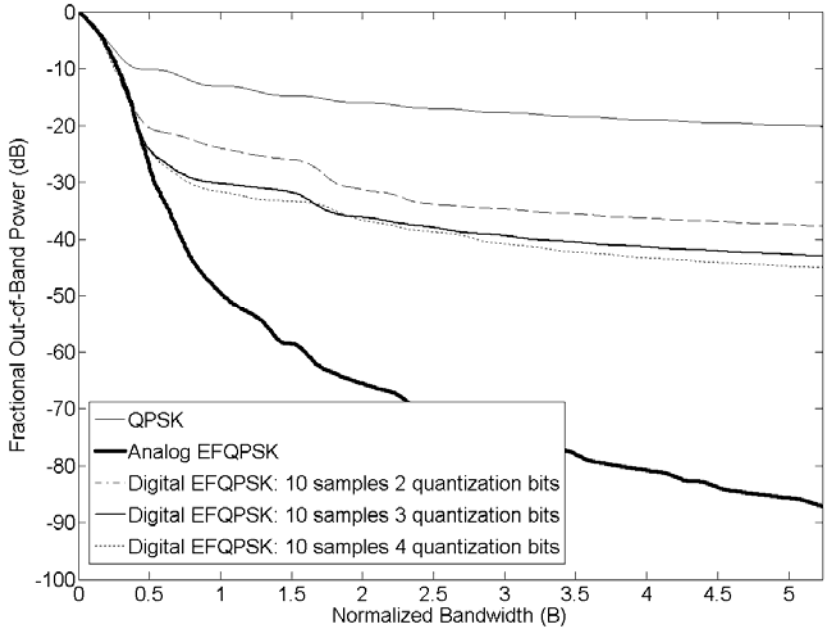

Fig. 4.11. The effect a low amount of quantization bits has on the out-of-band power of a 10-sample EFQPSK signal.

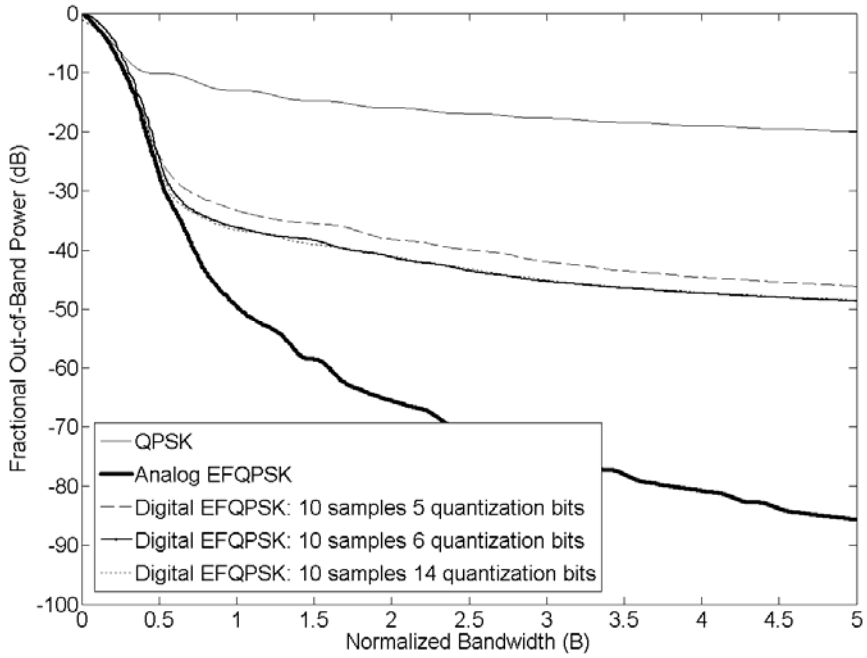

Fig. 4.12. The effect a moderate-to-high amount of quantization bits has on the out-of-band power of a 10-sample EFQPSK signal.

Fig. 4.11. As stated above, this is because the SQNR of the 5-bit case is large enough that it no longer dominates the signal because the spectral leakage of the signal is almost reached. The 6-bit quantization case is slightly better than the 5-bit quantization case as one would expect since the SQNR of the 6-bit case is ~38 dB as opposed to the 5-bit SQNR of ~32 dB. Note that the 6-bit quantization case converges to the 14-bit quantization case. The fact that the SQNR of the 14-bit quantization case is much larger than the SQNR of the 6-bit case is irrelevant because the spectral leakage has been reached with the 6-bit case so there is no advantage in utilizing more than 6 bits of quantization when trying to reduce out-of-band power. When utilizing more than 6 bits of quantization, the effects of distortion are no longer witnessed in the 10 sample EFQPSK signal, but instead, only the effects of the leftover artifact in taking the DFT and aliasing are observed. Since high power side-bands in the PSD are bunched together, the out-of-band power is also high compared to analog EFQPSK.

Fig. 4.13 illustrates the effect a low amount of quantization bits has on the out-of-band power of a 20-sample EFQPSK signal. Comparing Figs. 4.11 and 4.13, note the striking similarities in the 2-bit, 3-bit, and 4-bit quantization cases of the 10-sample and 20-sample signals. For all practical purposes, these sample signals are approximately the

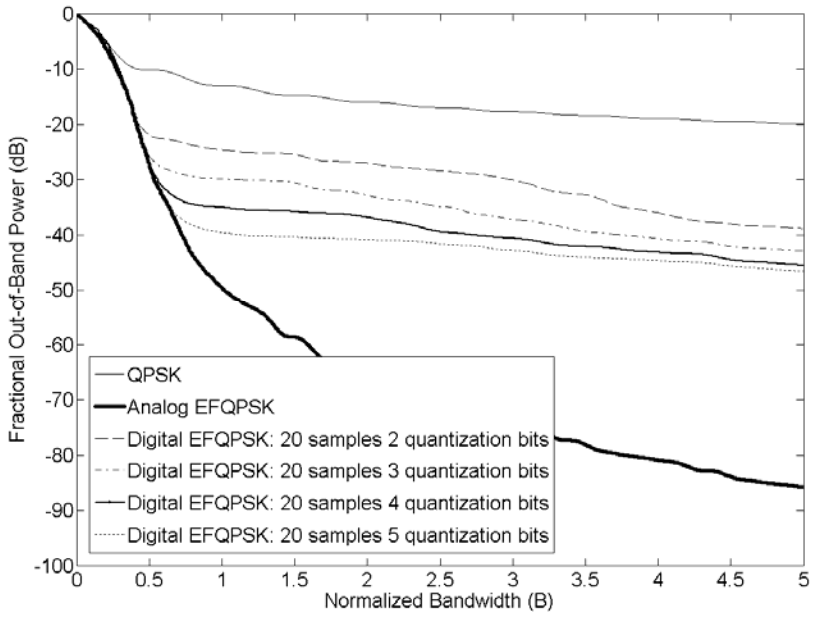

Fig. 4.13. The effect a low amount of quantization bits has on the out-of-band power in a 20-sample EFQPSK signal.

same in terms of out-of-band power at these quantization levels. The only difference between the two signals is that the 20-sample signal deviates from analog EFQPSK at twice the bandwidth the 10- sample signal does for a 5 quantization bit case, as witnessed when comparing Fig. 4.13 with Fig. 4.12. Since the sampling interval for the 20-sample signal is one-half as long as it is for the 10-sample signal, the period of the PSD for the 20-sample signal is twice the period for the 10-sample signal. This means the sidebands that a bunched together in the 20-sample signal are lower in power than the sidebands bunched together in the 10- sample signal. The lower side-band power does not contribute to the degradation of the 20-sample signal's out-of-band power until the side-band power becomes greater than the side-band power of analog EFQPSK. Another reason for the degradation of out-of-band power in the 20-sample signal is aliasing. Quantization is the final reason for the degradation of the 20-sample signal in Fig. 4.13. The SQNRs of these signals are equivalent to the SQNRs of the 10-sample signals.

Fig. 4.14 shows the effect a moderate-to-high amount of quantization bits has on the out-of-band power of a 20-sample signal.

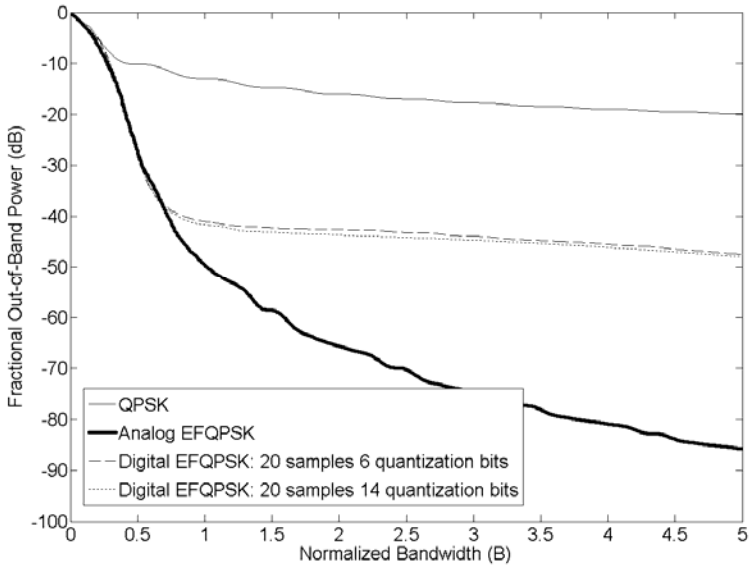

Fig. 4.14. The effect a moderate-to-high amount of quantization bits has on the out-of-band power of a 20-sample EFQPSK signal.

Note that the 6 quantization bit and 14 quantization bit cases are about the same because the 6-bit quantization case has converged to its best state. The spectral leakage has been reached for the 6-bit quantization case and aliasing plays a minor part compared to the spectral leakage in the degradation of the 20-sample out-of-band power. Looking at Fig. 4.12 and 4.14, we notice that the 10-sample and 20-sample signals have about the same out-of-band power for the 6-bit and 14-bit quantization cases at higher bandwidths. The only improvement the 20-sample signal offers over the 10-sample signal in terms of PSD and out-of-band power is a lower amount of power at lower frequencies. However, because the sampling intervals of the 10-sample and 20-sample signals are still relatively long, the two signals demonstrate many similarities in terms of PSD and out-of-band power. Therefore, with a 10-sample and 20-sample EFQPSK signal, it is not advantageous to use more than 6 bits of quantization when required to reduce out-of-band power.

Fig. 4.15 shows the effect a low-to-moderate amount of quantization bits has on the out-of-band power of a 50-sample EFQPSK signal. Note that this signal is nearly the same as the 10-sample and 20-sample signals for the 2-bit, 3-bit, and 4-bit quantization

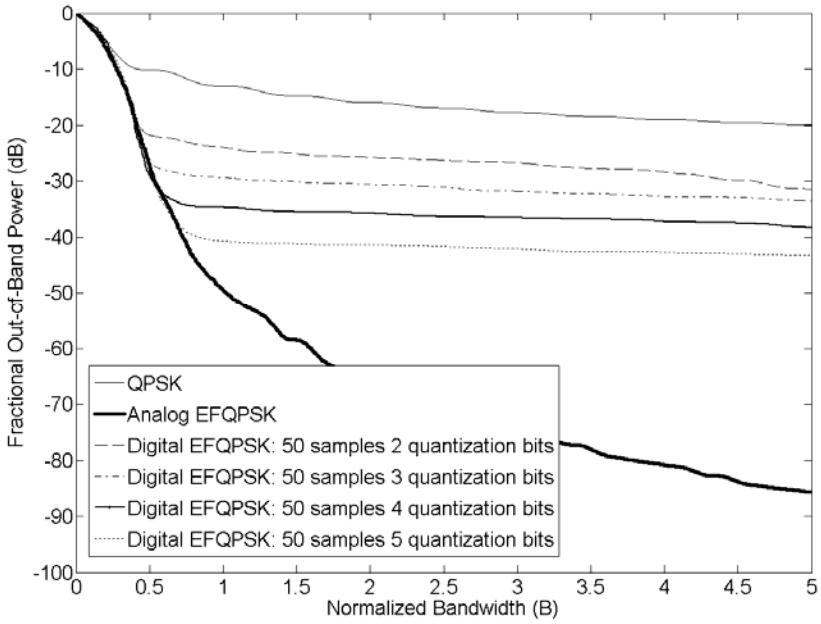

Fig. 4.15. The effect a low-to-moderate amount of quantization bits has on the out-of-band power of a 50-sample EFQPSK signal.

cases from Figs. 4.11 and 4.13. The reason the 50-sample signal has high out-of-band power for these cases of quantization bits is because the power of the distortion is very large compared to the power in the spectral leakage. Looking at the 6-bit quantization case, we notice that the 50-sample signal is better than the 10-sample and 20-sample signals in terms of out-of-band power, and that the 50-sample signal deviates from analog EFQPSK at a higher bandwidth. This results because the sampling interval is much shorter, meaning the side-bands that bunch together are lower in power than the side-bands that bunch together in the 10-sample and 20-sample cases. Aliasing in the 50-sample signal occurs at $f \geq 62.5\ kHz$, which is not represented in Fig. 4.15. With the 50-sample case, aliasing is not present and the power in the spectral leakage is small enough that quantization plays the largest role in the degradation of the out-of-band power of the digital signal compared to the out-of-band power of the analog signal in Fig. 4.15.

Fig. 4.16 illustrates the effect a high amount of quantization bits has on the out-of-band power of a 50-sample EFQPSK signal. Notice that the 8-bit quantization signal has converged to the 14-bit quantization signal. In Fig. 4.16, the power in the spectral leakage is the most dominant factor contributing to the degradation of the out-of-band power of the digital signal as compared to the out-of-band power of the analog signal. The power in the distortion of the 8-bit quantization case is much larger than the power in the distortion of the 14-bit quantization case, but in both cases the power in the distortion is lower than the power in the spectral leakage. To conclude, for a 50-sample signal, the power in the distortion for a low amount of quantization bits plays a larger role than does the power in the spectral leakage. However, for a high amount of quantization bits, the power in the distortion plays an insignificant role compared to the power in the spectral leakage in the degradation of the out-of-band power of a 50-sample signal. From Fig. 4.16, there is no advantage in using more than 8 quantization bits when trying to reduce out-of-band power in a 50-sample EFQPSK signal.

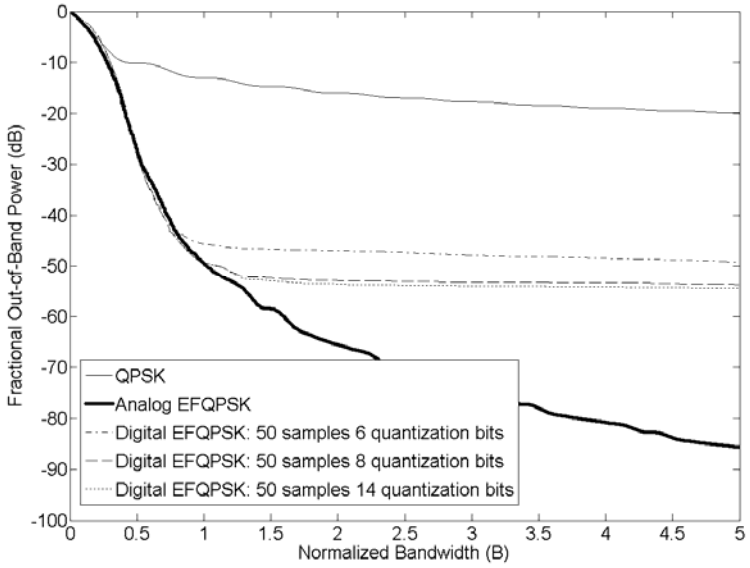

Fig. 4.16. The effect a high amount of quantization bits has on the out-of-band power of a 50-sample EFQPSK signal.

Fig. 4.17 illustrates the effect quantization with a low-to-moderate amount of bits has on the out-of-band power of a 100-sample EFQPSK signal. Looking at the 2-bit and 4-bit quantization, 100-sample signal in Fig. 4.17 and comparing it to all of the 10-sample signals of Figs. 4.11 and 4.12, the 100-sample signals are worse in terms of out-of-band power than the 10-sample signals. The distortion power from the 2-bit and 4-bit quantization dominates the signal in the 100 sample signals more than in the 10-sample signal because the power in the spectral leakage plays a more significant role compared to the distortion power from 2-bit and 4-bit quantization. In the 100-sample signal the distortion is the more dominant factor in the degradation of the PSD and out-of-band power than the power in the spectral leakage. The sampling interval for the 100-sample signal is relatively short. Since this is small compared to the bit period, the frequency spacing of the replicated spectra of the 100-sample signals is large. Therefore, the leftover artifact in taking the DFT of the signal is much smaller because the side-lobes that do interfere with one another are very low in power. So, the 100-sample cases deviate from analog at much lower power than do 10-sample cases. The 6-bit quantization case shows a better improvement in out-of-band power over the 2-bit and 4-bit cases because the SQNR for the 6-bit case is much larger than those of the 2-bit and 4-bit cases.

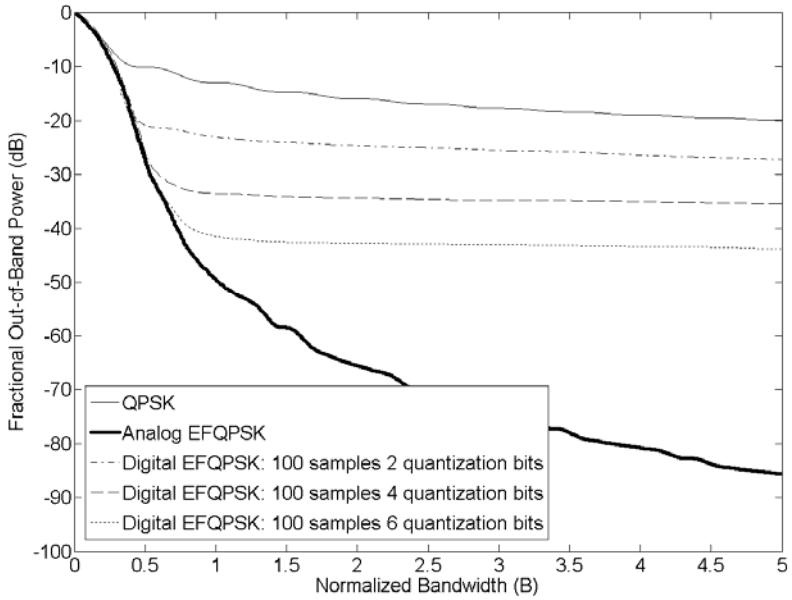

Fig. 4.17. The effect a low-to-moderate amount of quantization bits has on the out-of-band power of a 100-sample EFQPSK signal.

The frequencies at which aliasing occurs are greater than $125\ kHz$. Therefore, aliasing is not a factor in the degradation of the digital signal compared to the analog signal in the frequency ranges specified. Therefore, at higher frequencies, the out-of-band power of the 100-sample EFQPSK signal is affected by both the distortion from quantization and the power in the spectral leakage.

Fig. 4.18 shows the effect a high number of quantization bits have on the out-of-band power of a 100-sample EFQPSK signal. Looking at the 8-bit quantization case, the distortion of the signal is low enough that it becomes a good approximation to analog EFQPSK. At low frequencies, the 8-bit signal nearly matches the analog signal. At higher frequencies, especially at $B \geq 3.0$, the out-of-band power is somewhat higher than analog EFQPSK. The distortion from quantization changes the shapes of the side-bands that are bunched together, and as stated previously, swells the spectral content of those

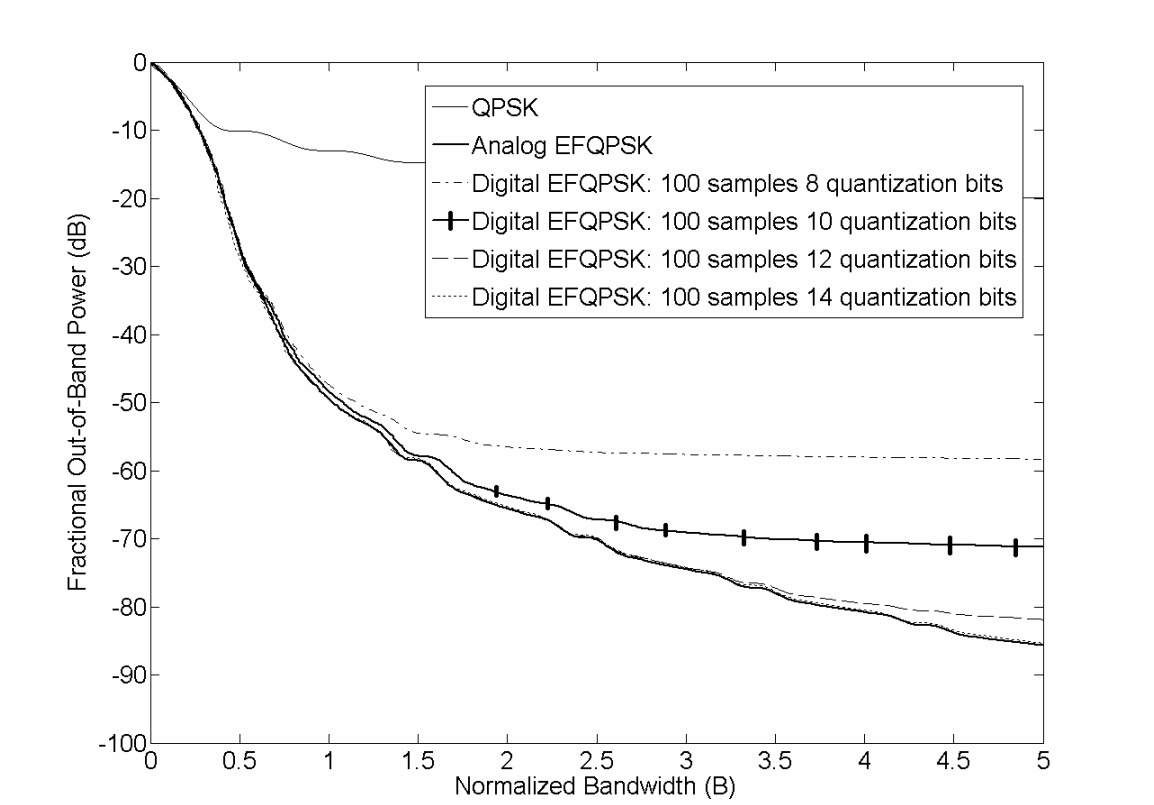

Fig. 4.18. The effect a high amount of quantization bits has on the out-of-band power of a 100-sample EFQPSK signal.

artifacts. The 12-bit case starts to deviate from analog EFQPSK before adjacent side-lobe interference occurs. This means that there is very little spectral leakage in the 100-sample signal and that the SQNR of the 12-bit quantization process still plays a significant role in the out-of-band power. In other words, in order to witness only the effect that power in the spectral leakage has on the 100-sample signal, one would have to raise the SQNR of the quantization process to match that of the spectral leakage in the frequency ranges discussed previously. The signal that shows this effect is the 100-sample, 14-bit quantization EFQPSK signal. The 14-bit quantization has a distortion power that has reached the power in the spectral leakage and therefore the only reason the digital signal deviates from the analog signal is due to the spectral leakage. In the frequency range of Fig. 4.18, there is negligible degradation. Although Fig. 4.9 indicates it is not advantageous to use more than 12 quantization bits for a 100-sample EFQPSK signal when trying to reduce side-band power at lower frequencies, it is beneficial to use

14-bit quantization when trying to reduce out-of-band power at higher frequencies. In other words, if very stringent bandwidth requirements force the system designer to space channels closely and the system designer can only have negligible interference for a bandwidth of $25\,kHz$, then the designer will want to use 14 quantization bits. Otherwise, if more interference is tolerable, the 12-bit quantization will do.

Fig. 4.19 is a plot that shows varying sized sample signals with 6-bit, 6-bit, 8-bit, and 14-bit quantization, respectively. The plot illustrates the concept that it is not advantageous to use more bits of quantization for these signals when trying to reduce out-of-band power. System designers can study Fig. 4.19 and quickly determine which signal best suits the needs of the system given certain bandwidth requirements and certain computational limits. For example, if a system designer has very limited computational resources and relaxed bandwidth requirements, then the 10-sample, 6-bit quantization case will probably suit the designer's needs. On the other hand, if computational resources are ample and bandwidth requirements are strict, then the 100-sample, 14-bit quantization case will probably suffice.

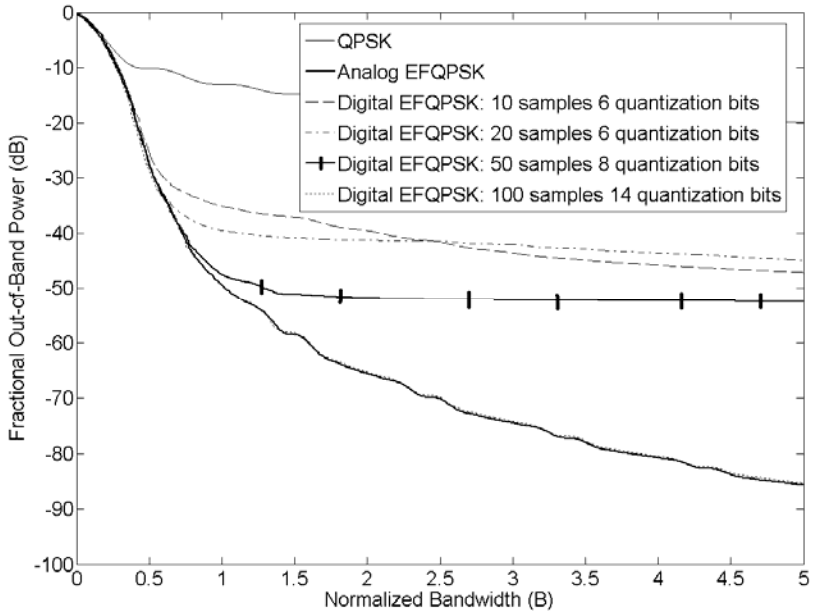

Fig. 4.19. Optimized out-of-band power of a 10, 20, 50, and 100-sample EFQPSK signal with 6-bit, 6-bit, 8-bit, and 14-bit quantization, respectively.

4.3 Maximum Envelope Fluctuation for Digital EFQPSK

The results of this section show simulations of analog EFQPSK and digital EFQPSK for 10, 20, 50, and 100 samples with varying quantization bits. There are two factors that contribute to the degradation of the envelope of digital EFQPSK compared to the envelope of analog EFQPSK: sampling and quantization. When the sampling interval is long, a large amount of data is lost and the sampled waveforms are jagged and discontinuous. When the last value of the present waveform $s_i(t)$ is concatenated with the first value of the next waveform, $s_{i+1}(t)$, the two values will not always equal one another, and shape discontinuity will exist at that point. Modulating the in-phase and quadrature phase channels, and adding the two together, create large fluctuations in the envelope. Quantization with a low amount of bits introduces both overload noise and granularity noise [15]. Overload noise is noise created when the value of the highest quantization interval is less than the value of the original signal [15]. Modulating this overloaded signal creates a distorted envelope in the transmitted signal. Granularity noise is noise introduced when the quantization spacing is too large [15]. Modulating this signal also creates a distorted envelope but does not affect the envelope as much as overload noise affects the envelope.

Fig. 4.20 is a plot that shows the effect the number of quantization bits has on the envelope fluctuation of a 10-sample EFQPSK signal. Sampling the underlying waveforms at 10 samples-per-bit creates jagged and sharp discontinuities in the newly sampled waveforms because the sampling interval is relatively large. These discontinuities also contribute to the spectral splatter in the PSD of the 10-sample signal because the derivative of these discontinuities creates higher frequencies within the signal. These are not the only places where the 10-sample EFQPSK signal expresses higher envelope fluctuation. The parts of the waveforms that are interpolated to create deviations from their analog counterparts also create larger envelope fluctuations. Looking at Fig. 4.20, the 2-bit quantization case expresses an almost 4 dB amount of envelope fluctuation. This makes sense because there are only four levels of quantization and, the 10 sample, 2-bit quantization signal hardly resembles its analog counterpart. Thus, for the 10 sample, 2-bit quantization case, there are interpolated values of the original waveform that did not exist before; there are discontinuities at of

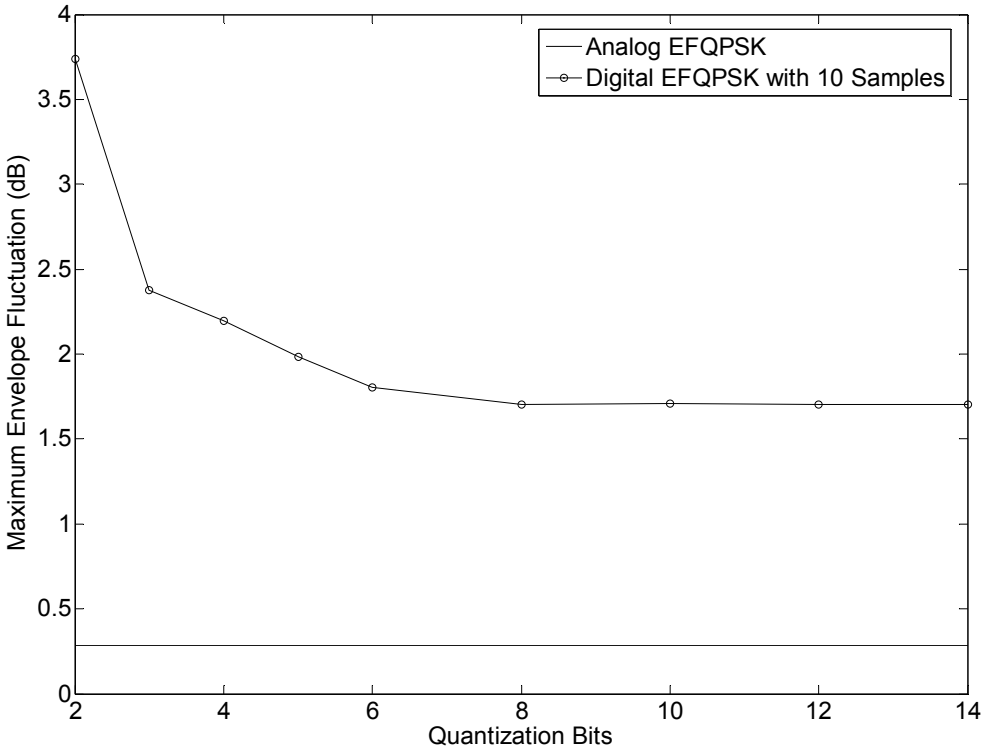

Fig. 4.20. The effect the number of quantization bits has on the envelope fluctuation of a 10-sample EFQPSK signal.

concatenation points in the string of bits; and, there is distortion from quantization. Together, these three factors create the ~4 dB envelope fluctuation. Notice as the number of quantization bits increases, the maximum envelope fluctuation decreases. This is because as the number of quantization bits increases the distortion decreases by $6\ dB$ per bit of quantization. With a 3 or more bits of quantization, the signal starts to resemble its analog counterpart. When 8 or more bits of quantization are used the maximum amount of envelope fluctuation is practically stationary. Similar to what was stated previously, the distortion from quantization with 8 or more bits no longer plays a significant role in the envelope fluctuation of this signal. So, with 8 or more bits of quantization, the distortion for all practical purposes is negligible and the only two factors that contribute to envelope fluctuation are: the interpolated values between samples that do not exist in analog EFQPSK, and the discontinuities at concatenation points in the string of pulse-shaped bits. If a system designer

is required to design a transmitter that must communicate with a satellite, then it needs to be amplified with a nonlinear amplifier and this signal will not meet the specifications (this last clause isn't clear within the context of the sentence). However, if the requirements do not advocate a need for long distance transmission, then the designer may want to use fewer quantization to save power or to decrease computational complexity.

Fig. 4.21 illustrates the effect the number of quantization bits has on the envelope of a 20-sample EFQPSK signal. The sampling interval of this signal is shorter than the sampling interval of the 10-sample signal and therefore fewer discontinuities exist when modulating the signal. However, when the waveforms are concatenated, the magnitudes of the discontinuities are larger than the magnitudes of the discontinuities for the 10-sample signal. When only 2-bit quantization is used, the quantization operation penalizes larger magnitudes more than it does smaller magnitudes. This is evident for the 2-bit quantization case of the 20-sample signal of Fig. 4.21 by comparing it to the same quantization case of Fig. 4.20. However, when more quantization bits are used in the 20- sample signal, the maximum envelope fluctuation falls below that of the fluctuation of the 10-sample signal. Once 8 or more bits of quantization is used for the 20- sample signal, the maximum envelope fluctuation converges to about $1.088\ dB$. The

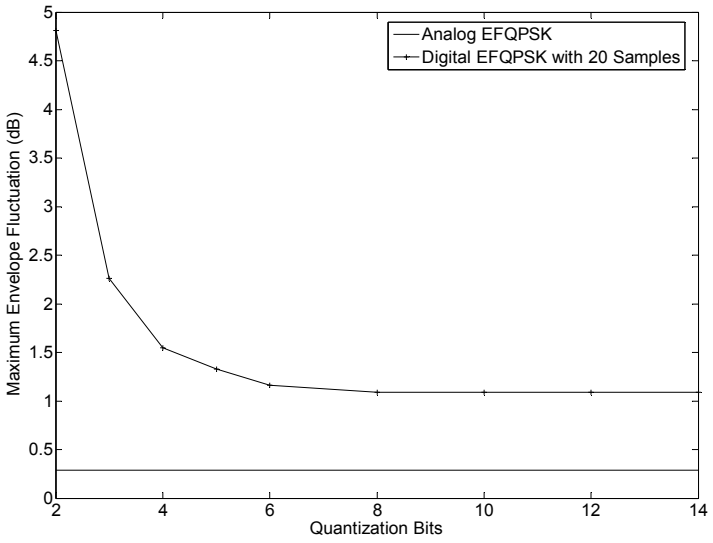

Fig. 4.21. The effect the number of quantization bits has on the envelope fluctuation of a 20-sample EFQPSK signal.

distortion from quantization with 8 or more bits plays an insignificant role and the only the long sampling interval and interpolation degrade the envelope of this case of EFQPSK.

Fig. 4.22 shows the effect the number of quantization bits has on the envelope of a 50-sample EFQPSK signal. With 2-bit quantization, the 50-sample signal has almost the same magnitude of envelope fluctuation as the 20-sample case for the same reasons. Note that for the 50-sample, 3-bit quantization case, the magnitude of the maximum envelope fluctuation is larger than in the 10 and 20 sample, 3-bit quantization cases. The magnitude of the distortion for the 50-sample, 3-bit quantization case is larger than the sum of the magnitudes of the discontinuities from the sampling interval. Using 4 or more bits of quantization in the 50-sample case yields lower envelope fluctuation than either of the 10-sample or 20-sample cases for the same number of quantization bits. Once 8 or more bits of quantization is used in the 50-sample signal, the maximum envelope fluctuation converges to about $0.44\ dB$. Since the sampling interval is relatively short, the sum of the magnitudes of the discontinuities is relatively small and therefore a small magnitude in envelope fluctuation is witnessed in Fig. 4.22.

Fig. 4.23 illustrates the effect the number of quantization bits has on the envelope fluctuation of a 100-sample EFQPSK signal. Again, as in the 10-sample case, the maximum envelope fluctuation of the 2-bit quantization case is almost 4 dB. This can be expected for any EFQPSK signal that uses 2 bits of quantization and is samples sized 100 or less. This is because the distortion from 2-bit quantization is extremely high. In other words, the shape of the signal is completely changed as compared to its analog counterpart. From Fig. 4.23, the maximum envelope fluctuation decreases considerably with each bit added to quantization. As the number of quantization bits increases the maximum envelope fluctuation converges to that of analog EFQPSK. For all practical purposes, a 10-bit quantization, 100-sample EFQPSK envelope is equivalent to an analog EFQPSK envelope.

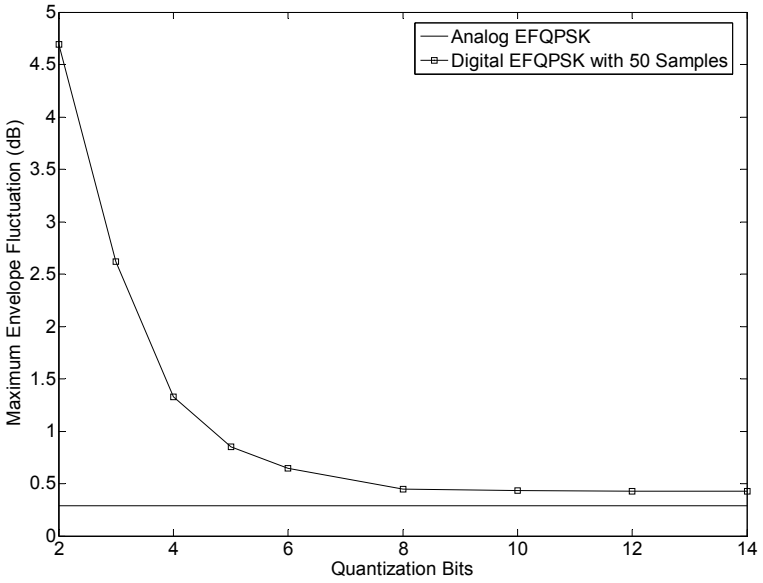

Fig. 4.22. The effect the number of quantization bits has on the envelope fluctuation of a 50-sample EFQPSK signal.

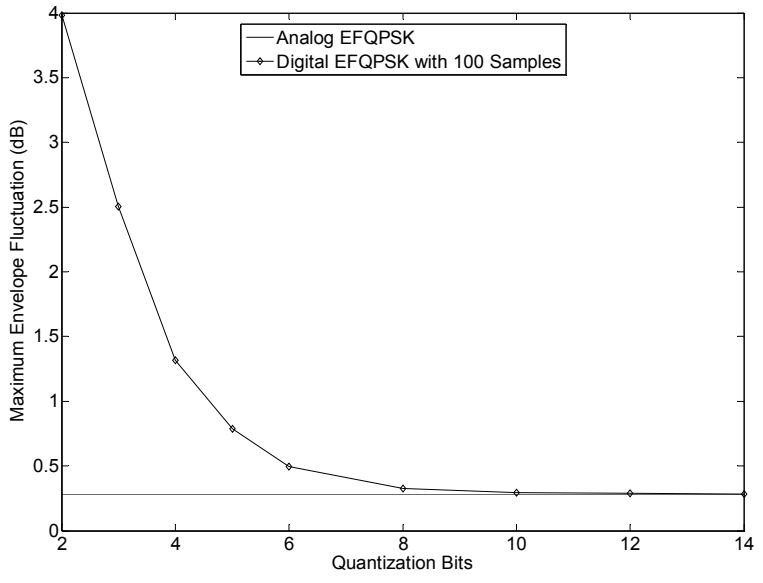

Fig. 4.23. The effect the number of quantization bits has on the envelope fluctuation of a 100-sample EFQPSK signal.

The 100-sample EFQPSK signal does not need to be interpolated because the space between samples is small. When the previous waveform is concatenated with the present waveform, there are negligible discontinuities because the last sample of the previous waveform is approximately equivalent to the first sample of the present waveform. Therefore, the only dominant variable that contributes to the degradation of envelope fluctuation in a 100-sample EFQPSK signal is the distortion from quantization.

Fig. 4.24 plots the maximum envelope fluctuations of 10, 20, 50, and 100 sample EFQPSK signals. A system designer can refer to Fig. 4.24 to quickly determine what signal best suits the designer's needs. For example, if the systems designer is transmitting only over short distances, then the 10-sample signals may suffice. However, if the designer is restricted to deep space communications, then the designer may find the 100-sample signals with a high amount of quantization bits more beneficial.

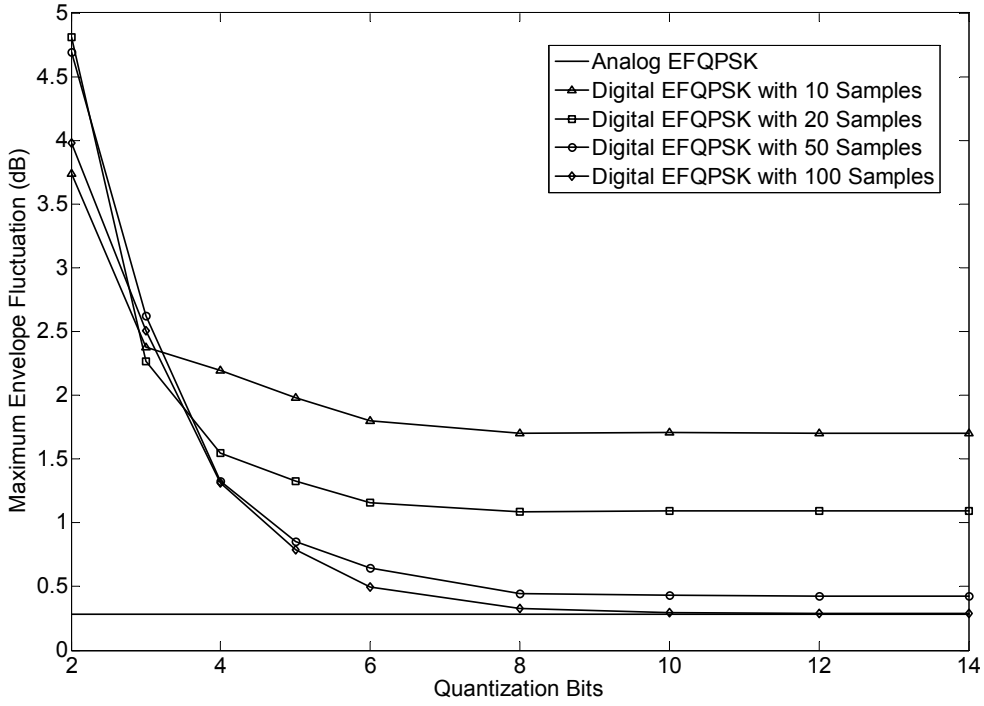

Fig. 4.24. Optimized plot of the maximum envelope fluctuation of 10, 20, 50, and 100-sample EFQPSK signals with varying quantization bits.

4.4 Bit-Error-Rate (BER) for Digital EFQPSK

The BER results of this section are of OQPSK, analog EFQPSK, and digital EFQPSK with 3, 5, 10, 20, 50, and 100 samples with varying quantization bits. The reason the 3 and 5 sample signals were simulated in this section and not in other sections is because for BER, the length of the digital signal does not have to equal the size of the analog signal when comparing BER plots.

Fig. 4.25 illustrates the effect the number of quantization bits has on the BER of a 3-sample EFQPSK signal. The signal has been sampled at $F_S = 1.5N_q$ and the equivalent sampling interval is $T = 1.333 \times 10^{-4}\ s$. Since the Nyquist theorem is not met for this signal, much of the information in this signal is lost. Therefore we can expect the BER to be much worse than analog EFQPSK. Looking at Fig. 4.25 we see a 3-sample signal with 2, 3, and 4 quantization bits. For analog EFQPSK, we note that at $\frac{E_b}{N_0} \approx 10.3\ dB$ a resulting BER of $P_e = 10^{-4}$ is expected. Looking at the 2 quantization bit case, we see that for a BER of $P_e = 10^{-4}$, an $\frac{E_b}{N_0} \approx 11.05\ dB$ is required. The only one reason why the BER of this case is worse than the BER of analog EFQPSK is the low sampling frequency. Much of the information is lost in sampling the signal at $1.5N_q$ and therefore much of $\overline{E}_b$ is also lost. Looking at Fig. 4.25, the BER for the 3 sample, 2-bit quantization signal is deceiving because one might assume that by sampling only at $1.5N_q$, less than $1\ dB$ of $\overline{E}_b$ is lost. The 2 bits in the quantization process restore much of the energy lost in the sampling operation. While the 2-bit quantization operation has only four levels of precision, this is more than enough precision for a signal that has only one analog voltage value. However, for a sinusoid with an infinite number of voltages in the range $-1\ V \le amplitude \le 1\ V$, four levels of precision offer an inadequate representation of the signal. At certain instances in the quantization process, some of the positive analog voltages are mapped to a positive quantization level that is larger than the voltage being mapped, which adds to $\overline{E}_b$. At other instances, some of the negative analog voltages are mapped to a negative quantization level that is smaller than the

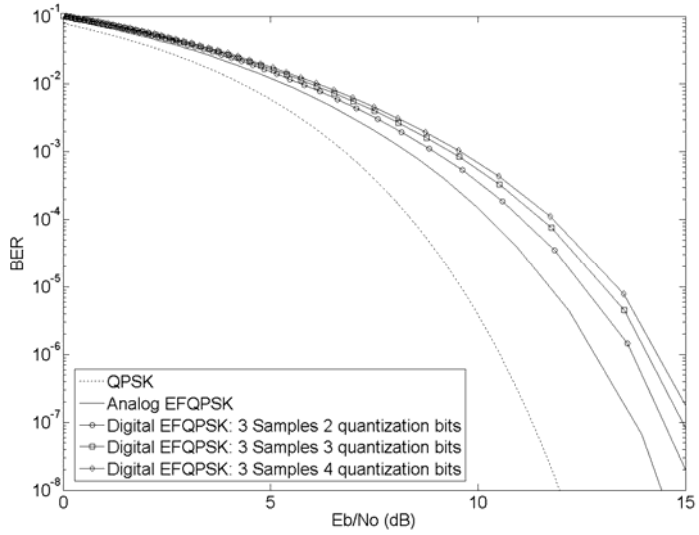

Fig. 4.25. The effect a low number of quantization bits has on the BER of a 3-sample EFQPSK signal.

voltage being mapped, which subtracts from $\overline{E}_b$. By inspection of Fig. 3.2, more positive analog voltages are mapped to quantization levels that are larger than the voltage being mapped than negative analog voltages mapped to quantization levels that are smaller than the voltage being mapped. Therefore, on the average, more energy will be added to than subtracted from $\overline{E}_b$ when a low amount of quantization bits are used. The correlation coefficients of (3.6) behave the same way as $\overline{E}_b$ does when various sampling frequencies and quantization bits are used, and this has a significant effect on the BER. The average magnitude of the correlations of each waveform for digital EFQPSK is computed as

$$\overline{C}_{S\overline{S}} = \frac{1}{8}\sum_{i=0}^{7}\left(\frac{1}{T_S}\int_0^{T_S} S_i(t)\overline{S}(t)dt\right)^2 . \qquad (4.8)$$

Assuming that $\overline{C}_{S\overline{S}}$ has larger magnitude than $\overline{E}_b$, $\overline{C}_{S\overline{S}}$ has a more significant effect on the BER than does $\overline{E}_b$. For the remainder of this study, the variables $\overline{E}_b$ and $\overline{C}_{S\overline{S}}$ are combined to form the variable $\overline{E}_b\overline{C}_{S\overline{S}}$ for the sake of simplicity. So, for the 3-sample signal with 2-bit quantization, the low sampling frequency subtracts more $\overline{E}_b\overline{C}_{S\overline{S}}$ than the 2-bit quantization adds to $\overline{E}_b\overline{C}_{S\overline{S}}$. The same concept applies to the 3-bit and 4-bit

quantization cases. However, with 3-bit and 4-bit quantization, less energy is added to $\overline{E}_b \overline{C}_{S\overline{S}}$ because there are 8 and 16 quantization levels, respectively. Note that the 4-bit quantization signal is about $1.5\ dB$ worse than the analog signal for $P_e = 10^{-4}$.

Fig. 4.26 shows the effect a moderate-to-high number of quantization bits have an EFQPSK signal with 3 samples-per-bit. The cases shown are for 5-bit, 6-bit, and 8-bit quantization. Note that the BER of all the digital cases are particularly close to one another. When 5 or more quantization bits are used, the BER deviation from analog EFQPSK is negligible and the BER converges to its worst state. This is because the energy gained in using 5 or more bits of quantization is very small compared to the energy lost in sampling with only 3 samples-per-bit.

In conclusion, if a system designer requires a bandwidth and power efficient modulation scheme with good BER, then the designer will want to use the 2-bit quantization signal

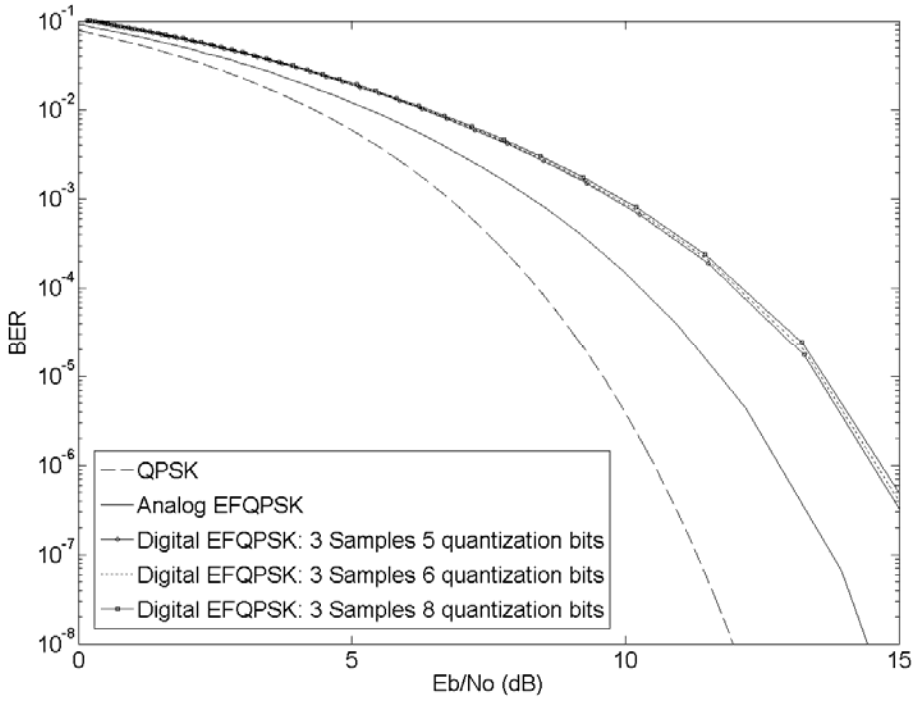

Fig. 4.26. The effect a moderate-to-high number of quantization bits have on the BER of a 3-sample EFQPSK signal.

over any of the other signals of Figs. 4.25 and 4.26 if BER is of utmost importance. However, if the same requirements exist for the designer but BER is of no concern, then the designer would want to use the 8-bit quantization signal because that signal has the best power and bandwidth efficient characteristics over all the digital signals presented in Figs. 4.25 and 4.26.

Fig. 4.27 shows the effect a low number of quantization bits have on the BER of a 5-sample EFQPSK signal. BER for 2-bit, 3-bit, and 4-bit quantization is presented. The signal has $F_S = 2.5N_q$ and $T = 8\times10^{-5}\ s$. Although Nyquist's theorem is met for this signal, F_S is too low a frequency to represent the various sinusoids of this signal. For example, if a sinusoid is sampled at $F_S = 2N_q$, the samples taken may be at zero crossings or at the peaks of the magnitudes of the sinusoids, depending on the phase of the sinusoid. If the sinusoid is sampled at $F_S = 4N_q$, then the worst case scenario would be that the samples taken are from the magnitudes of the peaks and the zero crossings of the sinusoid, both of which contain the bulk of the information. Therefore, it is desired in practice to sample at a minimum of $F_S = 4N_q$. Clearly the 5-sample signal exhibits a considerable loss of information, which is the reason BER is worse than the BER for the analog case. Note that the BER for all of the quantization cases are vary close to one another. The energy lost in $\overline{E}_b\overline{C}_{S\bar{S}}$ when increasing the quantization bits from 2-4 is a minute $0.0671\ {}^{W}\!/_{Hz}$. The small loss in energy is due to the the loss of data in sampling at 5 samples-per-bit is large enough that the loss of energy in adding quantization bits is negligible. Note that the digital BER is $\sim 0.70\,dB$ worse than BER for analog EFQPSK. Therefore, if using a 5-sample signal with low quantization bits, the amount of information lost in the transmitter is equivalent to the amount of power saved in the transmitter, and vice versa for the receiver.

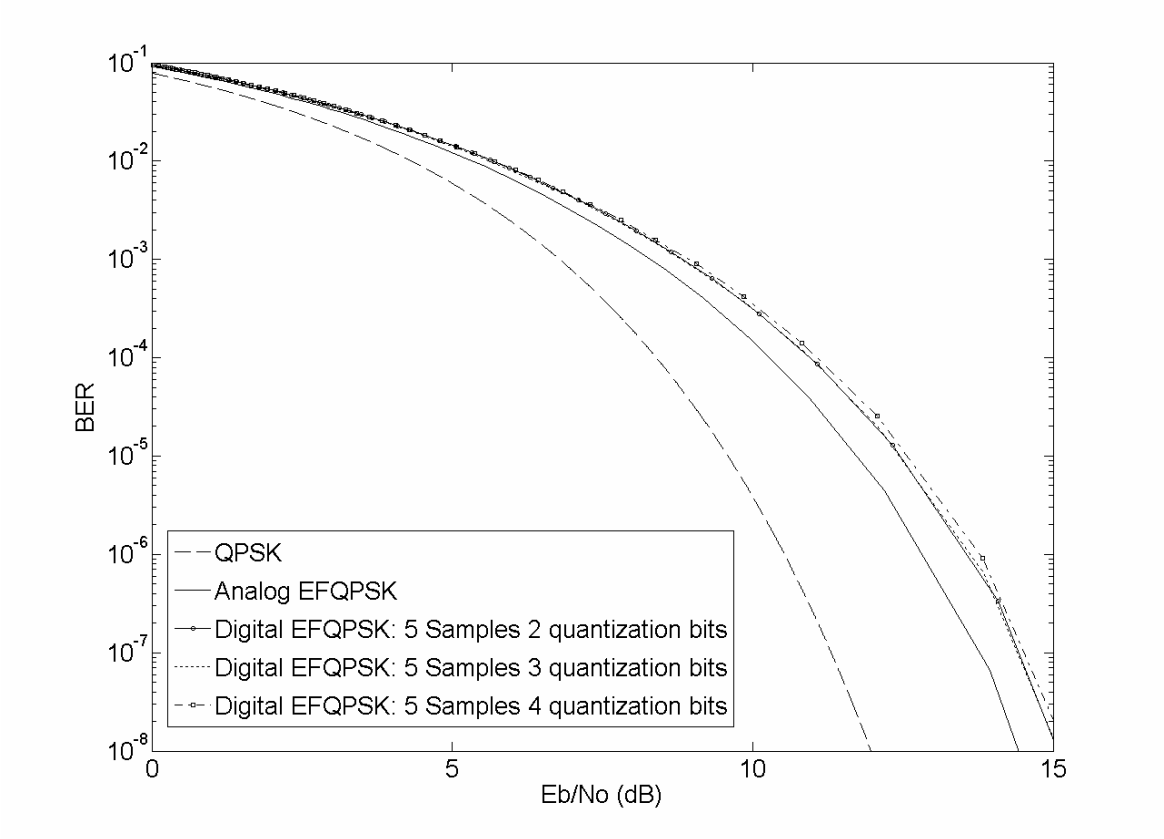

Fig. 4.27. The effect a low number of quantization bits has on the BER of a 5-sample EFQPSK signal.

Fig. 4.28 shows the BER of a 5-sample EFQPSK signal with a 5-bit and 6-bit quantization case. Both plots show that for $P_e = 1 \times 10^{-4}$, the 5-bit and 6-bit quantization cases are $\sim 0.80\ dB$ worse than analog EFQPSK. Practically speaking, for the 6-bit quantization case, the BER has converged to its worst possible state. As with the 2-bit, 3-bit, and 4-bit quantization cases, the loss of information with the large sampling interval is more dominant than the loss of energy in using more quantization bits for the 5-bit and 6-bit cases. The constant $\overline{E}_b \overline{C}_{S\bar{S}}$ is approximately the same for the 5-bit and 6-bit cases. Therefore, the BER of the 5-bit and 6-bit cases is approximately the same.

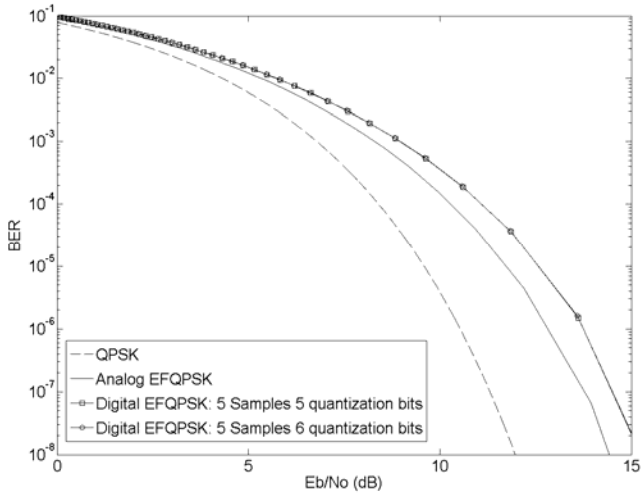

Fig. 4.28. The effect a moderate number of quantization bits has on the BER of a 5-sample EFQPSK signal.

Fig. 4.29 shows the effect a moderate number of quantization bits has on the BER of a 10-sample EFQPSK signal. The digital BER shown is for a 2-bit and 6-bit quantization case. Note that the BER of the 2-bit signal is $\sim 0.20\ dB$ better than the BER for analog EFQPSK. This is because the 4-level quantization process adds energy to $\overline{E}_b\overline{C}_{S\bar{S}}$ for the same reasons stated at the beginning of the chapter. Hence, $\overline{E}_b\overline{C}_{S\bar{S}}$ is higher for the 2-bit quantization case than $\overline{E}_b\overline{C}_{S\bar{S}}$ for the analog case. Sampling the signal at 10 samples-per-bit generally decreases $\overline{E}_b\overline{C}_{S\bar{S}}$, but for a 2-bit quantization case the distortion from quantization adds more to $\overline{E}_b\overline{C}_{S\bar{S}}$ than the loss from sampling with 10-samples subtracts from $\overline{E}_b\overline{C}_{S\bar{S}}$. That is, the distortion of the 2-bit quantization case is high enough that it dominates more than the loss of information in the sampling process. Notice that the 6-bit quantization case exhibits a worse BER than does its analog counterpart. This is because $\overline{E}_b\overline{C}_{S\bar{S}}$ of the 10-sample EFQPSK signal is lower than its analog counterpart. The 6-bit quantization has 64 levels of quantization, which means that the analog waveforms voltages can be relatively accurately mapped to these 64 levels without any sudden gains in $\overline{E}_b\overline{C}_{S\bar{S}}$ from large quantization spacing. The distortion

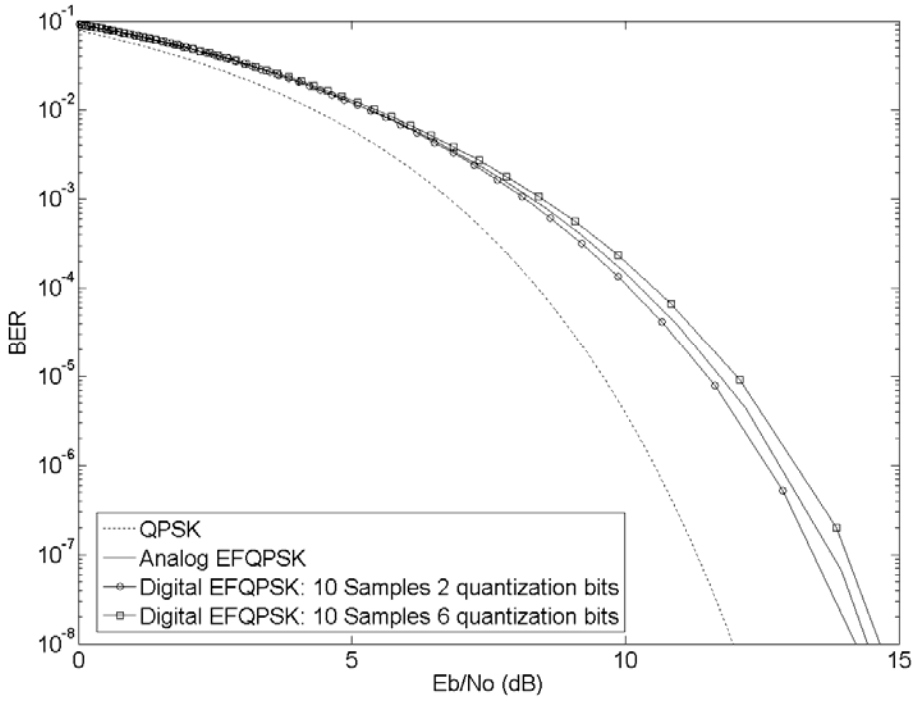

Fig. 4.29. The effect a low-to-moderate number of quantization bits has on the BER of a 10-sample EFQPSK signal.

of the 6-bit quantization is low enough that it does not dominate $\overline{E}_b \overline{C}_{S\bar{S}}$ as much as the sampling operation does.

Fig. 4.30 shows the effect a large number of quantization bits have on the BER of a 10-sample EFQPSK signal. Looking at Figs. 4.29 and 4.30, the BER for the 6-bit and 8-bit quantization cases are nearly identical since the energy added to $\overline{E}_b \overline{C}_{S\bar{S}}$ is negligible compared to the energy lost in the sampling operation. The difference in BER between the 6-bit and 8-bit quantization cases for $P_e = 1 \times 10^{-4}$ is $\sim 0.03\ dB$. Therefore, BER for the 8-bit quantization case has converged to the worst case BER for a 10-sample EFQPSK signal. Note that the BER of the 8-bit quantization case is $\sim 0.345\ dB$ worse than the BER of the analog case and $\sim 3.67\ dB$ worse than the BER of conventional QPSK at $P_e = 1 \times 10^{-4}$. This is a small price to pay given that the spectral efficiency from Fig. 4.3 for the 10-sample signal is $\sim 30\ dB$ better than that of QPSK.

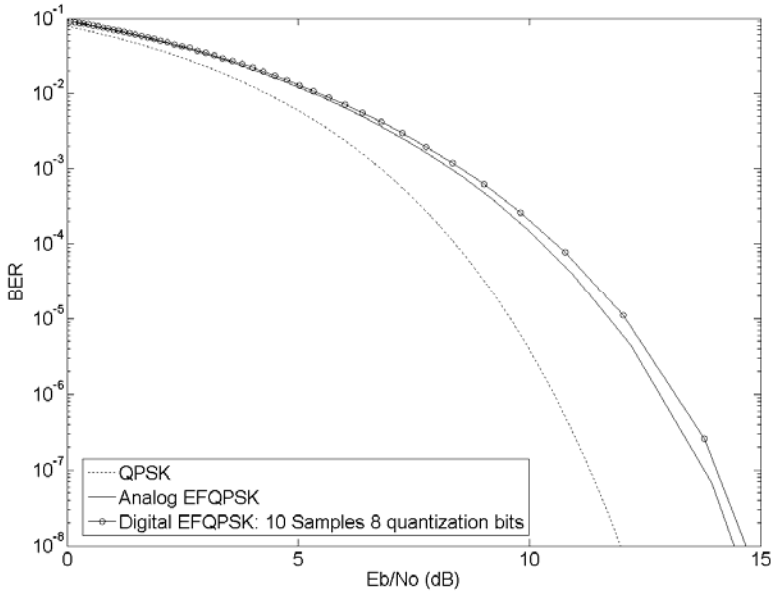

Fig. 4.30. The effect a high number of quantization bits has on the BER of a 10-sample EFQPSK signal.

Fig. 4.31 illustrates the effect a low number of quantization bits have on the BER of a 20-sample signal. The cases presented are for 2-bit, 3-bit, and 4-bit quantization. Note that the BER of the 2-bit quantization case, 3-bit quantization case, and 4-bit quantization case are $\sim 0.35\ dB$, $\sim 0.24\ dB$, and $\sim 0.05\ dB$ worse than the BER of analog EFQPSK, respectively. For all of these digital cases, more energy is added to $\overline{E}_b\overline{C}_{S\bar{S}}$ in the quantization process than is subtracted from $\overline{E}_b\overline{C}_{S\bar{S}}$ in the sampling process.

Fig. 4.32 shows BER for a 20-sample signal with 5-bit and 6-bit quantization. Note that the 5-bit quantization case has approximately the same BER as that of the analog case. For this case, the energy added to $\overline{E}_b\overline{C}_{S\bar{S}}$ in the quantization process is about the same as the energy lost in the sampling procedure. For the 6-bit quantization case, the BER is $\sim 0.12\ dB$ worse than that of analog EFQPSK. Slightly more energy is lost in the sampling operation than is gained in the quantization operation. For this case, the BER has converged to the worst-case BER for a 20-sample EFQPSK signal. Therefore, a system designer may use more than six bits of quantization to improve maximum envelope fluctuation with virtually no penalty in BER.

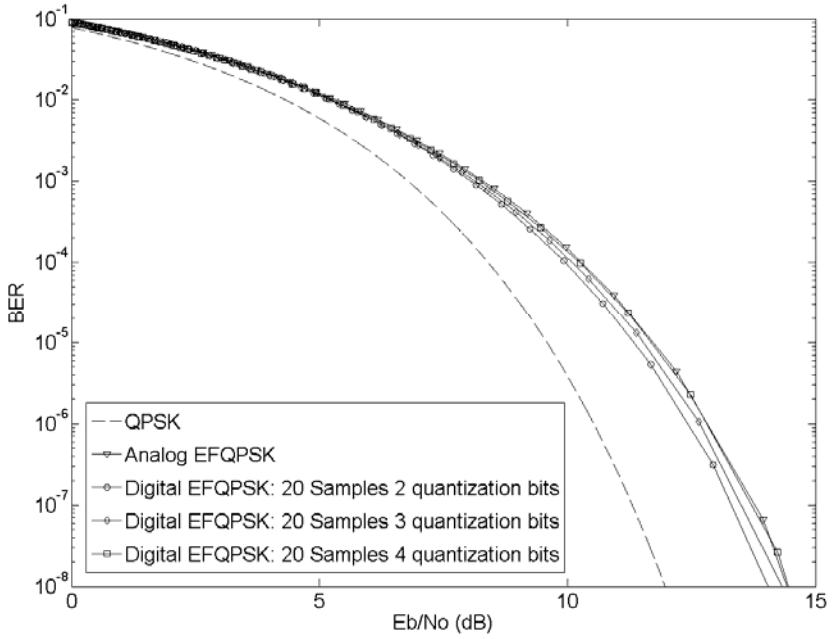

Fig. 4.31. The effect a low number of quantization bits has on the BER of a 20-sample EFQPSK signal.

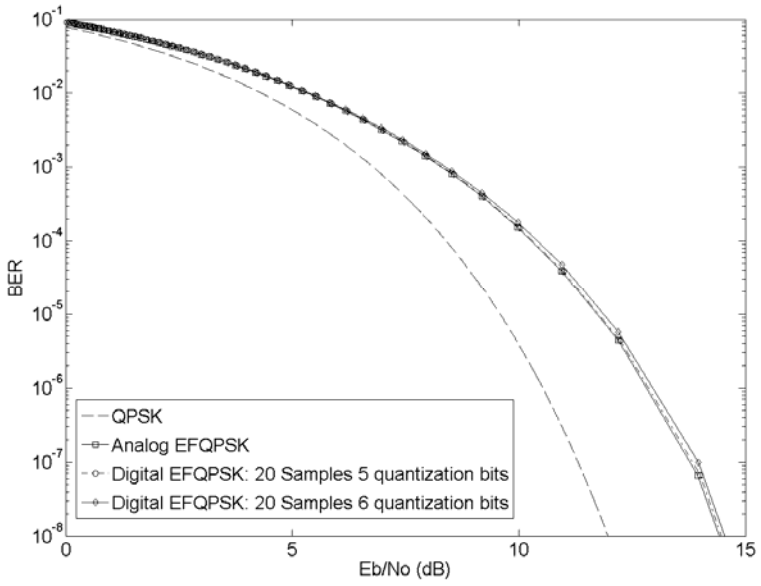

Fig. 4.32. The effect a moderate-to-high number of quantization bits have on the BER of a 20-sample EFQPSK signal.

Fig. 4.33 illustrates the effect a low number of quantization bits have on the BER of a 50-sample EFQPSK signal. The digital cases shown are for 2-bit, 3-bit, and 4-bit quantization. In the 2-bit, 3-bit, and 4-bit cases, the BER is $\sim 0.60\ dB$, $\sim 0.375\ dB$, and $\sim 0.15\ dB$ better than analog EFQPSK for $P_e = 1\times 10^{-4}$, respectively. As in cases with lower sampling frequencies, more energy is added to $\overline{E}_b \overline{C}_{S\bar{S}}$ with the 2-bit, 3-bit, and 4-bit quantization process than is subtracted from $\overline{E}_b \overline{C}_{S\bar{S}}$ in the sampling process. For the 50-sample signal, very little information is lost in the sampling process and therefore the quantization process has the most significant impact on BER. It is important to point out that $\sim 99\ \%$ of the signal energy is contained within the null-to-null bandwidth of digital EFQPSK. By inspection of Figs. 4.6 and 4.7, we can see that vary little of that energy is lost in the null-to-null bandwidth of the 50-sample EFQPSK signal. The energy that is lost is contained outside of that bandwidth, which is the same energy that is lost in the BER of Fig. 4.32. Although in Fig. 4.33 it is not evident that any energy is lost in the sampling process, we will show that in fact an insignificant amount of energy is lost in the sampling process in terms of BER.

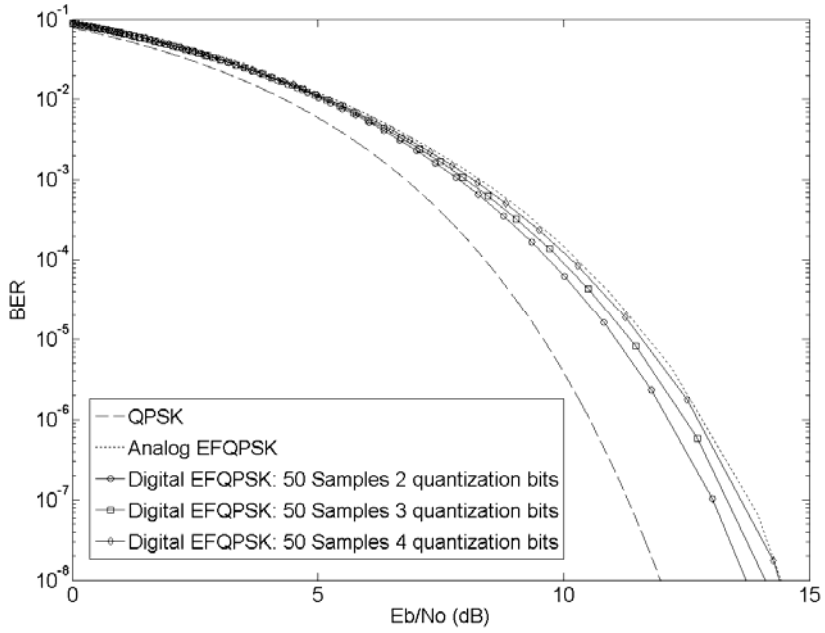

Fig. 4.33. The effect a low number of quantization bits has on the BER of a 50-sample EFQPSK signal.

Fig. 4.34 shows the effect a moderate number of quantization bits have on the BER of a 50-sample EFQPSK signal. The cases shown are for 5-bit and 6-bit quantization. Note that the BER of the 5-bit quantization case is slightly better than the BER of the analog case and that the BER of the 6-bit case is slightly worse than the BER of the analog case. For the 5-bit quantization case, a little more energy is added to $\overline{E}_b\overline{C}_{S\bar{S}}$ in the quantization process than is subtracted from $\overline{E}_b\overline{C}_{S\bar{S}}$ in the sampling operation. In the 6-bit quantization case, the reverse is true. The BER of the 6-bit quantization case has converged to the worst case BER for a 50-sample EFQPSK signal.

Fig. 4.35 illustrates the effect a low-to-moderate number of quantization bits have on the BER of a 100-sample signal. The cases presented are for 2-bit, 3-bit, and 6-bit quantization. The BER of the 2-bit and 3-bit cases are $\sim 0.60\ dB$ and $\sim 0.35\ dB$ better than the BER of analog EFQPSK. As with the 50-sample case, the energy added to

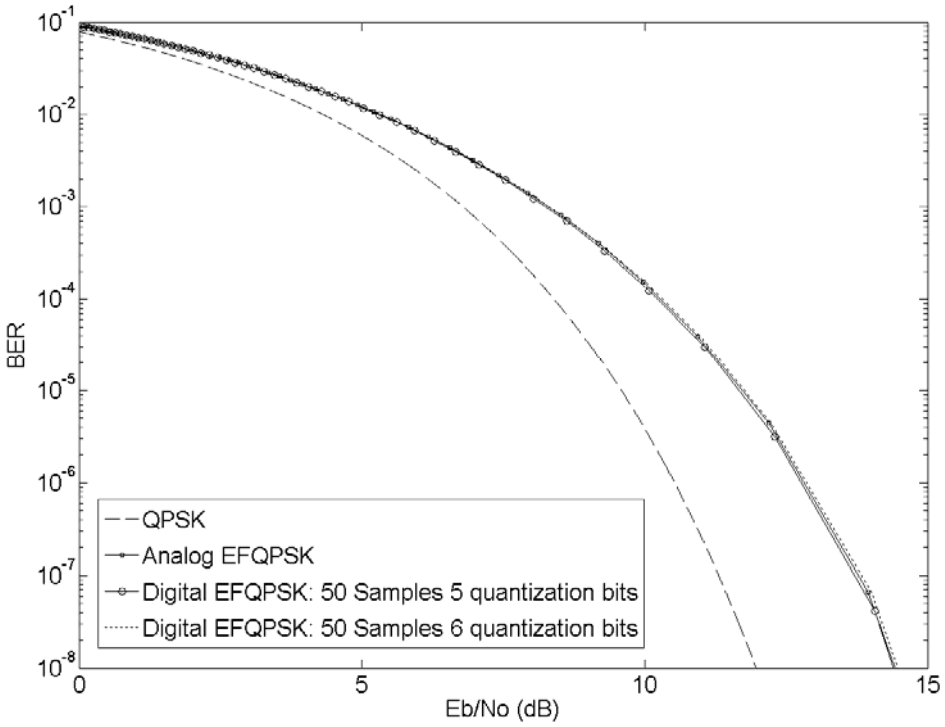

Fig. 4.34. The effect a moderate number of quantization bits has on the BER of a 50-sample EFQPSK signal.

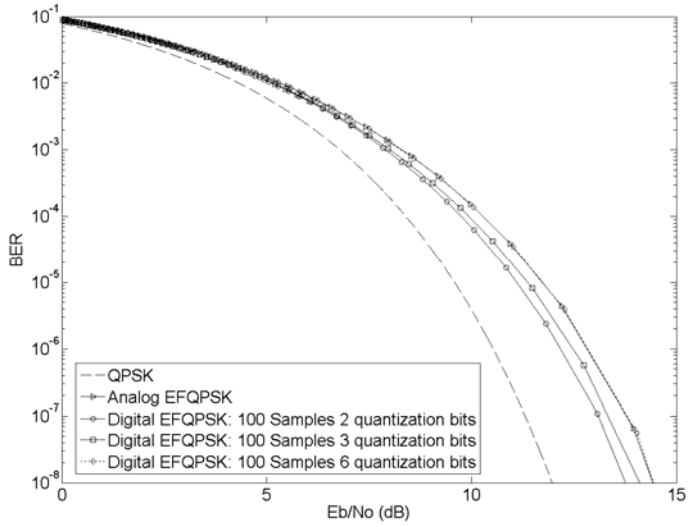

Fig. 4.35. The effect a low-to-moderate number of quantization bits has on the BER of a 100-sample EFQPSK signal.

$\overline{E}_b\overline{C}_{S\bar{S}}$ in the quantization process is greater than the energy subtracted from $\overline{E}_b\overline{C}_{S\bar{S}}$ in the sampling process. As a matter of fact, virtually no energy is lost in the sampling process because the signal is sampled with sampling frequency $F_S = 50N_q$, which greatly exceeds the required $F_S = 4N_q$ for accurate recovery of a signal. Since the 100-sample signal is over-sampled, the quantization process has the most dominant effect on the BER of the signal. Note that the BER of the 6-bit quantization case is approximately the same as the BER of the analog case. The BER for this case has converged to the worst case BER for a 100-sample EFQPSK signal. This further supports the fact that hardly any energy is lost in sampling the signal with $F_S = 50N_q$.

Figs. 4.36 and 4.37 are best-case and worst-case BER curves for digital EFQPSK signals with various sampling frequencies. Both plots show BER for 3, 5, 10, 20, 50, and 100 sample EFQPSK signals. All cases for Fig. 4.36 are for 2-bit quantization and all cases for Fig. 4.37 are for 6-bit quantization, except for the 3 sample signal which has 8-bit quantization. A system designer can study these figures to quickly decide which signal best meets the designer's needs in terms of BER. For PSD, out-of-band power, and envelope fluctuation, the best-case scenarios often translate to the worst-case scenarios for BER in digital EFQPSK.

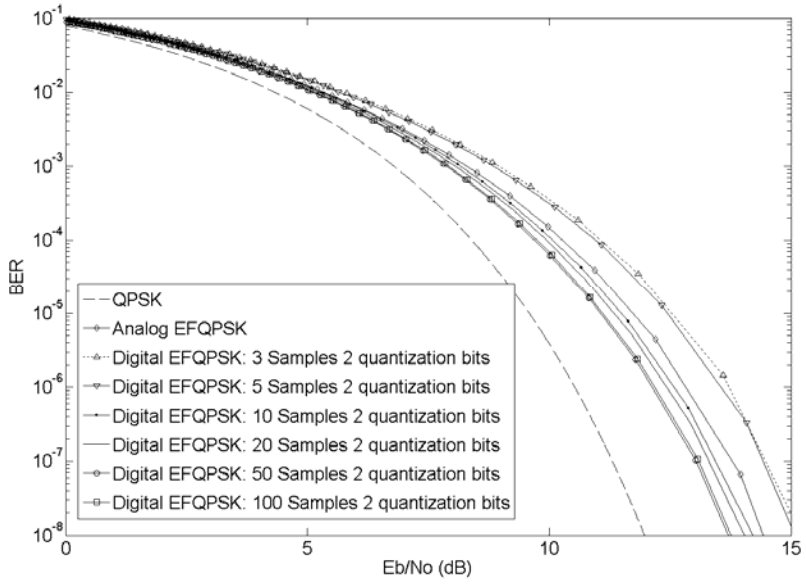

Fig. 4.36. Best case BER for signals with various sampling frequencies.

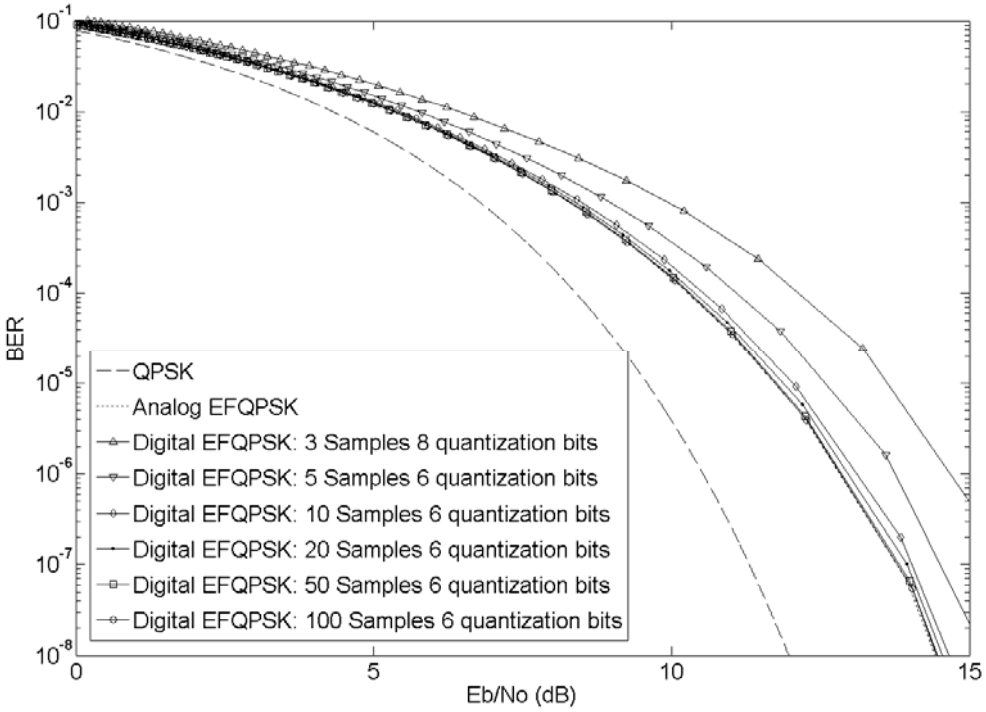

Fig. 4.37. Worst case BER for signals with various sampling frequencies.

Tables 4.1 and 4.2 shows $\overline{E}_b$ and $\overline{C}_{S\bar{S}}$ versus various sampling frequencies and quantization bits of digital EFQPSK compared to analog EFQPSK. The purposes of the tables are to show the effect $\overline{E}_b$ and $\overline{C}_{S\bar{S}}$ have on the BER of the figures presented in Section 4.4 of this study. The value of $\overline{E}_b$ for analog EFQPSK is $\overline{E}_b = 0.4973\ {}^{W}\!/_{Hz}$. The value of $\overline{C}_{S\bar{S}}$ for analog EFQPSK is $\overline{C}_{S\bar{S}} = 0.8792$. Keep in mind that these are statistically averaged values of these parameters. A system designer can quickly look at the values for $\overline{E}_b$ and $\overline{C}_{S\bar{S}}$ and make a conclusion as to the approximate outcome of BER for any case not shown in the figures of Section 4.4. As technology permits, we can greatly increase the sampling frequency and decrease the number of quantization bits to study the values of $\overline{E}_b$ and $\overline{C}_{S\bar{S}}$ and compare them to Tables 4.1 and 4.2 to see if a tradeoff can be made between high sampling frequency and low quantization bits.

Table 4.1. Various sampling frequencies and quantization bits versus $\overline{E}_b$.

Number of quantization bits	3-sample	5-sample	10-sample	20-sample	50-sample	100-sample
2	0.4583	0.5125	0.5824	0.5893	0.6029	0.6083
3	0.4505	0.4844	0.5385	0.5513	0.5610	0.5634
4	0.4485	0.4832	0.5140	0.5304	0.5347	0.5386
5	0.4251	0.4599	0.4897	0.5027	0.5098	0.5127
6	0.4250	0.4572	0.4855	0.4979	0.5029	0.5062
8	0.4194	0.4509	0.4782	0.4889	0.4957	0.4980
10	0.4173	0.4486	0.4755	0.4863	0.4932	0.4956
12	0.4168	0.4480	0.4750	0.4857	0.4926	0.4950
14	0.4167	0.4479	0.4749	0.4856	0.4925	0.4949

Table 4.2. Various sampling frequencies and quantization bits versus $\overline{C}_{S\bar{S}}$.

Number of quantization bits	3-sample	5-sample	10-sample	20-sample	50-sample	100-sample
2	0.5801	0.8384	1.0569	1.1496	1.2254	1.2442
3	0.5647	0.7875	0.9595	1.0145	1.0695	1.0815
4	0.5572	0.7503	0.8846	0.9535	0.9817	0.9957
5	0.4967	0.6777	0.8132	0.8731	0.9095	0.9212
6	0.4950	0.6650	0.8028	0.8566	0.8872	0.8995
8	0.4804	0.6485	0.7818	0.8329	0.8647	0.8758
10	0.4752	0.6424	0.7746	0.8257	0.8582	0.8694
12	0.4739	0.6407	0.7732	0.8241	0.8566	0.8678
14	0.4752	0.6404	0.7729	0.8238	0.8563	0.8675

4.5 PSD for Digital EFQPSK with Soft Limiting

The fundamental transmitter architecture for EFQPSK is OQPSK. When OQPSK undergoes band limiting, the envelope fluctuates slightly from constant envelope [4]. However, since 90° is the maximum discrete phase transition, the envelope does not go to zero and therefore when the signal is hard-limited, the phase is preserved [4]. Since the phase is preserved, no high frequency content will be generated in the spectrum, rendering the spectrum of hard-limited OQPSK virtually the same as the spectrum of OQPSK without amplification [4].

Since the envelope of analog EFQPSK does not go to zero and there are no discrete phase transitions in the envelope, we should expect that the spectrum of amplified analog EFQPSK to be about the same as that of the spectrum of analog EFQPSK without amplification. Fig. 4.38 illustrates this effect and also illustrates the effect a nonlinear amplifier has on the spectrum of a 10-sample EFQPSK signal with various quantization bits. The cases presented are for 2-bit, 3-bit, 4-bit, and 5-bit quantization. Comparing Figs. 4.2 with 4.38, we see that there is virtually no spectral re-growth in the spectrum of amplified analog EFQPSK. Comparing the two figures for the 10-sample, 2-

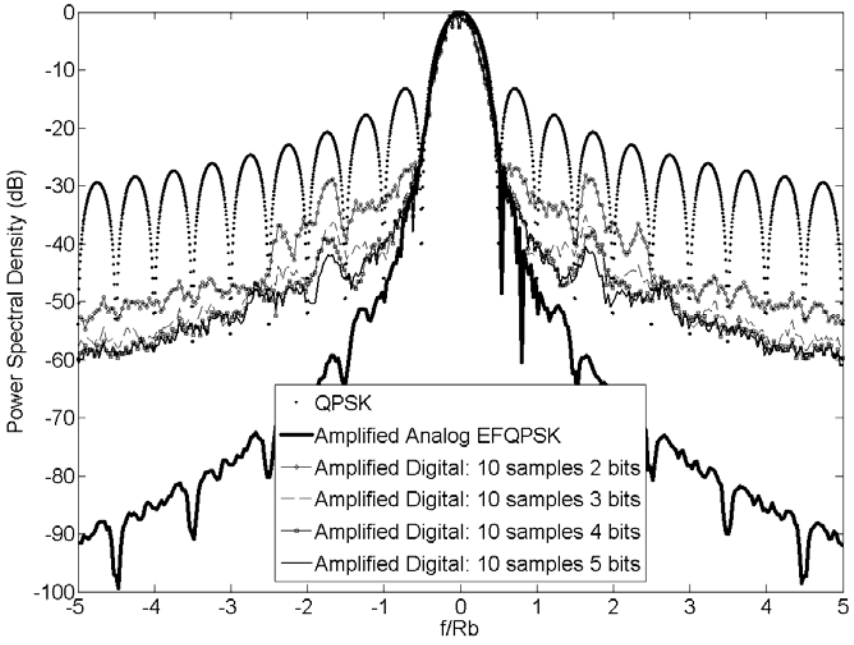

Fig. 4.38. The effect a low-to-moderate number of quantization bits have on the spectrum of a 10-sample EFQPSK signal with amplification.

bit quantization case we see some spectral re-growth at $f/R_b \geq \sim 2.5$ in the amplified case. This re-growth is introduced only by the limiting of the non-constant envelope of this particular signal. Comparing Fig. 4.2 and 4.38, the same degradation exists between signals with 3-bit, 4-bit, and 5-bit quantization with and without amplification. The maximum envelope fluctuation of the 10-sample signals with 2-bit, 3-bit, 4-bit, and 5-bit quantization ranges from $\sim 3.75\ dB$ to $\sim 2\ dB$, respectively. Since this large amount of fluctuation is filtered through the limiting process, the resulting AM/AM conversion and AM/PM conversion introduces spectral re-growth in all of the cases of digital EFQPSK presented in Fig. 4.38 at $f/R_b \geq \sim 2.5$.

Fig. 4.39 illustrates the effect amplification has on the spectrum of a 10-sample EFQPSK signal with quantization bits of 6 and 14. Comparing Fig. 4.3 and 4.39, we see that there is some spectral re-growth in both the 6-bit and 14-bit quantization cases at higher

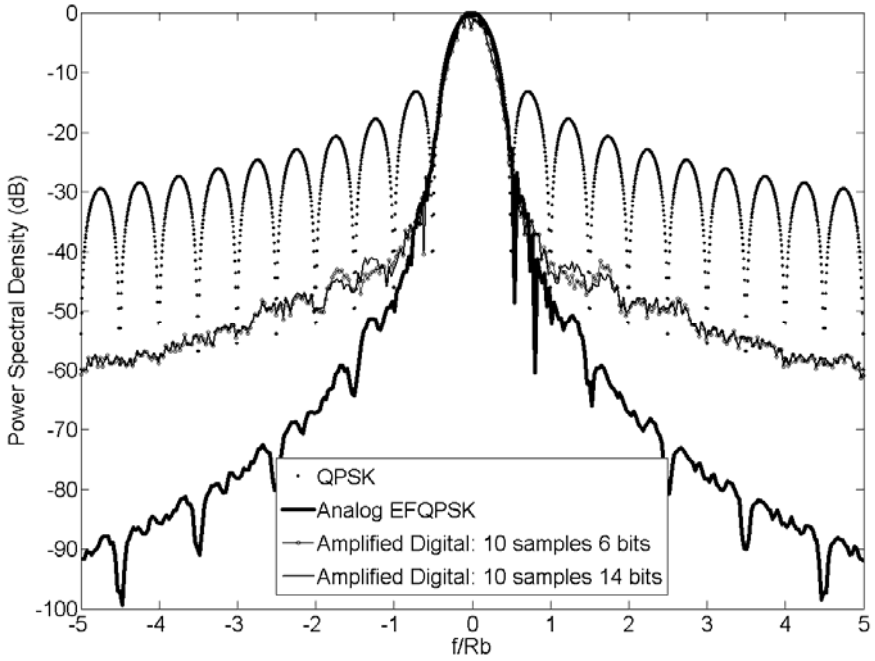

Fig. 4.39. The effect a moderate-to-high number of quantization bits have on the spectrum of a 10-sample EFQPSK signal with amplification.

frequencies. However, there is very little re-growth because the maximum envelope fluctuation ranges from $\sim 1.75\ dB$ to $\sim 1.6dB$ when increasing quantization bits from 6 to 14. However, the spectral re-growth has increased the power in the side-lobes of the 6-bit and 14-bit quantization cases by $\sim 1.0\,dB$ at $f/R_b = 5.0$. Similar to the conclusion drawn from Fig. 4.3, the spectrum of the 6-bit quantization case of the 10-sample signal has converged to the best spectral state of a 10-sample EFQPSK signal.

Fig. 4.40 illustrates the effect amplification has on a 20-sample EFQPSK signal with quantization bits of 2, 3, 4, and 5. Note that for all of the digital cases, some spectral re-growth is witnessed compared to the results of Fig. 4.4. Overall, at higher frequencies, the side-band power is only slightly higher for the amplified cases compared to the cases without amplification. The maximum envelope fluctuation in the cases presented in Fig. 4.40 ranges from $\sim 4.75\ dB$ to $\sim 1.40\ dB$ when increasing the quantization bits from 2 to 5. As with the 10-sample cases, the resulting AM/AM conversion and AM/PM conversion in the 20-sample cases creates the spectral re-growth witnessed in Fig. 4.40.

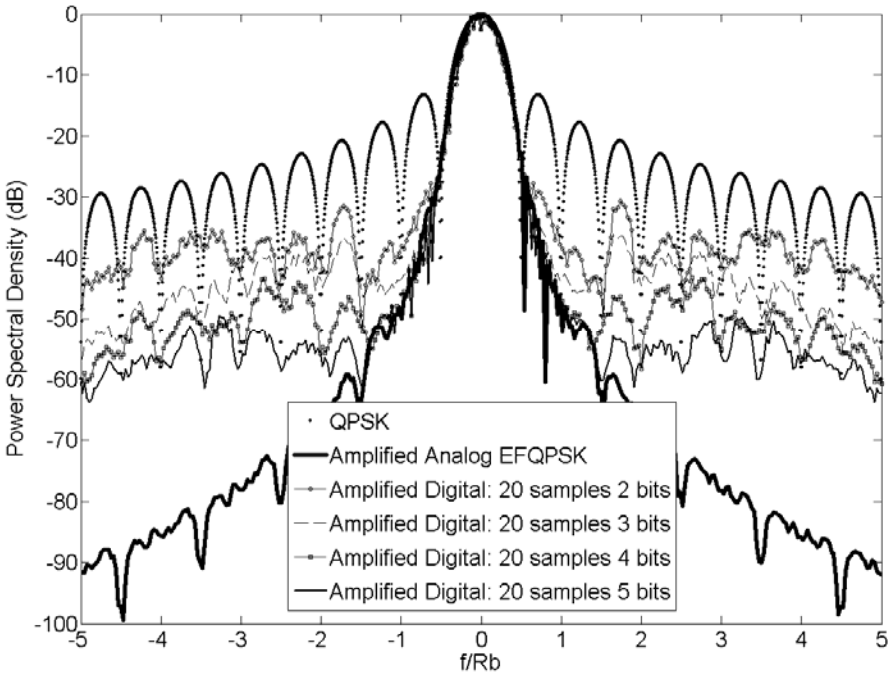

Fig. 4.40. The effect a low-to-moderate number of quantization bits have on the spectrum of a 20-sample EFQPSK signal with amplification.

Fig. 4.41 shows spectral plots of amplified 20-sample EFQPSK signals with quantization bits of 6 and 14. The maximum envelope fluctuations in these two cases are $\sim 1.2\ dB$ and $\sim 1.1\ dB$, respectively. Although these amounts of envelope fluctuation are not comparatively large, it is great enough that the resulting AM/AM conversion and AM/PM conversion in the limiting process creates some spectral re-growth. Note that for both the 6-bit and 14-bit quantization cases, there is a significant amount of re-growth in the frequency range $\sim 0.75 \le {}^{f}\!/_{R_b} \le \sim 2.50$. However, at frequencies greater than this, the re-growth is minor. For the 20-sample EFQPSK signal with 6-bit quantization, the spectrum has converged to the best spectral state with amplification.

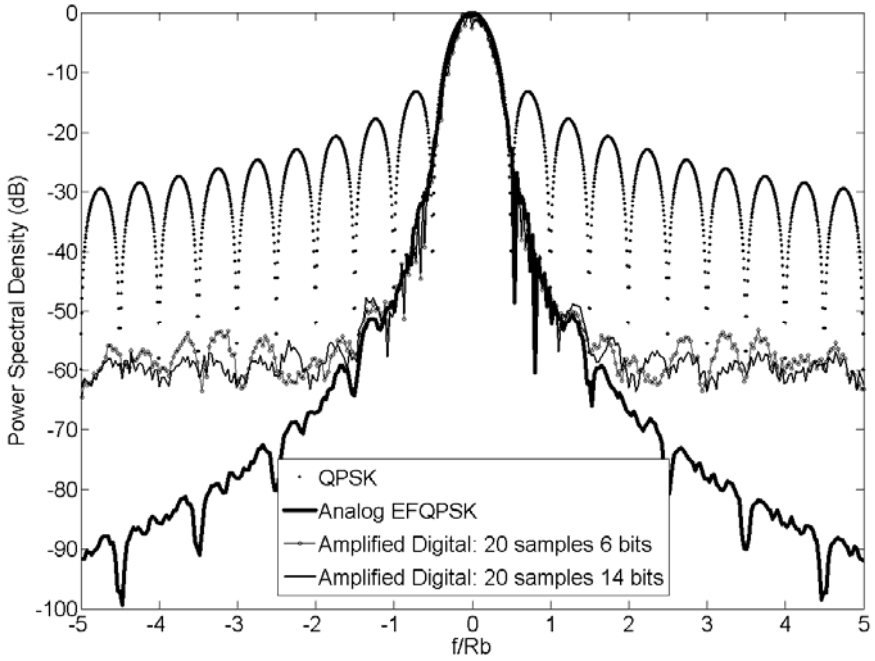

Fig. 4.41. The effect a moderate-to-high number of quantization bits have on the spectrum of a 20-sample EFQPSK signal with amplification.

Fig. 4.42 illustrates the effect amplification has on the spectrum of a 50-sample EFQPSK signal with 2-bit, 3-bit, 4-bit, and 5-bit quantization. The maximum envelope fluctuation of these signals ranges from $\sim 4.75\,dB$ to $\sim 0.75\,dB$, respectively. Note that for these signals, the spectral re-growth is about the same as the re-growth for the 10-sample and 20-sample signals.

Fig. 4.43 shows an amplified 50-sample EFQPSK signal with 6-bit, 8-bit, and 14-bit quantization. The maximum envelope fluctuations of these signals are $\sim 0.6\ dB$, $\sim 0.50\ dB$, and $\sim 0.45\ dB$, respectively. The spectra of these signals are considerably better than the spectra of the 10-sample and 20-sample EFQPSK signals with the same number of quantization bits, even with amplification. Note that from Figs. 4.7 and 4.423, the convergence of the best spectral state of a 50 sample EFQPSK signal occurs with 8-bit quantization.

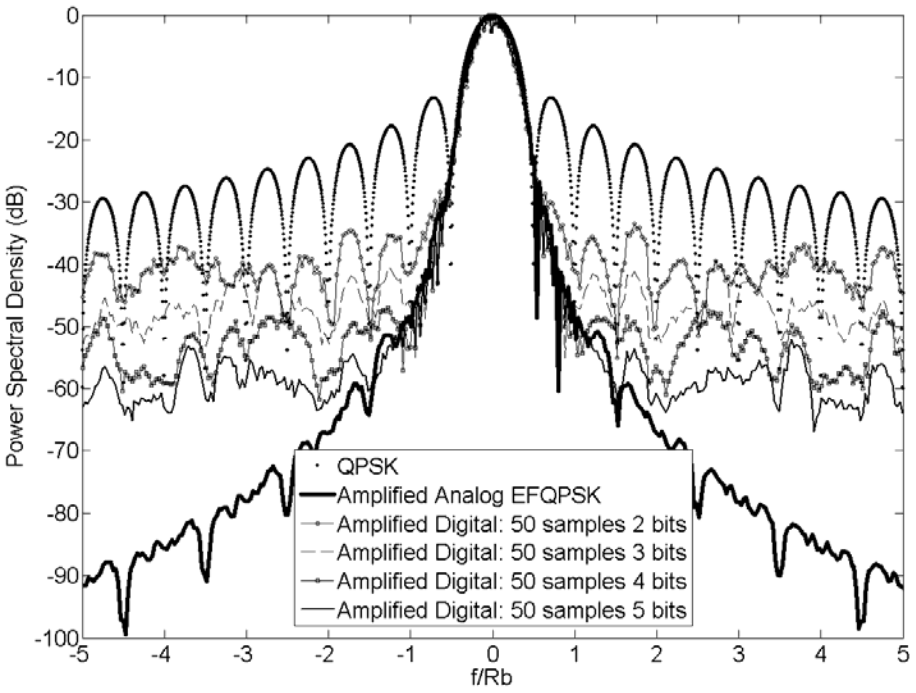

Fig. 4.42. The effect a low-to-moderate number of quantization bits have on the spectrum of a 50-sample EFQPSK signal with amplification.

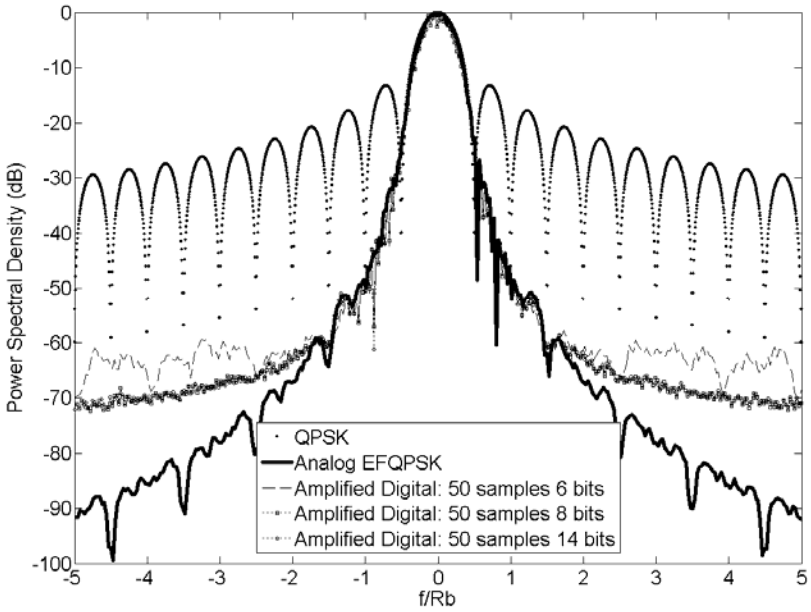

Fig. 4.43. The effect a moderate-to-high number of quantization bits have on the spectrum of a 50-sample EFQPSK signal with amplification.

Fig. 4.44 illustrates the effect amplification has on the spectrum of a 100-sample EFQPSK signal with 2-bit, 3-bit, 4-bit, and 5-bit quantization. Comparing Fig. 4.8 and 4.44 we see some spectral re-growth between the amplified signals and the signals without amplification. The maximum envelope fluctuation ranges from $\sim 4.0\ dB$ to $\sim 0.75\ dB$, respectively. Note that for a low number of quantization bits in a 100-sample EFQPSK signal with amplification, the spectral re-growth is of minor significance compared to the quantization operation in the degradation of the spectrum. The quantization operation for a low number of bits has drowned out most of the effects AM/AM conversion has on a 100-sample EFQPSK signal with amplification.

Fig. 4.45 illustrates the effect amplification has on the spectrum of a 100-sample EFQPSK signal with 6-bit, 8-bit, 10-bit, and 12-bit quantization. Note there is some spectral re-growth in the 6-bit quantization case and somewhat more spectral re-growth in the 8-bit quantization case. However, since the maximum side-band power in these cases is below $60\ dB$, this re-growth has little effect on the degradation of the spectra. The maximum envelope fluctuation of all the digital cases presented in Fig. 4.45 ranges from $\sim 0.5\ dB$ to $\sim 0.28\ dB$, where $\sim 0.28\ dB$ is the maximum envelope

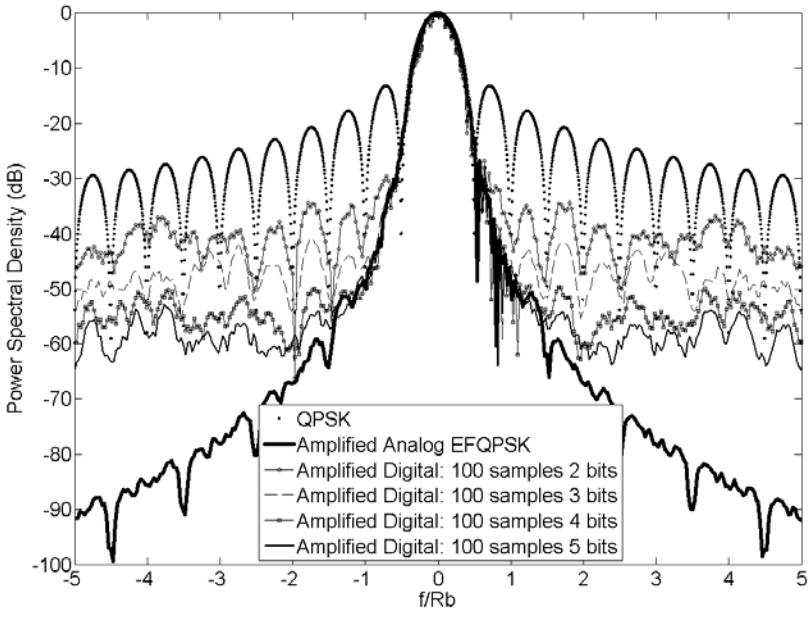

Fig. 4.44. The effect a low-to-moderate number of quantization bits have on the spectrum of a 100-sample EFQPSK signal with amplification.

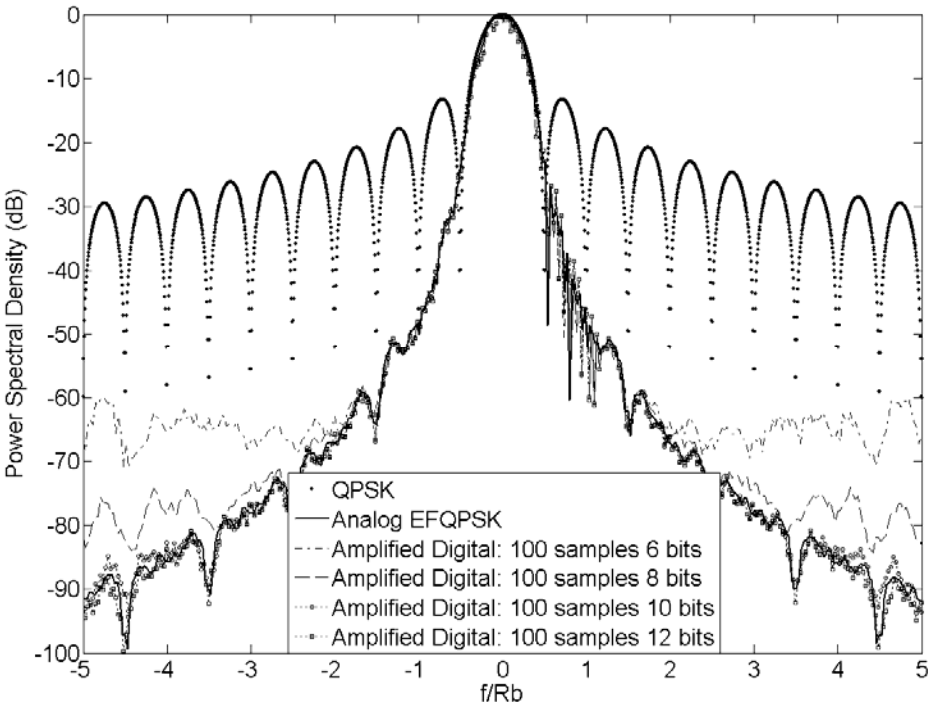

Fig. 4.45. The effect a moderate-to-high number of quantization bits have on the spectrum of a 100-sample EFQPSK signal with amplification.

fluctuation of analog EFQPSK. Once 10-bit quantization is used in the 100-sample EFQPSK signal, the envelope has reached the best state of the envelope of EFQPSK. That is why when comparing Figs. 4.9 with 4.45, there is no evidence that spectral re-growth occurs in the 100-sample, 10-bit and 12-bit quantization cases.

In conclusion, due to no discrete phase transitions in the envelope of EFQPSK, high frequency components are not generated when limiting the envelope. However, with many versions of digital EFQPSK, the resultant envelope fluctuation creates a large amount of AM/AM and AM/PM conversion in the limiting process. The digital cases where this phenomenon is most prevalent are when fewer number of quantization bits is used. When the maximum envelope fluctuation of digital EFQPSK is much greater than that of analog EFQPSK and both are soft-limited, the resulting spectral re-growth coupled with the quantization operation of the digital case significantly distorts the spectrum. When the envelope fluctuation of digital EFQPSK is very close to that of analog EFQPSK, spectral re-growth is not evident.

Fig. 4.46 is an optimized plot showing the effects soft-limiting has on the spectrum of digital EFQPSK with varying sampling frequency and quantization bits. The cases shown are for 10, 20, 50, and 100 samples with quantization bits of 6, 6, 8, and 12, respectively. By looking at Fig. 4.46, we can see that the spectrum of digital EFQPSK becomes less affected by non-linear amplification with increasing sampling frequency and increasing quantization bits. The spectrum becomes less affected by non-linear amplification with decreasing envelope fluctuation. Fig. 4.46 allows a system designer to make a quick conclusion as to which signal best suits the designer's needs.

4.6 Out-of-Band Power of Digital EFQPSK with Soft Limiting

The results of this section compare the out-of-band power of digital EFQPSK to the out-of-band power of QPSK and analog EFQPSK. Since the spectrum of analog EFQPSK is virtually unaffected by amplification, the out-of-band power is likewise virtually unaffected by amplification. The results of this section present digital EFQPSK signals with sampling frequencies of 10, 20, 50, and 100 samples-per-bit, each of which vary in the number of quantization bits.

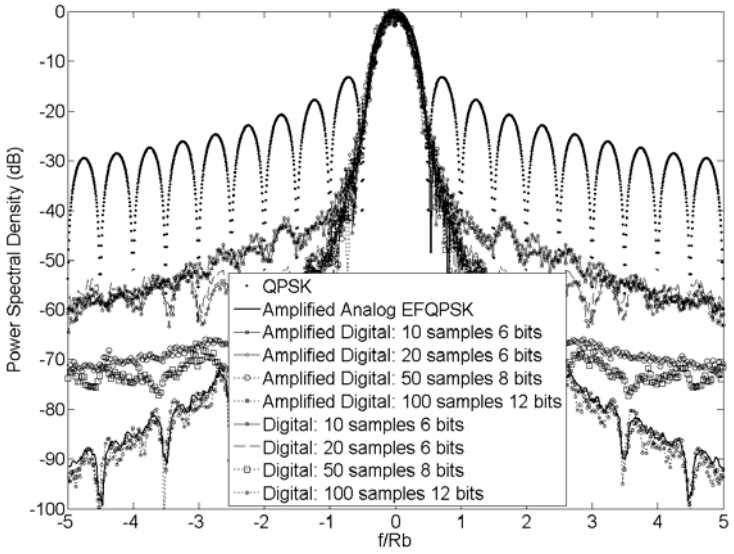

Fig. 4.46. Optimized plot showing the effects amplification has on the spectrum of digital EFQPSK with various sampling frequencies and quantization bits.

Fig. 4.47 illustrates the effect amplification has on the out-of-band power of a 10-sample EFQPSK signal with quantization bits of 2, 3, 4, and 5. Note that for the 2-bit, 3-bit, 4-bit, and 5-bit quantization cases, the out-of-band power is approximately the same for the amplified cases as it is for the cases without amplification. This is because the spectrum of these cases exhibits very little spectral re-growth with amplification. The spectral re-growth contributes a minimal amount of power to the total out-of-band power of the cases presented in Fig. 4.47.

Fig. 4.48 demonstrates the effect amplification has on the out-of-band power of a 10 sample EFQPSK signal with quantization bits of 6 and 14. Note that for both cases the out-of-band power is $\sim 4\ dB$ worse for the amplified cases at higher bandwidths. This is because the total power of the spectral re-growth is higher than the power of the distortion from the quantization operation. In other words, for the low-to-moderate quantization bit cases, the distortion power is the most dominant factor in the degradation of the spectrum of the 10 sample signal. For 6-bit to 14-bit quantization, the total power of the spectral re-growth is more significant than the distortion power from

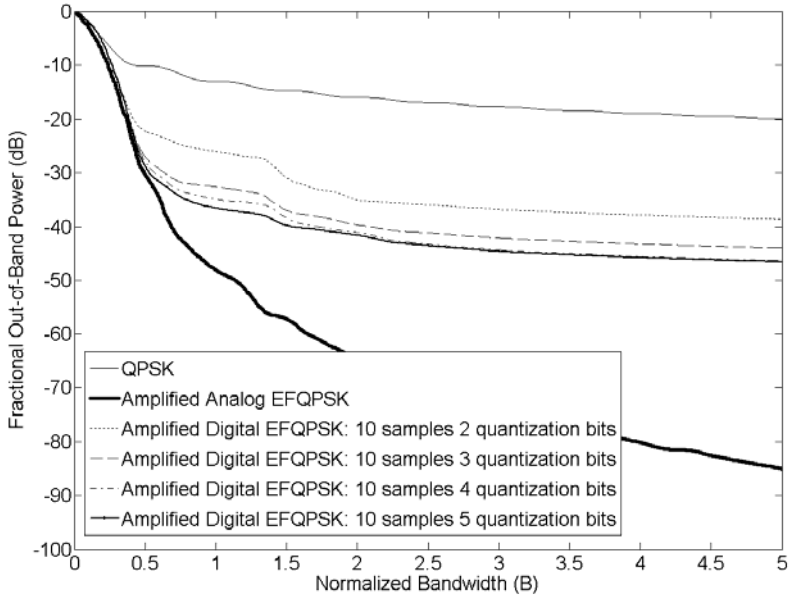

Fig. 4.47. The effect a low-to-moderate amount of quantization bits has on the out-of-band power of a 10-sample EFQPSK signal with amplification.

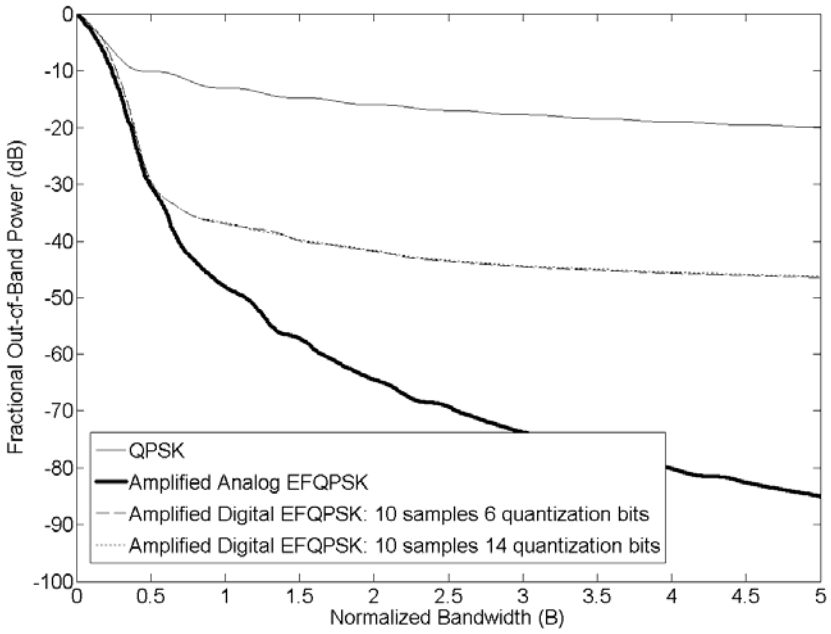

Fig. 4.48. The effect a moderate-to-high amount of quantization bits has on the out-of-band power of a 10-sample EFQPSK signal with amplification.

the quantization operation. For example, in the 2-bit quantization case the total power of the spectral re-growth is a small fraction of the distortion power from the quantization operation, which is why an increase in out-of-band power is not witnessed in Fig. 4.47. However, for the 6-bit quantization case the total power of the spectral re-growth is larger than the distortion power from the quantization operation, resulting in out-of-band power slightly higher for the case with amplification.

Fig. 4.49 depicts the effect amplification has on the out-of-band power of a 20-sample EFQPSK signal with quantization bits of 2, 3, 4, and 5. For each of these cases the out-of-band power is approximately the same for cases with amplification as cases without amplification. As with the cases for the 10-sample signal, the 20-sample signal with 2, 3, 4, and 5-bit quantization has approximately the same spectrum with amplification as the spectrum without amplification.

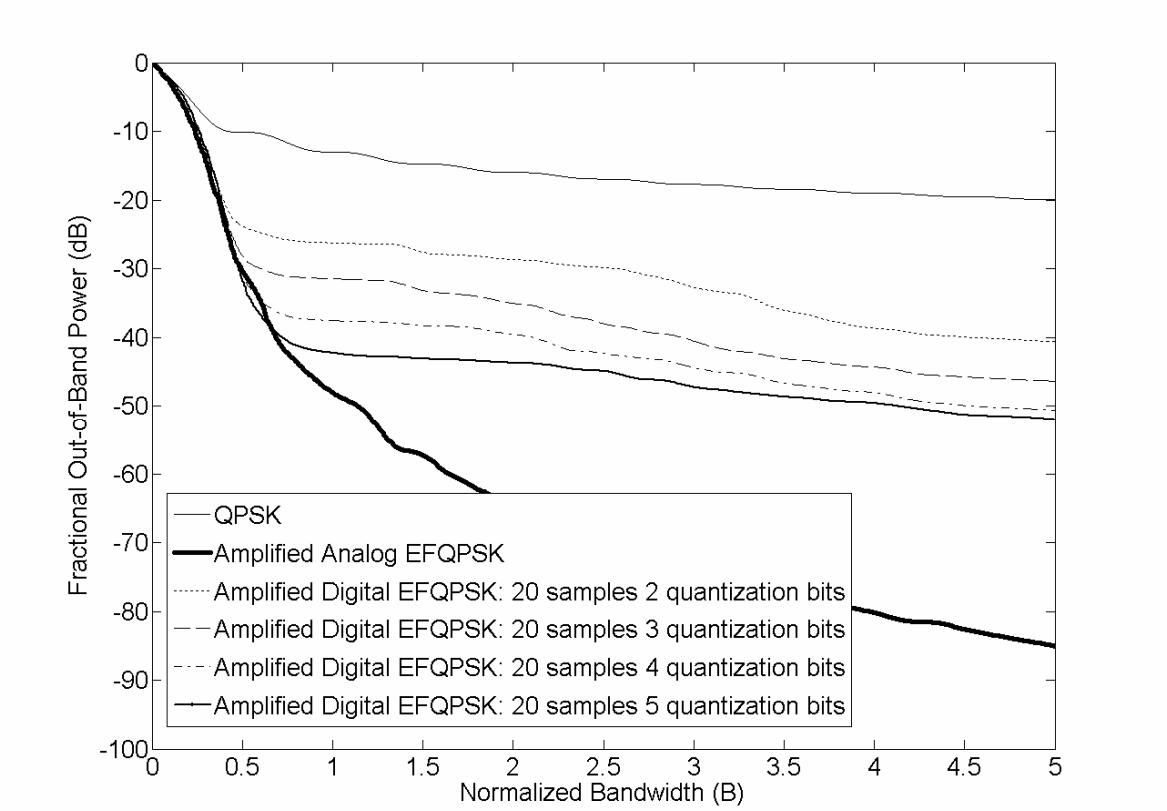

Fig. 4.49. The effect a low-to-moderate amount of quantization bits has on the out-of-band power of a 20-sample EFQPSK signal with amplification.

Fig. 4.50 shows the effect amplification has on the out-of-band power of a 20-sample EFQPSK signal with quantization bits of 6 and 14. Since the spectrum of each of these two cases exhibit a slight increase in side-band power compared to their counterparts without amplification, the total out-of-band power of each of these cases is slightly higher. As with the 10-sample cases, the total power of the spectral re-growth is larger than the power from the distortion in the quantization process, which is why the spectrum and out-of-band power is slightly larger for the 20-sample, 6-bit and 14-bit quantization cases with amplification than the cases without amplification.

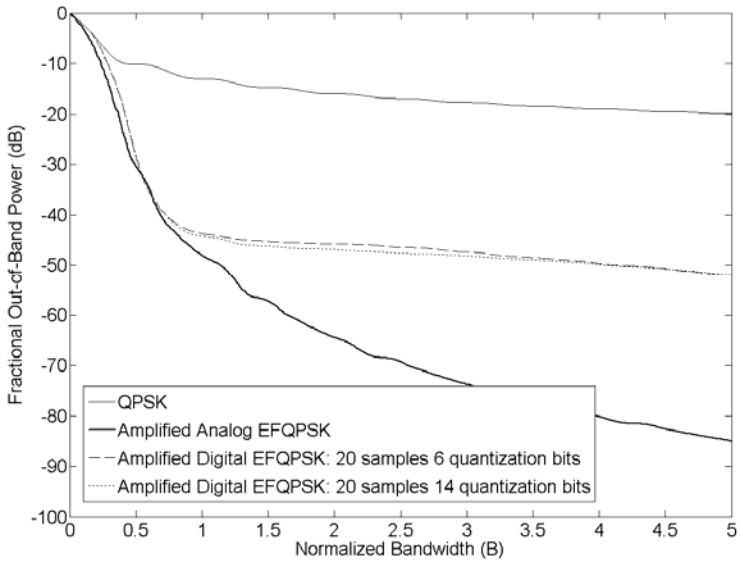

Fig. 4.50. The effect a moderate-to-high amount of quantization bits has on the out-of-band power of a 20-sample EFQPSK signal with amplification.

Fig. 4.51 depicts the effect amplification has on the out-of-band power of a 50 sample EFQPSK signal with quantization bits of 2, 3, 4, and 5. Note that the total out-of-band power of each of the cases is about the same with amplification than without amplification. The total power of the spectral re-growth is a fraction of the power of the distortion, which is why the out-of-band power exhibits a negligible change compared to the cases without amplification.

Fig. 4.52 shows the effect amplification has on the out-of-band power of a 50-sample EFQPSK signal with quantization bits of 6 and 14. Comparing Figs. 4.16 and 4.52, we notice that the out-of-band power of each of these cases is about the same for the cases with and without amplification. This is due to negligible AM/AM and AM/PM conversion from the limiting process, which translates to approximately the same spectra for these two particular cases. As discussed in the previous section, for a 50-sample EFQPSK signal with quantization bits ranging from 6-14, when the signal is limited the resulting total power of the spectral re-growth is about the same as the power in the distortion from the quantization process. This is why the spectra and out-of-band power of the cases with amplification are about the same as the spectra and out-of-band power without amplification.

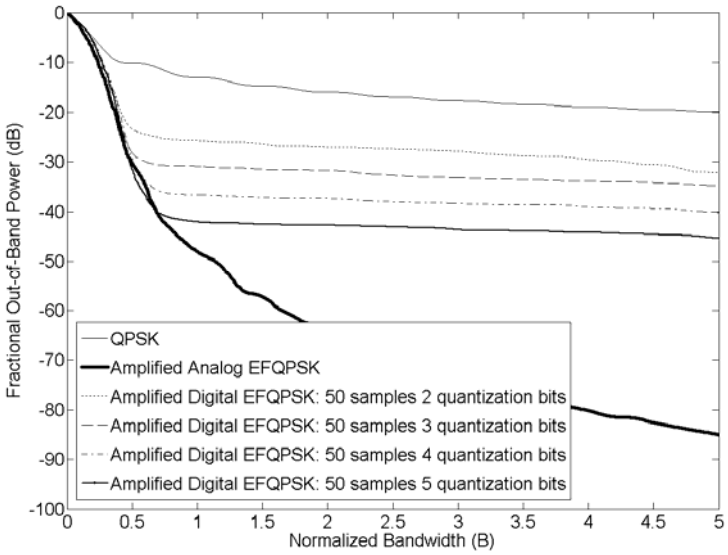

Fig. 4.51. The effect a low-to-moderate amount of quantization bits has on the out-of-band power of a 50-sample EFQPSK signal with amplification.

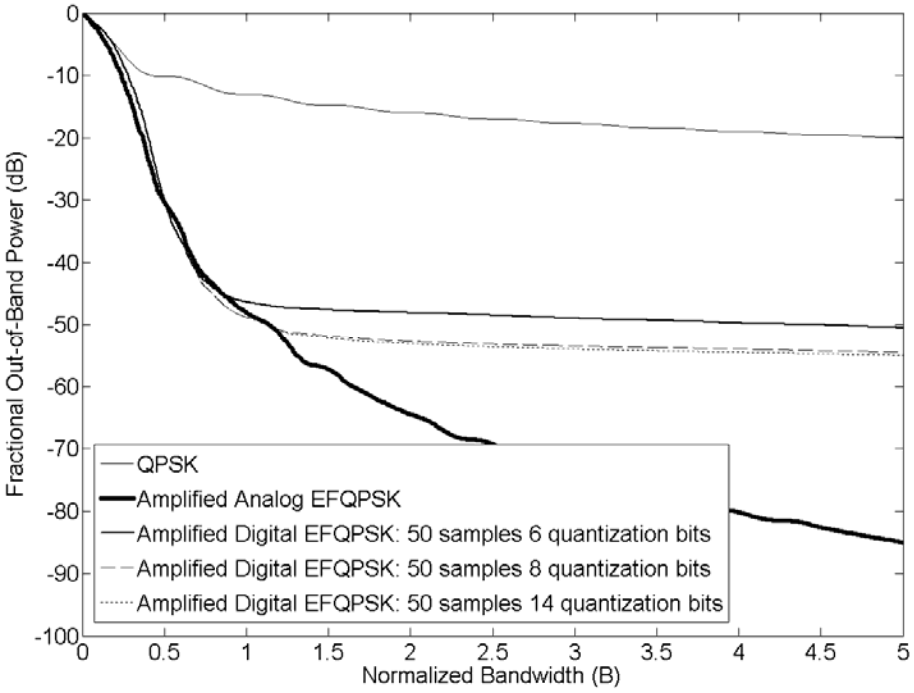

Fig. 4.52. The effect a moderate-to-high amount of quantization bits has on the out-of-band power of a 50-sample EFQPSK signal with amplification.

Fig. 4.53 illustrates the effect amplification has on the out-of-band power of a 100 sample EFQPSK signal with quantization bits of 2, 3, 4, 5, and 6. Note that the out-of-band power appears to decrease at a uniform rate with each increasing quantization bit. The total out-of-band power of each of these cases is slightly worse with amplification than without amplification. This is expected because the spectra of each of these cases are slightly worse with amplification than without amplification.

Fig. 4.54 shows the effect amplification has on the out-of-band power of a 100-sample EFQPSK signal with quantization bits of 8, 10, 12, and 14. Comparing Figs. 4.18 with 4.54, we notice that with 8-bit quantization, the total out-of-band power is slightly better with amplification than without amplification. However, considering the statistical average of the spectra of these two cases, they are about the same. For the cases of 10, 12, and 14-bit quantization, the total out-of-band power is about the same for each case with amplification as without amplification. This is because the envelope fluctuation of each of these three cases has approached that of analog EFQPSK.

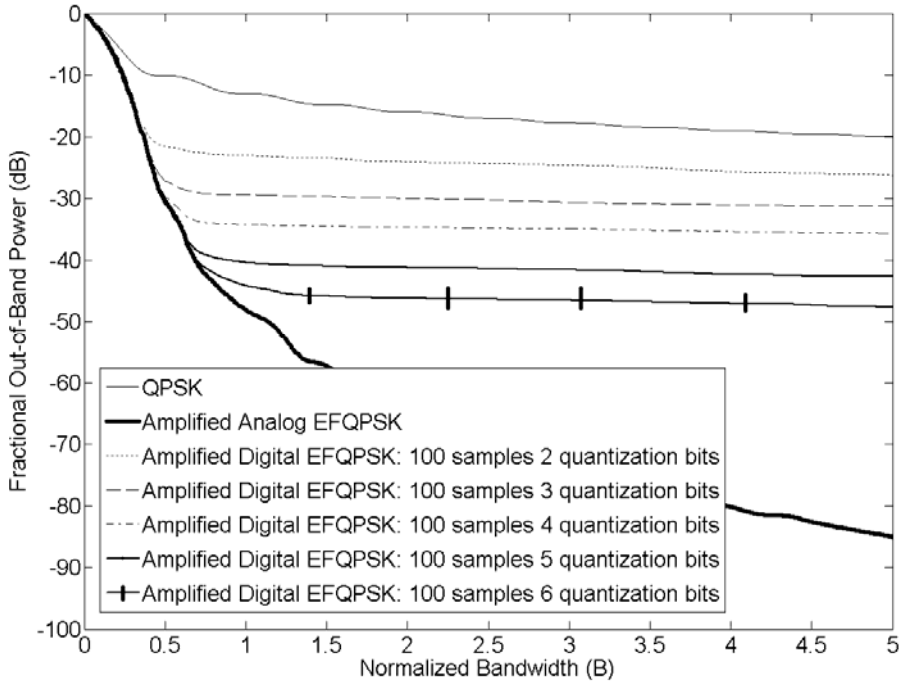

Fig. 4.53. The effect a low-to-moderate amount of quantization bits has on the out-of-band power of a 100-sample EFQPSK signal with amplification.

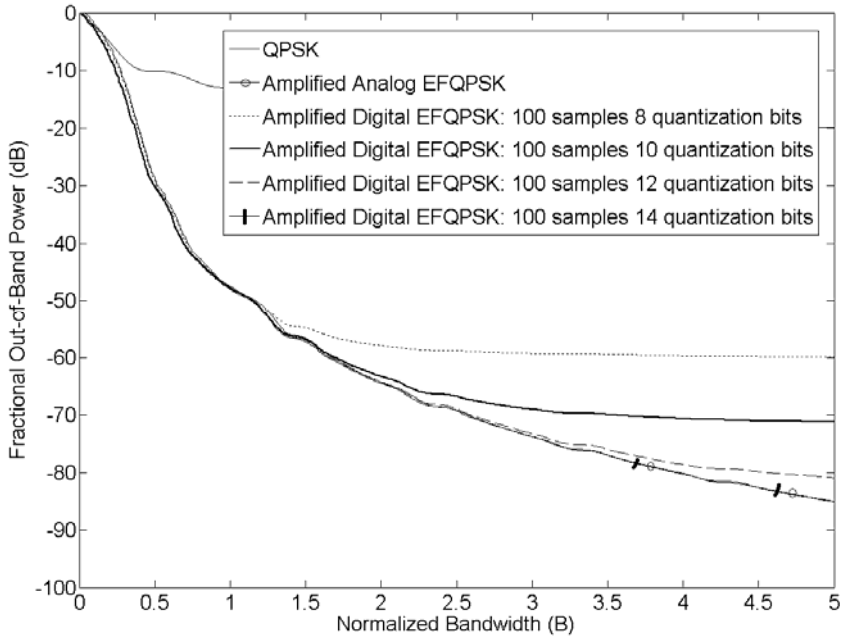

Fig. 4.54. The effect a moderate-to-high amount of quantization bits has on the out-of-band power of a 100-sample EFQPSK signal with amplification.

Fig. 4.55 shows an optimized plot of the out-of-band power of amplified cases of 10, 20, 50, and 100 sample EFQPSK signals with 6, 6, 8, and 14-bit quantization. Note that the total out-of-band power of the 10, 20, and 50 sample cases are very close to one another. Comparing Fig. 4.55 to Fig. 4.19, we notice that the 10-sample and 20-sample cases are slightly worse with amplification than without amplification. However, for the 50-sample case the out-of-band power is about the same with and without amplification. For the 100-sample case, the out-of-band power is the same for both cases because the maximum envelope fluctuation is approximately the same as that of analog EFQPSK. A system designer can take a quick look at this plot and easily determine that it is best to use a 100-sample EFQPSK signal if required to transmit over long distances.

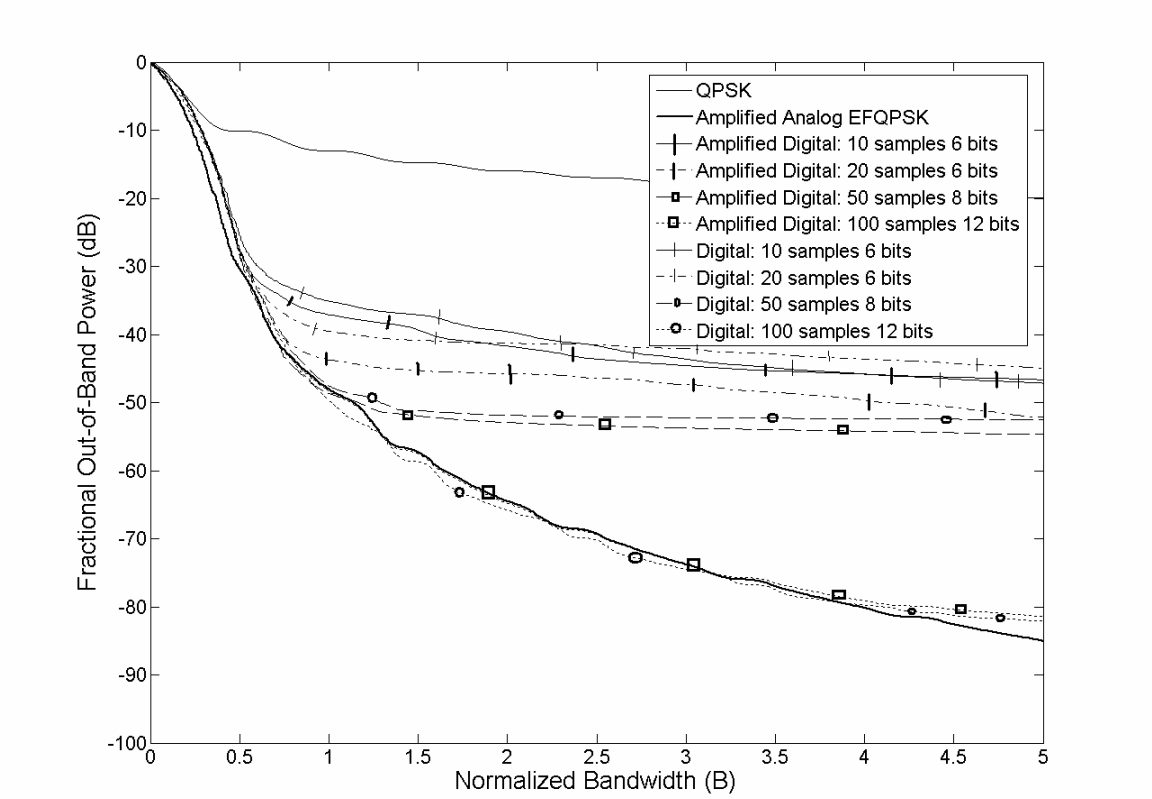

Fig. 4.55. Optimized out-of-band power plot of amplified 10, 20, 50, and 100-sample EFQPSK signals with 6, 6, 8, and 14-bit quantization, respectively.

4.7 Summary

In this chapter we have studied the effects sampling frequency and quantization has on four aspects of value in EFQPSK: PSD, out-of-band power, maximum envelope fluctuation, and BER. By varying the sampling frequency and the number of quantization bits we have both degraded and enhanced these four aspects of EFQPSK. Utilizing a poorly digitized signal we have shown that BER is the only aspect in EFQPSK that can experience an enhancement compared to its analog counterpart. Next we studied the effects soft-limiting a digital EFQPSK signal has on the spectral efficiency of EFQPSK. Overall, this chapter allows a system designer to quickly decide which digital signal is sufficient to fulfill the designer's requirements. The next chapter will conclude this work and present possible future research utilizing the system of this study.

Chapter 5: CONCLUSIONS

5.1 Conclusions of Results

In our study we characterized the merit of analog EFQPSK in terms of spectral efficiency, envelope fluctuation, and BER. For spectral efficiency, we have shown that analog EFQPSK is an especially spectral efficient modulation scheme and that EFQPSK can be digitized in such a way that the spectral efficiency of the digital signal is approximately the same as that of the analog signal, given a certain bandwidth. Through simulation we have shown that superior spectral efficiency over conventional QPSK can be achieved utilizing a poorly digitized EFQPSK signal. Finally, we have shown that a range of digitized EFQPSK signals gives a variety of results, each of which showing an improvement over conventional QPSK in terms of spectral efficiency.

Envelope fluctuation for analog EFQPSK was shown to be minimal. Through simulation, this study indicates that digital EFQPSK can approach minimum envelope fluctuation with a feasible sampling frequency and viable number of quantization bits. We have demonstrated that as the sampling frequency and number of quantization bits become smaller, the maximum envelope fluctuation becomes larger. However, because this is a continuous phase modulation scheme no discrete phase transitions are possible in the envelope in which case, no new high frequency components will be generated when soft limiting the signal. We have also shown that as the sampling frequency and number of quantization bits increase, the maximum envelope fluctuation decreases; and, when the maximum envelope fluctuation is small very little spectral re-growth will take place if the signal is soft-limited.

The BER of analog EFQPSK was revealed to be worse than conventional QPSK. We have demonstrated that an EFQPSK signal with a high sampling frequency and high number of quantization bits will exhibit approximately the same BER as analog EFQPSK. In this study we have also shown that as the sampling frequency decreases, the BER of digital EFQPSK increases; whereas when the number of quantization bits decreases the BER of digital EFQPSK decreases.

5.2 Future Research

Additional work can be done studying the effects digitization has on EFQPSK:

1. BER of digital EFQPSK after soft-limiting can be studied.
2. We used an average matched filter receiver of EFQPSK in this study. Further study of various P_e with a range of digital cases utilizing a Viterbi receiver would expand upon this work.
3. It would also be interesting to investigate the effects digital EFQPSK has in a multi-user environment.
4. In this study we assumed an AWGN channel for the BER . However, it would be useful to study the BER of digital EFQPSK over a Rayleigh fading channel
5. Lastly, we never studied the tradeoff between over-sampling and a low number of quantization bits. As technology advances, it would be interesting to study the effects from increasing the sampling frequency by a couple orders of magnitude and decreasing the quantization bits on the four aspects of EFQPSK studied herein.

LIST OF REFERENCES

REFERENCES

[1] Theodore S. Rappaport, *Wireless Communications: Principles and Practice 2nd Ed*. Upper Saddle River, NJ: Prentice Hall, 2002.

[2] Marvin K. Simon, *Bandwidth-efficient digital modulation with application to deep space communications*. Hoboken, NJ: John Wiley & Sons, 2003.

[3] Ziemer/Tranter, *Principles of Communications: Systems, Modulation, and Noise, 2nd Ed*. Dallas: Houghton Mifflin Company, 1985.

[4] Pasupathy, S., "Minimum Shift Keying: A Spectrally Efficient Modulation," *IEEE magazine*, pp. 14-22, July 1979.

[5] Mark C. Austin and Ming U. Chang, "Quadrature Overlapped Raised-Cosine Modulation", *IEEE Transactions on Communications*, vol. com-29, no. 3, March 1981.

[6] Shuzo Kato and Kamilo Feher, "A New Cross-Correlated Phase-Shift Keying Modulation Technique", *IEEE Transactions on Communications*, vol. com-31, no. 5, May 1983.

[7] Marvin K. Simon and T.-Y. Yan, "Unfiltered FQPSK: Another Interpretation and Further Enhancements: Part 1: Transmitter Implementation and Optimum Reception", *Applied Microwave and Wireless Magazine*, pp. 76-96, February 2000.

[8] Terrance J. Hill, "A Non-Proprietary, Constant Envelope, Variant of Shaped Offset QPSK (SOQPSK) for Improved Spectral Containment and Detection Efficiency", *MILCOM Conference Record*, vol. 1, Los Angeles, California, pp. 347-352, October 23-26, 2000.

[9] John G. Proakis and Dimitris G. Manolakis, *Digital Signal Processing: Principles, Algorithms, and Applications 3rd Ed*. Upper Saddle River, NJ: Prentice Hall, 1996.

[10] Jeffrey H. Reed, *Software Radio: A modern approach to radio engineering*. Upper Saddle River, NJ: Prentice Hall PTR, 2002.

[11] William H. Tranter, K. Sam Shanmugan, Theodore S. Rappaport, Kurt L. Kosbar, *Principles of communication systems simulation with wireless applications*, low price Ed. Patparganj, Delhi, India: Pearson Education (Singapore) Pte. Ltd, 2004.

[12] Israel Korn, *Digital Communications*, New York, NY: Van Nostrand Reinhold Company, 1985.

[13] John G. Proakis, *Digital Communications, 4th ed.* New York, NY: McGraw Hill, 2001.

[14] Marvin K. Simon and T.-Y. Yan, "Unfiltered FQPSK: Another Interpretation and Further Enhancements: Part 2: Suboptimum reception and performance comparisons", *Applied Microwave and Wireless Magazine*, pp. 100-105, March 2000.

[15] Leon W. Couch, II, *Digital and Analog Communication Systems, 6th ed*. Upper Saddle River, NJ: Prentice Hall, 2001.

VITA

Fall B. Taylor Jr. was born in Berlin, Germany and raised in Louisiana (where his interest in technology began) and Tennessee. He was a bi-athlete for several years before and during high school in baseball and football. After high school, he attended the University of Tennessee, Knoxville where he received his Bachelor's of Science degree in Electrical Engineering in May, 2004. Originally, plan number one had Fall playing baseball while pursuing his Bachelor's in Electrical Engineering as a backup. Due to a shoulder injury, he reformulated his plans and concentrated all of his energy into pursuing a degree. In June, 2004 he began working at Oak Ridge National Laboratory in Oak Ridge, TN in pursuit of his Master's of Science in Electrical Engineering with a concentration in Communication Theory at the University of Tennessee, Knoxville.